"Mechanism of Amphoteric Liposomes

&

Application for siRNA Delivery"

Dissertation

zur Erlangung des akademischen Grades

Doctor rerum naturalium (Dr. rer. nat.)

vorgelegt an der

Naturwissenschaftlichen Fakultät I-Biowissenschaften

der Martin-Luther-Universität Halle-Wittenberg

Fachbereich Biochemie/Biotechnologie

von

Evgenios Siepi

geboren am 19.08.1978 in Zypern

Gutachter :

1. Prof. Dr. Sven-Erik Behrens
2. Prof Dr. Andreas Langner
3. PD Dr. Hans Binder

Halle (Saale), Februar 2010

To my parents

TABLE OF CONTENTS

ABBREVIATIONS..... 05

ABSTRACT..... 08

1. INTRODUCTION..... 10

1.1 Antisense and siRNA molecules..... 10
1.1.1 Unassisted cellular uptake of oligonucleotides..... 11

1.2 Overcoming extra- and intracellular barriers..... 13
1.2.1 Liposomal carriers for nucleic acid delivery..... 14

1.3 Lipid structures – charged and neutral lipids..... 17
1.3.1 Neutral "helper" lipids..... 17
1.3.2 Cationic and anionic lipids..... 18

1.4 Lipid properties – An Overview..... 21
1.4.1 Lipid shape theory and lipid geometry..... 21
1.4.2 The role of counterions in lipid membranes..... 23

1.5 Membrane fusion through hexagonal phase..... 24

1.6 pH-sensitive liposomes..... 25
1.6.1 Mixtures of charged lipids present pH-dependent properties..... 25
1.6.2 Biphasic stability of amphoteric liposomes..... 26

1.7 Scope of this thesis..... 28

2 MATERIALS & METHODS..... 29

2.1 Chemicals and Reagents..... 29
2.1.1 Lipids..... 29
2.1.2 SiRNA sequence..... 30

2.2 Fusion in response to pH..... 30
2.2.1 Preparation of particles..... 30
2.2.2 Lipid mixing – FRET assay..... 30

2.3 Fusion after counterion discharge..... 31
2.3.1 Preparation of particles..... 31
2.3.2 Lipid mixing – FRET assay..... 31

2.4 Counterion dependent fusion..... 32
2.4.1 Preparation of particles..... 32
2.4.2 Lipid mixing – FRET assay..... 32

2.5 Fluorescence Resonance Energy Transfer (FRET) measurements..... 32

2.6 Size measurement..... 33

2.7 Fluorescence microscopy studies with fluorescently labelled lipid..... 33
2.7.1 Preparation of labelled MoChol/CHEMS liposomes..... 33
2.7.2 Fluorescence microscopy studies..... 34

2.8 Transfection of siRNA into HeLa and RAW264.7 cells..... 34
2.8.1 Preparation of particles..... 34
2.8.2 Cell culture and transfection procedure..... 36

2.8.3 Cell proliferation assay..... 36
2.9 APPENDIX: Structures and physical properties of lipids used in this study..... 38

3. RESULTS..... 46

3.1 The role of counterions in the fusogenic behaviour of lipid bilayers..... 46

3.2 Amphoteric liposomes and their biphasic stability..... 49
3.2.1 Amphoter I system..... 50
3.2.2 Amphoter II system..... 52
3.2.3 Amphoter III system..... 53

3.3 High-Throughput Screen for lipid fusion..... 55
3.3.1 Charge only systems-Size of headgroup can modulate amphoteric membrane fusion..... 57
3.3.2 Fine tuning of amphoteric membrane fusion by the addition of neutral or zwitterionic lipids..... 58
3.3.3 Algorithm predicts impact of neutral lipid..... 61

3.4 Fusion studies with vesicular models of the cell membrane..... 63

3.5 Intracellular delivery of siRNA mediated by amphoteric liposomes..... 67
3.5.1 Screen design for siRNA *in vitro* application..... 68
3.5.2 Transfection efficiency based on the molecular shape theory..... 72
3.5.3 The shape parameter κ_{MIN} dictates cellular transfection potency..... 74

4. DISCUSSION..... 78

4.1 Counterion binding causes shape transition..... 79

4.2 Amphoteric lipid membranes present pH-guided, biphasic stability 80

4.3 Influencing fusogenicity through the addition of neutral/zwitterionic lipids. 81

4.4 Algorithm – Rational optimization of liposome design..... 83

4.5 The fusion determinant κ_{MIN} guides activity of amphoteric liposomes..... 84

REFERENCES..... 87

TABLES & FIGURES..... 98

ACKNOWLEDGEMENTS..... 100

CURRICULUM VITAE..... 101

PUBLICATIONS & PATENTS..... 102

STATEMENT/ERKLÄRUNG..... 103

ABBREVATIONS

$Å^3$	cubic Ångstrom
ApoB-100	Apolipoprotein B-100
ASOs	Antisense oligonucleotides
C:A	cation to anion molar ratio
CPP	Critical packing parameter
DGAT2	diacylglycerol O-acyltransferase 2
DMEM	Dulbecco modified eagle medium
DMPC	1,2-dimyristoyl-sn-3-phosphatidylcholine
DMRIE	1,2-dimyristyloxypropyl-3-dimethyl-hydroxyethylammonium bromide
DNA	Deoxyribonucleic acid
DODAC	N,N-dimethyl-N,N-di-9-cis-octadecenylammonium chloride
DOIM	4-(2,3-bis-oleoyloxy-propyl)-1-methyl-1H-imidazole
DOSPA	2,3-dioleoyloxy-N-[2(sperminecarboxamido)ethyl]-N,N',-dimethyl-1-propanaminium-trifluoroacetate
DOTMA	N-[1-(2,3-dioleyloxy)propyl]-N,N,N-trimethylammonium chloride
DOPC	1,2-dioleoyl-sn-3-phosphatidylcholine
DOPS	1,2-dioleoyl-sn-3-phosphatidylserine
DPIM	4-(2,3-bis-palmitoyloxy-propyl)-1-methyl-1H-imidazole
DSPC	1,2-distearoyl-sn-glycero-3-phosphocholine
Ex/Em	Excitation/Emission wavelengths
FCS	Fetal calf serum
FRET	Fluorescence resonance energy transfer
h, min	hour, minute
H_{II}	Hexagonal phase
L_α	Lamellar phase
mM, µM, nM	millimolar, micromolar, nanomolar
ms	millisecond
OA	Oleic acid
ONs	Oligonucleotides
PA	Phosphatitic acid
PBS	Phosphate buffered saline
PC	Phosphatidylcholine

PE	Phosphatidylethanolamine
PEG	Polyethyleneglycol
PG	Phosphatidylglycerol
pH	negative decadic logarithm of the hydrogen ion (H^+) concentration
pK_α	negative logarithm of the dissociation constant K
Plk1	Polo-like kinase 1
PS	Phosphatidylserine
RISC	RNA-induced silencing complex
RNAs	Ribonucleic acids
RT	Room temperature
SAINT	Synthetic, Amphiphilic, INTeractive
SALPS	Stabilized antisense- lipid particles
siRNA	small interfering RNA
SNALPS	Stabilized nucleic acid- lipid particles
∑FRET	sum of FRET signals

*Abbreviations and names of the lipids used in this study are provided in MATERIALS & METHODS section (see Appendix 2.9).

ABSTRACT

Oligonucleotides are molecules that have the ability to inhibit gene expression in a specific manner, being therefore potentially active for the treatment of numerous diseases, such as cancer and metabolic diseases. Liposomal delivery systems are frequently used for the intracellular delivery of pharmaceutical substances and have thus attracted substantial interest as transporters for oligonucleotides. Over the last twenty years, several studies have focused on the principles and mechanism of intracellular delivery. However, the transfection efficiency mediated by these liposomal gene delivery vectors varies widely and is still not well elucidated. Therefore, intracellular delivery of a cargo can only be improved through insights into transfection related mechanisms at the molecular levels. An important and usually rate limiting step in liposomal drug delivery is the release of the encapsulated oligonucleotides into the target cell. Following the endocytic pathway, the cargo release is thought to occur by fusion of the liposome and the endosomal membrane. After cellular contact, these carriers need to undergo a structural change in order to release their cargo into the cytosol and often this process requires pH dependent driven fusion between the liposomal and endosomal membrane. Consequently, a detailed understanding of the transition between stable and fusogenic carrier states is critical for the effective function of the carrier.

In the past years, it has been suggested that anionic liposomes constructed from ionizable lipids, such as cholesterol hemissucinate, can undergo a structural transition by adopting a stable lamellar phase at neutral pH and exhibiting an hexagonal, fusogenic orientation in the lower pH found within the endosomes. Such pH-sensitive liposomes fuse as the pH is reduced toward the pK_α of the acidic lipid and can mediate cytosolic delivery of oligonucleotides. However, a major practical limitation of these anionic pH-sensitive liposomes is the poor encapsulation of their cargoes due to lack of attraction. In order to circumvent the loading problem, a new generation of pH-sensitive liposomes has been lately introduced, named amphoteric liposomes. Amphoteric liposomes are able to become positively charged at acidic conditions, thus enabling the efficient encapsulation of nucleic acid molecules.

This thesis mainly focuses on the mechanism behind amphoteric liposomes and their lipids and furthermore intent to provide essential knowledge for the optimal design of liposomal delivery systems. Firstly, emphasis is placed on the role of counterions in lipid geometry and the mathematical model proposed by Panzner and colleagues, which suggests an extension of the

lipid shape theory. In this algorithm, volume elements of the lipids and solvent ion reveal that bilayer, in its charged state, recruits counterions from the solvent, thus promoting the formation of the lamellar phase. It is the first time, to my knowledge, that experimental evidence is provided demonstrating that counterions can be used to modulate the structure of lipid assemblies and promote stabilization of liposomal bilayers. Moreover, the data establish that the counterion recruitment is a common phenomenon in lipid membranes.

A further important contribution of this thesis is the profound analysis and description of the double pH-driven phase transition in amphoteric lipid materials through fusion experiments based on the FRET technique. Liposomes having amphoteric character form a lamellar phase both at acidic and neutral pH, but can undergo fusion at slightly acidic conditions. The obtained data attribute this to a reversible, pH-driven lipid salt formation, specific to amphoteric bilayers, which acts in combination with a recruitment of solvent ions to the bilayer, a general feature of charged membranes.

Eventually, in order to evaluate the utility of amphoteric liposomes capable of mediating efficient delivery of siRNA *in vitro*, selected liposomes from the fusion experiments were tested for siRNA transfection in human and murine cell lines. By comparing transfection efficacy with carrier properties described in the biophysical model, a link between transfection and fusogenic behaviour was found. The fusion determinant κ_{MIN} derived from the algorithm was identified as the rate limiting factor for the cellular transfection of liposomes, thereby establishing a quantitative structure activity relationship between liposome composition and cellular transfection efficacy. In summary, this thesis provides novel knowledge of liposomal membrane properties, which can lead to a global theory for the rational design of triggered lipid based delivery systems.

1. INTRODUCTION

The specific inhibition of target gene expression through oligonucleotides (ONs), such as antisense oligonucleotides (ASOs) and small interefering RNAs (siRNA) creates a new class of therapeutics with illimitable potential. However, poor bioavailability, biodistribution and intracellular delivery are still major obstacles on the way towards the development of nucleic acid-based therapeutics. In order to circumvent these obstacles, it has been suggested the use of carriers for effective drug delivery. Liposomal carriers have been successfully applied for nucleic acid delivery and their use has become a highly active field in current antisense and siRNA therapy (Behlke, 2006; de Foungerolles et al.,2007). Therefore, an improved understanding of the elementary mechanisms, from the formation of the liposomal carrier to the functional delivery of the oligonucleotide payload *in vivo*, is vital for the design of vehicles optimized for gene therapy applications.

In this chapter, the issues involved in the intracellular delivery of antisense oligonucleotides and small interfering RNAs are first presented and then followed by a short summary of liposomal delivery strategies. The main chapter will take a closer look into lipids and their molecular shape theory with respect to biophysical properties of liposomal membranes. Subsequently, the development of pH-sensitive liposomes will be described and discussed regarding their fusion properties for efficient endosomal escape of encapsulated oligonucleotides.

1.1 Antisense and siRNA molecules

The use of oligonucleotides for suppressing gene expression in both research and the therapeutic field has moved from basic science towards applied molecular biology and molecular medicine (Hannon and Rossi, 2004; Whitehead et al., 2009).

Two major classes of oligonucleotides are the catalytically active antisense oligonucleotides and small interfering RNA, which consist of approximately 20 (deoxy)ribonucleotides or chemically modified analogs thereof. In contrast to most common drugs, they can be applied to suppress gene expression in a specific manner (Stephenson and Zamecnik, 1978; Elbashir et al., 2001).

Antisense oligonucleotides (ASOs) are short single-stranded nucleotide sequences, typically with a length of 15 to 20 deoxyribonucleotides. Once the oligonucleotide crosses the cell membrane, it has the ability to bind with high degree of fidelity to the target messenger RNA sequence through Watson-Crick base pairing and therefore blocks the protein translation process. Basically, there are two antisense mechanisms to inhibit the translation of the targeted mRNA by an oligonucleotide. In the first one, the formation of the antisense-sense duplex is supported by a family of enzymes named ribonuclease H (RNAse H1 and RNAse H2). These proteins are present in all mammalian cells and recognize the DNA-RNA duplex (Cerritelli and Crouch, 2009). The RNAse H degrades the complementary RNA sequence resulting in a 5´-phosphate on the RNA product and the inhibition of target mRNA expression (Donis-Keller, 1979). An alternative antisense mechanism is the use of antisense oligonucleotides, which inhibit the translation process in the cytoplasm by blocking the ribosome (Hudziak et al., 2000). They simply block the interaction of the 40S ribosome subunit to the mRNA by binding to the 5´-cap region and therefore preventing the formation of the translation initiation complex (Bennett and Swayze, 2010).

Small interfering RNA (siRNA) are short (19-21) double-stranded RNA molecules, which are involved in the RNA interference (RNAi) pathway (Fire et al., 1998; Elbashir et al., 2001). Within the cytoplasm, long double-stranded RNA molecules are firstly cleaved by the enzyme Dicer, a member of the RNase III family of ribonucleases, into 21- to 23-nucleotide interfering RNAs comprising 3´- or 5´-overhangs of two to four nucleotides. After cleavage, these siRNA molecules are shuttled into a RNA-induced silencing complex (RISC), a multi-functional components complex which binds double-stranded RNA oligonucleotides (Kim et al., 2007). In the RISC, the enzyme helicase unwinds the strands and the siRNA molecules become separated. The RISC discards one strand and the remaining RISC bounded antisense strand binds to the target messenger RNA sequence resulting to an antisense-sense duplex. The nuclease component of RISC Argonaute 2 (Ago2) finally cleaves the target mRNA through hydrolysis at a specific site, 10 nucleotides from the 5´ end of the antisense-sense duplex, resulting to mRNA degradation by RNAses (Matranga et al., 2005, Kurreck, 2009).

1.1.1 Unassisted cellular uptake of oligonucletides

Entry into the target cell and translocation into the cytoplasm of nucleic acids is of major importance for sequence-specific gene silencing. Nucleic acids are large, negatively charged

molecules and therefore diffusion across the lipophilic cell membrane or cellular internalization by endocytosis is at least unlikely (Chiu et al., 2004; Yakubov et al., 1989).

The ability of free oligonucleotides (ONs) to traverse cell membranes has been observed but still their cellular internalization remains poor (Zhao et al., 1993; Sioud et al., 2005). The internalization of nucleic acids into the cells has been characterized through three mechanisms. The first one includes oligonucleotide cellular uptake via membrane channels, e.g. through anion channels in cultured bovine adrenal cells (Li et al., 1997). Furthermore, receptor-mediated intracellular transport of oligonucleotides has been observed in different cell types (Feinberg and Hunter, 2003). Binding of free antisense oligonucleotides to the cell membrane receptor has been found to be sufficient to trigger endocytosis or pinocytosis (Yakubov et al., 1989; Liang et al., 1996). Alternatively, proteins and ligands may serve the purpose of oligonucleotides delivery. The intracellular uptake of antisense oligonucleotides linked to transferring, folic acid and neoglycoproteins was more effective than the addition of unmodified ASOs (Bonfils et al., 1992; Citro et al. 1992; Citro et al. 1994). Nevertheless, the mechanism of nucleotide internalization in most tissues still remains unclear.

Cellular internalization is, however, only the first barrier to be overcome. Once nucleic acids enter the endosomal/lysosomal pathway, they are facing the next intracellular barrier: the endosomal membrane. Naked oligonucleotides can be directly taken up by cells *in vitro*, but they mainly localize in the endosomes and therefore cannot silence gene expression even at high concentrations (Zhang et al., 2006; Chiu et al., 2004). Oligonucleotides entrapped in the endosomal and lysosomal compartments can either be rapidly degraded by lysosomal enzymes, or may be released from the cell via exocytosis (Loke et al, 1989), whereas the perturbation of the endosomal membrane integrity leads to cytosol- and nuclear-localized nucleic acids. Therefore, unassisted oligonucleotide-mediated gene silencing is ineffective even at high oligonucleotide concentrations (Hu et al., 2002; Zhang et al., 2006).

Nevertheless, a number of reports support pharmacological activity of chemically stabilized, but otherwise unassisted oligonucleotides *in vivo* at high doses. For antisense oligonucleotides, *in vivo* studies by Graham and colleagues regarding the tissue distribution of oligonucleotides have shown that intravenously administered phosphorothioate oligodeoxynucleotide reached cellular and subcellular localisation in rat liver. At 5- and 10-mg/kg dose levels, nuclear and cytosolic oligo localization could be detected only in kupffer and endothelial cells. Nuclear localization in hepatocytes has been achieved only by increasing the input dose to 25 mg/Kg and above (Graham et al., 1998). Pharmacological responses in mice liver, achieved with ASO

dosages of 10-50 mg/kg, match these results. Antisense oligonucleotides mediated knockdown of the liver target Apolipoprotein B-100 (ApoB-100) and reduced LDL cholesterol in hyperlipidemic mice. Reduced diacylglycerol O-acyltransferase 2 (DGAT2) levels in the liver of obese mice have been also demonstrated upon i.v. administration of an antisense oligonucleotide (Crooke et al., 2005; Yu et al., 2005).

Duxpury and colleagues reported efficacy of siRNA in a murine pancreatic adenocarcinoma xenograft model. SiRNA was systemically administered bi-weekly at a dose of 150 µg/kg by tail vein injection in mice. Suppression of primary tumor growth was 68% compared to control siRNA (Duxpury et al., 2004). Although some reports claim entry of siRNA molecules into cells of the target tissue following i.v. injection, the vast majority of reports state that naked siRNA is not active *in viv*o. SiRNA molecules cannot passively penetrate cell membranes because in comparison to ASOs, they carry approximately twice the charge and are about twice as large. Thus, naked siRNA is used by many researchers as a negative control, since it fails to produce silencing effects after i.v. injection. Hydrodynamic injections have enabled experimental work *in vivo* using siRNA. However, this harsh and painful administration procedure lacks any clinical relevance (McCaffrey et al., 2002; Lewis et al., 2002). Important progress for the *in vivo* application of siRNAs was made by Soutschek and co-workers who attached a modified cholesterol molecule at the 3'-end of the sense strand of a siRNA. Following i.v. administration of this hybrid molecule, ApoB-100 levels were reduced in the liver and the jejunum on both, mRNA and protein level. Most convincingly, ApoB-100 mRNA was cleaved within the sequence targeted by the siRNA. Although these are impressive results, it has to be mentioned that the dosage at 50 mg/kg was relatively high (Soutschek et al., 2004).

The cellular barriers for the delivery of functional siRNA molecules are much higher than expected and not compensated by their higher potency compared to free antisense oligonucleotides, which are therapeutically active at sufficient high doses (Campbell et al, 1990). Therefore, assisted delivery of siRNA molecules at this point is required both for *in vitro* and *in vivo* application and is expected to improve their potential for research and therapeutic application.

1.2 Overcoming extra- and intracellular barriers

One main approach to overcome the issues associated with the functional delivery of nucleic acids is the chemical modification. In comparison to naked ONs, chemically modified

oligonucleotides demonstrate enhanced potency, increased tissue residence times and improved ability to resist nuclease-mediated degradation (Phillips and Zhang, 2000; Zhang et al. 2006). However, assisted delivery of naked and modified oligonucleotides still is an essential condition for solving challenges concerning the transport of oligonucleotides into cells and release from the endosome by permeating the endosomal membrane.

In order to circumvent these obstacles, it has been suggested to enhance the cellular uptake of nucleic acids by using delivery systems (Bennett et al. 1992). Synthetic non-viral vector systems have been developed over the last years. Commonly used non-viral vectors for delivery of nucleic acid-based therapeutics can be divided into 2 major classes: liposomal and polymeric delivery systems (for a review on the development of delivery systems see Reinsch et al., 2008). Most non-viral vectors have a cationic surface charge that promotes complex formation with nucleic acids. They enhance cellular accumulation of the nucleic acids, disrupt endosomes and release the nucleic acids into the cytoplasm. Several studies have demonstrated a localization of the delivery system on the cell surface and in the cytoplasm of cells *in vitro*. After cellular uptake the nucleic acids dissociate from the delivery systems followed by an accumulation in the cytoplasm and the nucleus, as well as specific down-regulation of the target mRNA (Zelphati and Szoka, 1996; Marcussson et al.,1998). It has become apparent that many fundamental issues on the mechanism of nucleic acid delivery can be conveniently and properly investigated *in vitro,* including intracellular processing and intracellular oligonucleotide stability. However, it has become equally clear that a direct extrapolation from *in vitro* to *in vivo* should only be done with extreme caution, since parameters such as biodistribution and bioavailability of the carrier can only be examined in an experimental model *in vivo*.

1.2.1 Liposomal carriers for nucleic acid delivery

In general, liposomal carriers for oligonucleotides delivery are cationic, neutral/anionic or amphoteric particles. Cationic liposomal carriers have a positive surface charge, which facilitates rapid complex formation with negatively charged oligonucleotides. In addition, complexes with a cationic net-charge are readily adsorbed onto the negatively charged cell membrane, leading to a high local oligonucleotide concentration at the cell surface, which supports internalization.

Neopharm has developed LErafAON-ETU, a commercially available cationic liposomal ASO formulation, which has shown inhibition of tumor growth in mouse models of human breast, ovarian and prostate cancer. NeoPhectin-AT, another cationic liposomal formulation, has been reported to facilitate the delivery of siRNA against c-raf (Kasireddy et al., 2005; Chien et al., 2005). Cellular attraction provides encouraging results, but unfortunately such rapid and unspecific binding of cationic lipids onto cell membranes is known to result in high toxicity levels. In addition, aggregate formation with serum components and relatively short circulation lifetimes represent major challenges of these carrier systems for systemic applications (Plank et al., 1996; Zelphati et al., 1998).

A common strategy to overcome such limitations is the PEGylation of the carrier. PEGylated liposomes (AtuFECT01) were designed by the group of Santel and functional delivery of a siRNA has been demonstrated by repeated applications of the formulation. However, due to the polycationic lipid used and the poor PEGylation, these cationic complexes (Figure 1.1, panel A) exhibit no organ specificity and adhere easily at endothelia, which limits their ability to penetrate into the organs (Santel et al., 2006a). Moreover, PEGylation of cationic/oligonucleotides complexes with such relatively non-exchangeable polyethylene

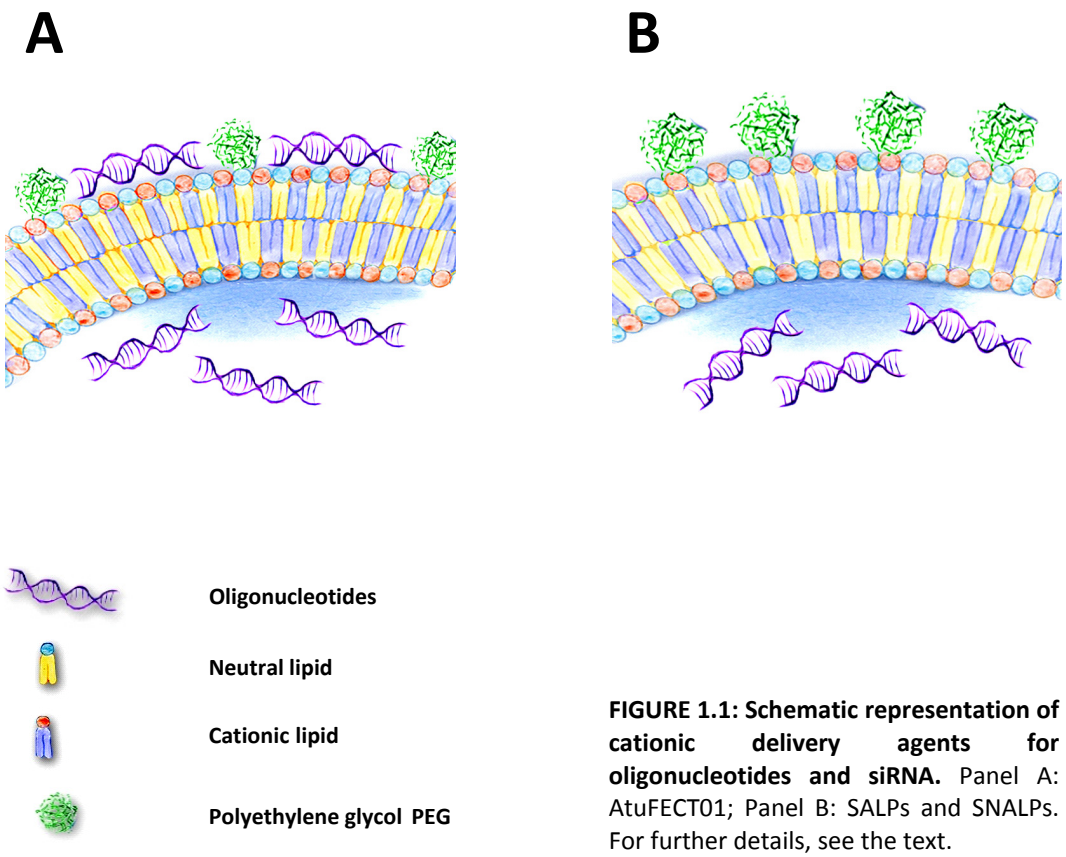

FIGURE 1.1: Schematic representation of cationic delivery agents for oligonucleotides and siRNA. Panel A: AtuFECT01; Panel B: SALPs and SNALPs. For further details, see the text.

glycol (PEG) conjugated-lipids can hinder the intracellular delivery of oligonucleotides by inhibiting their dissociation from the lipoplexes (Shi et al., 2002; Santel et al., 2006b). Another interesting strategy is the use of a transient, diffusible PEG-shielding, which has also aid to combine beneficial biodistribution properties with efficient cellular uptake (Zhang et al., 1999). Tekmiras SNALPs (Figure 1.1, panel B) are such liposomes and their use for efficient delivery of siRNA has been demonstrated in mice and cynomolgous monkeys (Morrissey et al., 2005; Zimmermann et al., 2006).

Compared to the cationic delivery systems, anionic and neutral liposomal systems show low toxicity and exhibit relatively longer circulation lifetimes. Despite the encouraging results from experimental *in vitro* and *in vivo* models using such carriers, relatively high concentrations of oligonucleotides were needed to obtain a pharmacological effect. Efficient oligonucleotide encapsulation and cellular uptake represent major obstacles for these delivery vectors, since they lack the electrostatic interaction between cargo and carrier, (Lubrich et al., 2000; Landen et al., 2005; Halder et. al., 2006; Klimuk et al., 2000).

Andreakos and co-workers have described the use of amphoteric liposomes as delivery system for antisense oligonucleotides. It has been demonstrated that a charge-reversible liposomal mixture designated as Nov038 is safe, well-tolerated in the circulation, devoid of nonspecific immunostimulatory effects, and effective for systemic oligonucleotide delivery *in vivo*. Nov038 enabled the systemic and targeted delivery of CD40-specific ASO to myeloid dendritic cells and macrophages and achieved potent gene knockdown effects *in vivo* (Andreakos et al., 2009). Their amphoteric character conceptually avoids the need for PEGylation. In addition, they efficiently encapsulate their cargo, which could explain the absence of immunogenicity of these carriers and their compatibility with unmodified oligonucleotides.

In systematic review of the recent literature, it becomes obvious that significant progress has been made in the construction of liposomal delivery systems that enable and improve *in vivo* efficacy of oligonucleotides. In the next sections, the lipids behind this carrier and their basic principles and properties will be introduced for a better understanding of the design of such vectors, which enable cytosolic delivery or nuclear uptake of oligonucleotides without affecting the cellular integrity.

1.3 Lipid structures - charged and neutral lipids

The general term "lipid" is used to denominate a chemically diverse group of substances, which comprise mainly carbon, hydrogen, oxygen and in several cases nitrogen and phosphorous. They are amphiphilic molecules meaning that they consist of both a hydrophilic and a hydrophobic region. The headgroup is attached via a linker to a usually single/double hydrocarbon chain or to cholesterol. A fatty acid side chain can be fully saturated by containing only carbon-carbon single bonds, whereas unsaturated chains contain at least one carbon-carbon double bond. With the exception of the lipid cholesterol, all lipids have ionic charges in their hydrophilic headgroups. For example, phospholipids have both a negatively charged phosphate and a positively charged ammonium moiety in their headgroup and can thus be termed as zwitterions (Ahn and Yun, 1999). Furthermore, only lipids bearing a net electric charge are considered as "charged". In Figure 1.2, a cholesterol- and a diacyl-based lipid are illustrated.

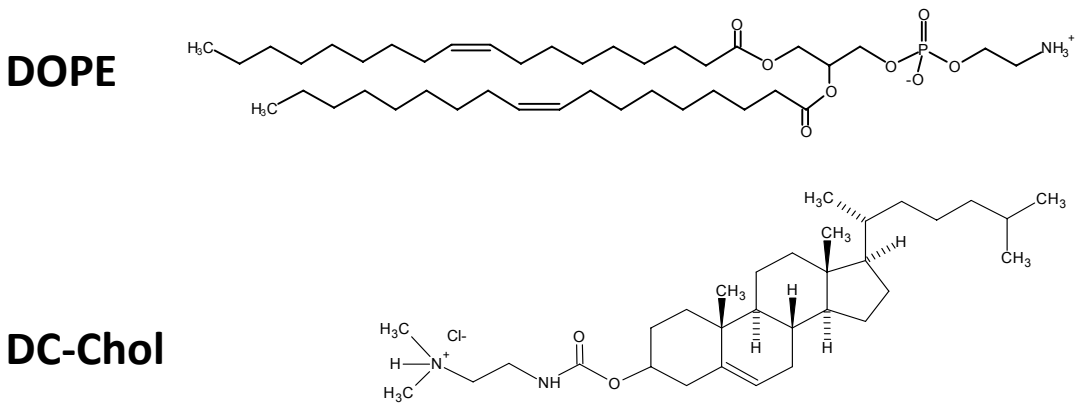

FIGURE 1.2: Chemical structures of typical amphiphiles used in liposome formation. DOPE contains a phosphatidylethanolamine polar head group, glycerol linker and two unsaturated oleoyl chains as hydrocarbon tail. DC-Chol is typified by a charged head group attached to cholesterol as hydrophobic tail. DOPE: 1,2-Dioleoyl-sn-glycero-phosphatidylethanolamine; DC-Chol: 3a-[N-(N,N"-dimethylaminoethane)-carbamoyl] cholesterol hydrochloride.

1.3.1 Neutral "helper" lipids

The neutral lipids are typically zwitterionic such as 1,2-dioleoyl-sn-glycero-phosphatidylcholine (DOPC) and 1,2-dioleoyl-sn-glycero-phosphatidylethanolamine (DOPE) or the neutral lipid cholesterol. In most cases, liposomal vectors include "helper" lipids in order to improve their transfection levels or to improve particles stability. In contrast to phosphatidylcholine (PC)

lipids, which form and stabilize bilayer formation, lipids that form non-bilayer phases promote destabilization of lipid bilayers and fusion with cellular membranes (Hui et al., 1981).

Cholesterol has a short a hydrocarbon moiety attached to a larger, hydrophobic fused ring structure with a small, hydrophilic hydroxyl group. In contrast, lipid molecules, such as DOPC or DOPE, have a larger hydrophilic headgroup and longer, more flexible, hydrocarbon tails. The zwitterionic lipid DOPE lipid has no net charge at physiological pH, and is a common component of a numerous liposome formulations (Ellens et al., 1984). DOPE is a fusion-promoting lipid and preferably adopts non-lamellar phase at room temperature (Cullis and de Kruijff, 1978). Lamellar phases of DOPE can be observed at low temperatures or high pH (Ellens set al., 1989; Siegel and Epand, 1997). Several *in vitro* studies have demonstrated enhanced transfection efficiencies when cholesterol or DOPE or mixture thereof is incorporated in the liposomal membrane (Felgner et al., 1987; Bennet et al., 1995). This has been attributed to their fusogenic character, which promotes destabilization of the endosomal membrane and release of the nucleic acids into the cytosol, resulting to improved transfection efficacy (Zhou and Huang, 1994; Farhood et al., 1995). Furthermore, cholesterol can stabilize DOPE containing liposomes in the presence of serum without any effect on their fusogenic activity (Liu et al., 1989).

Many studies have also focused on different forms of PC lipids as helper lipids in liposomal vectors for gene transfer. PC lipids such as 1,2-dimyristoyl-sn-3-phosphatidylcholine (DMPC) or 1,2-dipalmitoyl-sn-3-phosphatidylcholine (DPPC) have both fully saturated (carbon-carbon single bonds) hydrocarbon chains, whereas PC lipids like 1,2-dioleoyl-sn-3-phosphatidylcholine (DOPC) or 1-palmitoyl-2-oleoyl-sn-glycero-phosphatidylcholine (POPC) have only one saturated and one monounsaturated chain (Rappolt et al., 2003). Replacement of the fusogenic lipid DOPE or cholesterol with the bilayer lipid DOPC either completely inhibits or severely attenuates cytosolic delivery of nucleic acids (Farhood et al., 1995; Hui et al., 1996). Similar results could also be demonstrated using the lipid 1,2-distearoyl-sn-glycero-3-phosphocholine (DSPC) (Huang and Cullis 2000).

1.3.2 Cationic and anionic lipids

A cationic or anionic lipid is a positively or negatively charged amphiphile molecule. The charge is usually caused by the protonation or deprotonation of the headgroup regions. Besides

separating such lipids by the types of their electrical charge, they can also be classified into permanently charged and pH-sensitive at neutral and acidic conditions.

A number of *in vivo* studies have demonstrated successful cationic lipid-mediated gene transfer into cells, thereby establishing the importance of cationic lipids in the lipid-nucleic acid formulation (Zimmermann et al., 2006; Morrissey et al., 2005). Cationic lipids could lend the particle a net positive charge; therefore it can spontaneously interact during the formulation process with the negatively charged nucleic acids to form a complex. This results in high payloads concentration compared to liposomes containing only anionic or/and neutral lipids (Jeffs et al., 2005). Additionally, positively charged particles can interact with cell membrane surface anionic components, resulting in subsequent cellular uptake (Mislick and Baldschwieler, 1996; Mounkes et al., 1998).

A permanently positive charged lipid is the 1,2-dioleoyloxy-3-trimethylammonium-propane (DOTAP), which consists of two unsaturated diacyl side chains, ester linker and propyl ammonium headgroup (Leventis and Silvius, 1990). Other lipids may contain different linkers, such as the more stable ether linkages, for instance N-[1-(2,3-dioleyloxy)propyl]-N,N,N-trimethylammonium chloride (DOTMA). DOTMA consists of a quaternary ammonium connected to two unsaturated aliphatic hydrocarbon chains via ether groups (Felgner et al., 1987) and is a commercially available transfection lipid (Lipofectin®, Invitrogen Life Science). Another commercially marketed cationic lipid is the LipofectAMINE® reagent 2,3-dioleoyloxy-N-[2(sperminecarboxamido)ethyl]-N,N',-dimethyl-1-propanaminium-trifluoroacetate (DOSPA) (Hawley-Nelson et al., 1993).

Additional examples of permanently charged cationic lipids are the 1,2-dimyristyloxypropyl-3-dimethyl-hydroxyethylammonium bromide (DMRIE), which is a quaternary ammonium salt (Felgner et al., 1994), the bilayer forming lipid N,N-dimethyl-N,N-di-9-cis-octadecenylammonium chloride (DODAC) (Mok and Cullis, 1997) and pyridinium amphiphiles analogues (SAINT), which efficiently transfect eukaryotic cells (Lee et al., 1996; Meekel et al., 2000; Zuhorn and Hoekstra, 2002).

Moreover, Budker and co-workers have evaluated the cell transfection ability of cationic pH-sensitive lipids with an imidazole headgroup for several cell types. This set of *in vitro* results obtained with 4-(2,3-bis-palmitoyloxy-propyl)-1-methyl-1H-imidazole (DPIM) and 4-(2,3-bis-oleoyloxy-propyl)-1-methyl-1H-imidazole (DOIM) suggest that the transfection efficiency is a result of membrane fusion within the endosome. When the cells were treated with endosomal-inhibitory agents, the transfection efficiency of these lipids strongly decreased in

comparison to the transfection activity of liposomes comprising the permanently charged cationic DOTMA, which was slightly decreased. Similar results could also be demonstrated with the ionizable cholesterol derivate lipid CHIM (cholesterol-(3-imidazol-1-yl propyl)-carbamate) (Budker et al., 1996). Other examples for ionisable cholesterol based cationic amphiphile are the α-(3'O-cholesteryloxycarbonyl)-δ-(N-ethylmorpholine)-succinamide (MoChol) and 3a-[N-(N,N"-dimethylaminoethane)-carbamoyl] cholesterol hydrochloride) (DC-Chol) (Andreakos et al., 2009; Gao and Hui, 1991).

Cholesteryl hemisuccinate (CHEMS) and oleic acid (OA) are the most frequently used pH-sensitive anionic lipids. It was found that when these ionisable lipids are incorporated in the liposomal membrane, together with the helper lipid DOPE, the stability of the liposome becomes pH-dependent (Hope et al., 1983). Such vesicles are stable in neutral environment, but undergo fusion at acidic conditions. Similar results could also be retrieved with unsaturated phosphatidylserine lipids, such as the permanently acidic lipid 1,2-dioleoyl-sn-3-phosphatidylserine (DOPS) (Tilcock and Cullis, 1981; Slepushkin et al., 1997). 1,2-Dioleoyl-sn-glycero-3-phosphate acid (DOPA) has an ionisable phosphate group with at least one negative charge at pH values above ~3.0 (Fattal et al., 2004; Hafez et al., 2001). This lipid generally

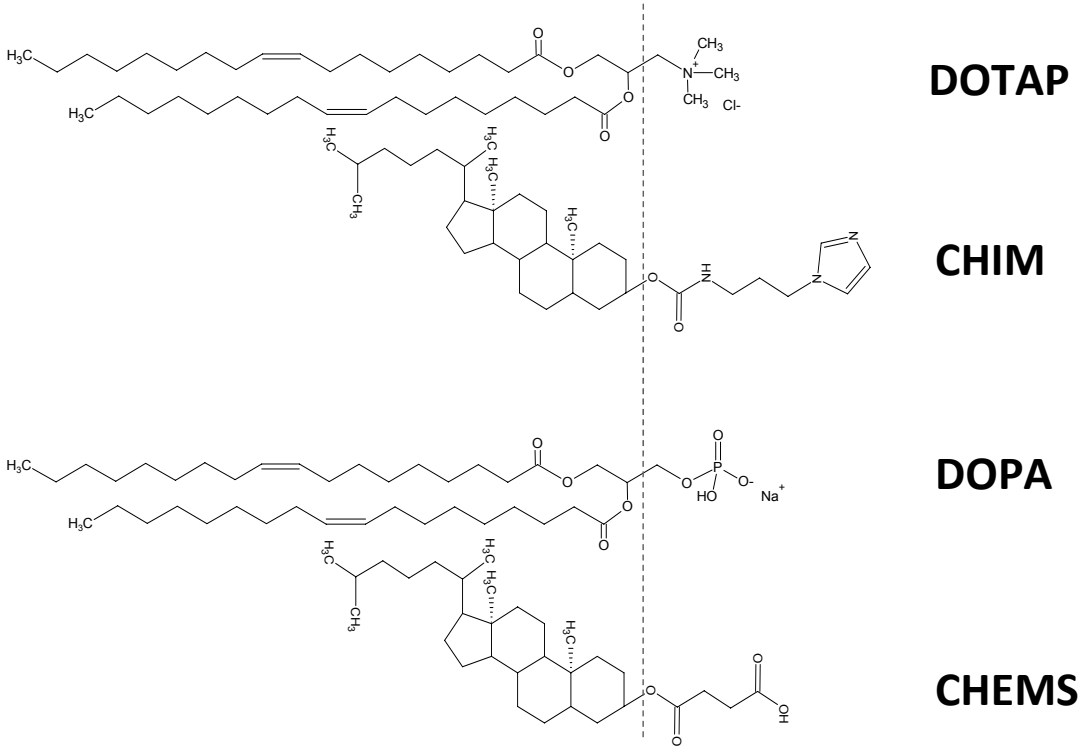

FIGURE 1.3: Schematic representation of positively and negatively charged lipids. The ester linked variant DOTAP consists of a quartenary ammonium charged headgroup. The ionisable lipid CHIM has an imidazole head group attached to cholesterol. DOPA and CHEMS are typified by a phosphatidic acid and a carboxylic head group, respectively.

produces micellar structures. When incorporated in DNA lipoplexes, it tends to destroy the initial lamellar structure of the lipoplexes in contrast to the also permanently anionic charged lipid 1,2-dioleoyl-sn-3-phosphatidylcholine (DOPG) (Tarahovsky et al., 2004).

1.4 Lipid properties - An overview

Lipids can adopt various structural phases, such as the lamellar (L_α) phase and the hexagonal inverted (H_{II}) phase (Figure 1.3), when dispersed in aqueous media. The fundamental driving force for membrane formation is the hydrophobic interactions ("Hydrophobic Effect") among lipid molecules (Lindblom and Rilfors, 1992; Kooijman et al., 2005).

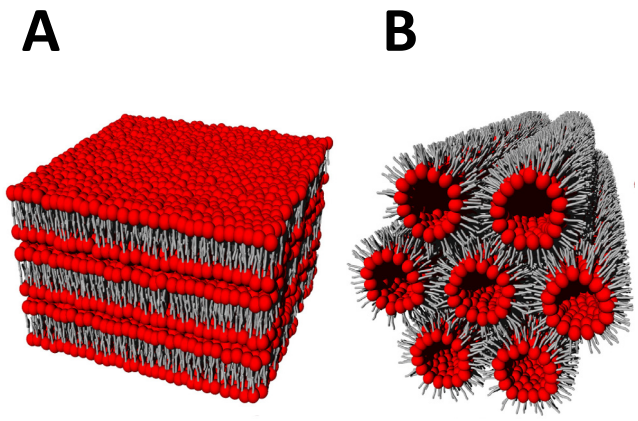

FIGURE 1.4: Schematic illustration of lamellar L_α (A) and inverted hexagonal H_{II} phase (B), (Tresser, 2009)**.**

Lipid geometry properties and molecular shape formation have been used to explain the lipid phase behaviour (Gruner et al., 1985; Cullis et al. 1986). Lipid bilayers comprise a hydrophobic core and a hydrophilic headgroup region. Both are further fine-tuned by various intermolecular forces, such as electrostatic interactions, bound and free counterions, hydrogen bonding, as well as bilayer associated interactions. Presence of divalent cations and temperature can also modulate the molecular shape and consequently the lipid phase behaviour (Ellens et al., 1985; Cullis and de Kruijff, 1979; de Kruijff and Cullis, 1980).

1.4.1 Lipid shape theory and lipid geometry

Groundbreaking theoretical understanding of the formation of lipid bilayers was provided by Israelachvili and co-workers, who described how the molecular lipid geometry influences the vesicle size and form (Israelachvili et al., 1980). Surface area, hydrocarbon chain volume and length of the hydrophobic part of a lipid are factors that determine whether spherical micelles,

non-spherical micelles or bilayers are formed. This molecular shape relationship is generally described by the "critical packing parameter" **CPP** defined as $v/(\alpha_0 \cdot l_c)$, where v is the effective volume of the hydrocarbon chains, α_0 is the optimal surface area occupied by the headgroup and l_c is the maximum or "critical" length of the hydrocarbon chains. The phase structures of different effective molecular shapes of lipids as a function of their "critical packing parameter" are illustrated in Figure 1.4.

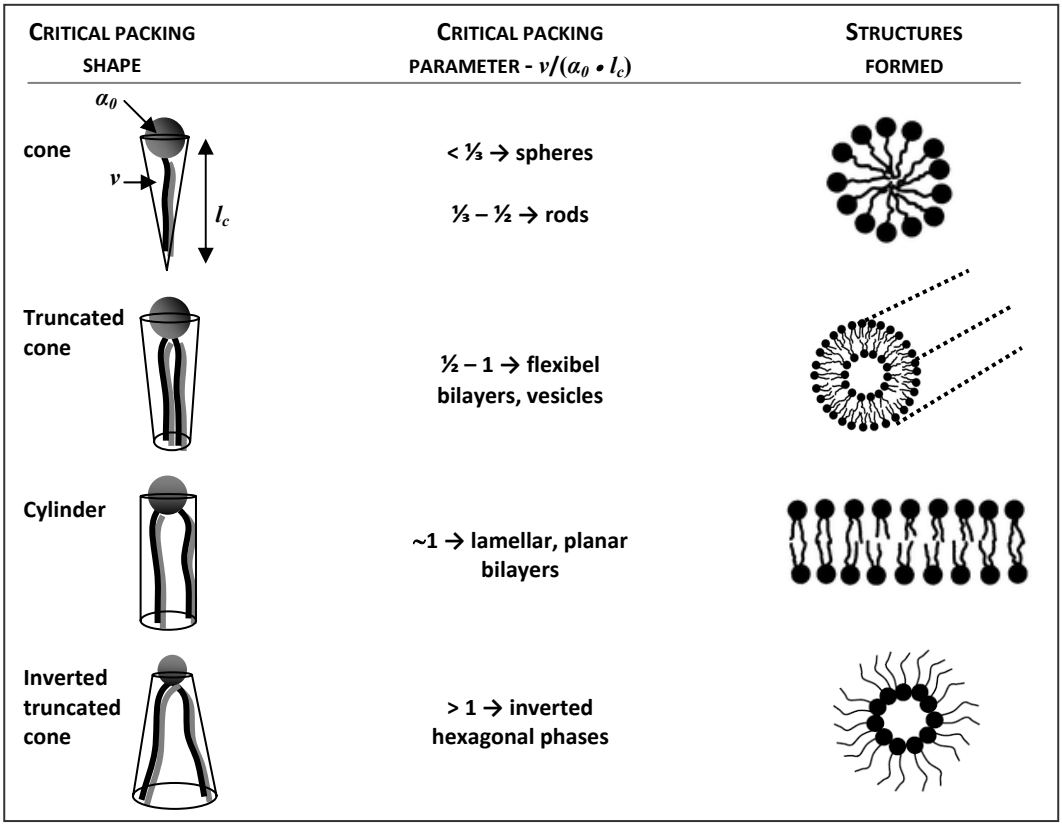

FIGURE 1.5: Schematic illustration of molecular lipid geometry and the related phase structures. The "critical packing parameter" defines the lipid geometry and determines the formation of lipid assemblies in aqueous solutions (Israelachvili et al., 1980).

Lipids, which are conical in shape, exhibit positive membrane curvature. They have a sufficiently large headgroup area and a small hydrocarbon region, i.e. $v/(\alpha_0 \cdot l_c) < ⅓$. These lipids have charged headgroups, since this leads to a large head group area and self assemble spherical micelles. Non-spherical and rod like micelles are formed from those lipids, which posses smaller headgroup cross-sectional areas, resulting to a truncated conical geometry such that $⅓ < v/(\alpha_0 \cdot l_c) < ½$ (Israelachvili et al., 1980).

Alternatively, the most important biologically mode of lipid forming structures is a lipid bilayer, which requires a cylindrical molecular shape. These lipids have nearly equal headgroup area α_0

to hydrocarbon chain region l_c. Therefore, for bilayer forming lipids, the value of the "critical packing parameter" $v/(\alpha_0 \cdot l_c)$ must be between **½** and **1**. These lipids cannot pack into micellar structures either due to their small headgroup region or their hydrocarbon chain area is too bulky to fit into such small structures. In the case of bilayer forming lipids, the hydrocarbon volume has to be twice that of micelle forming lipids and therefore, these lipids have two hydrocarbon chains. Lipids with a $v/(\alpha_0 \cdot l_c) > 1$ normally can not form bilayer structures due to their small headgroup area (Israelachvili et al., 1980). These lipids, such as cholesterol and DOPE, adopt ''inverted'' lipid phases due to their small headgroup surfaces. Such 'inverted'' lipid phases include the inverted hexagonal phase or cubic phases with negative spontaneous curvature.

1.4.2 The role of counterions in lipid membranes

Lipid geometry, molecular shape, net charge and distribution of partial charges are all important factors in determining bilayer properties and are strongly dependent on the ion concentration and environmental pH. In comparison to PG, PC and PS lipids, which have nearly equal headgroups, PA lipids have a very small headgroup. Under acidic conditions and in the presence of divalent cations, PA lipids have a negative spontaneous curvature. Interestingly, Kooijman and co workers suggest that pure DOPA forms billayers at neutral pH (pH 7.2) and physiological salt (150 Mm NaCl), while DOPA in mixtures with DOPE adopts H_{II} hexagonale phase under such physiological conditions. In such mixtures, DOPA will adopt a lamellar phase when the mixture is not in contact with salt, because of strong headgroup repulsions (Kooijman et al., 2003; Kooijman et al., 2005). In a simulation study using 1-palmitoyl-2-oleoyl-sn-glycero-phosphatidylglycerol (POPG), it was found that counterions strongly adsorb to the bilayer interface in the water-membrane interface, which results in reduced water dynamics (Zhao et al.; 2007). Therefore, it is able to form intramolecular and intermolecular hydrogen bonds, resulting to a small fluidity (Dickey and Faller, 2008).

In addition to the importance of the structure of the lipid itself, the lipid counterions also play an important role in determining the lipid activity. Most lipid headgroups are hydrated with water and may require counterions, which can influence the lipid biological activity. It was demonstrated in both biological and model experiments that the interaction of lipids with cellular membranes depends on the type of the salt these compounds constitute (Lai et al., 1985). Counterions are part of a group of factors, which decide the efficiency of the interaction

of an amphiphilic compound with cellular membranes (Sarapuk et al., 1997; Sarapuk et al., 1998). If the function of a transmembrane protein is to transfer positively charged ions across a membrane, negatively charged lipids solvating that protein will increase the concentration of positively charged ions near the protein opening (Lee, 2004). Aberle and colleagues suggest that ions with highly delocalized anionic charge enhance transfection of DNA plasmid using DOTAP analogs into NIH3T3 cells. The order of *in vitro* transfection efficiency is decreased as follows bisulfate > trifluormethylsulfonate ~ iodide ~ bromide > dihydrogenphosphate ~ chloride > acetate > and sulphate. Subsequently, a similar correlation of lipid hydration with transfection activity has also been demonstrated *in vivo* (Aberle et al., 1996; Benette et al., 1997).

1.5 Membrane fusion through hexagonal phase

The process of the fusion of two bilayer membranes to form a single one is of great importance for many processes in biological systems. Fusion of biological membranes is required for processes such as phagocytosis, exocytosis, cell division or viral infection (Lindau and Almers, 1995; Lentz et al., 2000). The primary route of internalisation of liposomes by cells is the endocytic pathway. The main barrier in liposome drug delivery is the escape of the sensitive material from the endosomes and lysosomes (Straubinger et al., 1983; Daleke et al., 1990, Chiu et al., 2004).

The most widely used description of membrane fusion divides the process into three steps. It has been argued that the initial connection between the two membranes is formed either through a formation of a pore or via a semitoroidal structure, named "stalk" (Markin et al., 1984; Siegel, 1999). In the fusion process, the first step is to promote aggregation in order to bring the outer bilayer of the liposomal membrane and the inner layer of the endosome into close contact. This initial state is called the hemifusion (Siegel and Epand, 1997). The expansion of the hemifused zone is the second step on the mechanism of membrane fusion by which the two opposing bilayers must be able to merge (Kozlovsky et al., 2002). In fact, a local departure from the lamellar (L_α) phase to the destabilizing hexagonal inverted (H_{II}) phase must take place in order to allow two lipid membranes to merge into a single bilayer membrane (Koltover et al., 1998). Finally, subsequent formation and expansion of a stable fusion pore complete the fusion reaction.

1.6 pH-sensitive liposomes

Lipids adopting the inverted hexagonal phase, such as DOPE or protonated PS lipids, promote fusion of liposomal membranes (Hope et al., 1993). In order to obtain membrane fusion in the endosome at acidic environments, one has to promote various pH-dependent physico chemical changes within the liposomes that generate inverted cone shaped molecules. The liposome has to be stable at neutral conditions and fusogenic at acidic conditions. These liposomes represent a class of liposomes being different from straight anionic or cationic liposomes. The first lipid combinations used were mainly the same type, meaning a combination of helper lipids with titratable fusogenic acidic amphiphiles, such as cholesteryl hemisuccinate or oleic acid (Ellens et al., 1984; Duzgunes et al., 1985).

1.6.1 Mixtures of charged lipids present pH-dependent properties

Hafez and colleagues first described the pH-dependent fusion of liposomal mixtures constructed by the ionizable anionic lipid CHEMS and the permanently charged cationic lipid DODAC by using a lipid mixing assay based on fluorescence resonance energy transfer. They have shown that such liposomal mixtures adopt a lamellar phase and form liposomes at neutral condition, but undergo fusion upon acidifications. In addition, the authors grappled with the limited control over the pH at which such fusion occurs and demonstrated a rational approach to fine-tune the fusion point by varying the proportions of cationic and anionic lipids. They found a correlation between the isoelectric point - the pH at which the surface charge is neutral - and the membrane fusion by plotting a function of the pH of half maximum fusion and the molar ratio of DODAC/CHEMS (Hafez et al., 2000).

Li and Schick applied a comparable approach to the well known pH-sensitive system CHEMS/DOPE using a mathematical model (Li and Schick, 2000 a,b,c). In addition, they analysed the fusion tendency for the amphoteric lipid mixtures DODAC/CHEMS. Their model predicts phase transition at a value of pH that depends on the concentration of the ionisable anionic (Li and Schick, 2001). They assumed that the stabilization mechanism of pH-sensitive liposomes is the attraction of counterions and their associated waters of hydration to the vicinity of the headgroups, which effectively increases their size. As the pH is reduced, the fraction of anionic amphiphiles that are ionized decreases and therefore, there are fewer counterions near the headgroups to stabilize them (Li and Schick, 2001). Hence, the reduction

in pH eventually triggers instability of the vesicle. Therefore the lipids revert to their more stable phase, which usually is the inverted hexagonal phase (H_{II}).

1.6.2 Biphasic stability of amphoteric liposomes

While known pH-sensitive systems have been restricted to one-way loss or gain of charge, the charge of amphoteric liposomes reversibly varies between negative and positive in response to changes in pH, providing a lamellar phase at both neutral and acidic pH and a fusogenic state at intermediate, slightly acidic pH. Amphoteric liposomes present an anionic state at neutral conditions, thus avoiding serum aggregation. On the other hand, at low pH, they adopt a cationic state, which enables efficient loading of nucleic acids (Panzner et al., 2008-WO 02/066012).

Andreakos and co-workers have described morpholine cholesterol (MoChol) as a novel parent compound of amphoteric liposomes. The pK_α of the MoChol compound was experimentally determined in liposomes in which a pK_α of 6.5 was observed. The combination of equal amounts of MoChol and CHEMS, which has a pK_α of ~5.8 (Hafez and Cullis, 2000), provided amphoteric character with an isoelectric point of ~6.3 (Andreakos et al., 2009). However for amphoteric mixtures of MoChol and CHEMS, the theory of Li and Schick, which assumes a pH-dependent association and dissociation of counterions to the charged lipids in a lipid membrane (Li and Schick, 2001), is insufficient to explain the biphasic stability of such assemblies. Due to the fact that only the pH-sensitive CHEMS would mediate fluctuations of counterions at pH 4, but not the positively charged MoChol. As a result, an admixture of MoChol would only dilute, but not alter the single-sided phase transition observed for CHEMS at low pH.

Panzner and co-workers in an extended algorithm consider an additional interlipid salt formation between the charged lipids within one monolayer (Panzner et al., 2008-WO 08/043575). For mixtures comprising monovalent ions with at least one lipid being pH-sensitive, three different systems exist: (i) Amphoter I, which comprises a stable cation and a chargeable anion (e.g. DOTAP/CHEMS or DOTAP/OA), (ii) Amphoter II, in which both lipids are chargeable (MoChol/CHEMS or CHIM/CHEMS) and (iii) Amphoter III composed of a chargeable cation and stable anion (e.g. MoChol/DOPA or CHIM/DOPA). Figure 1.5 illustrates the new extended theory as proposed by Panzner using as an example a MoChol/CHEMS mixture.

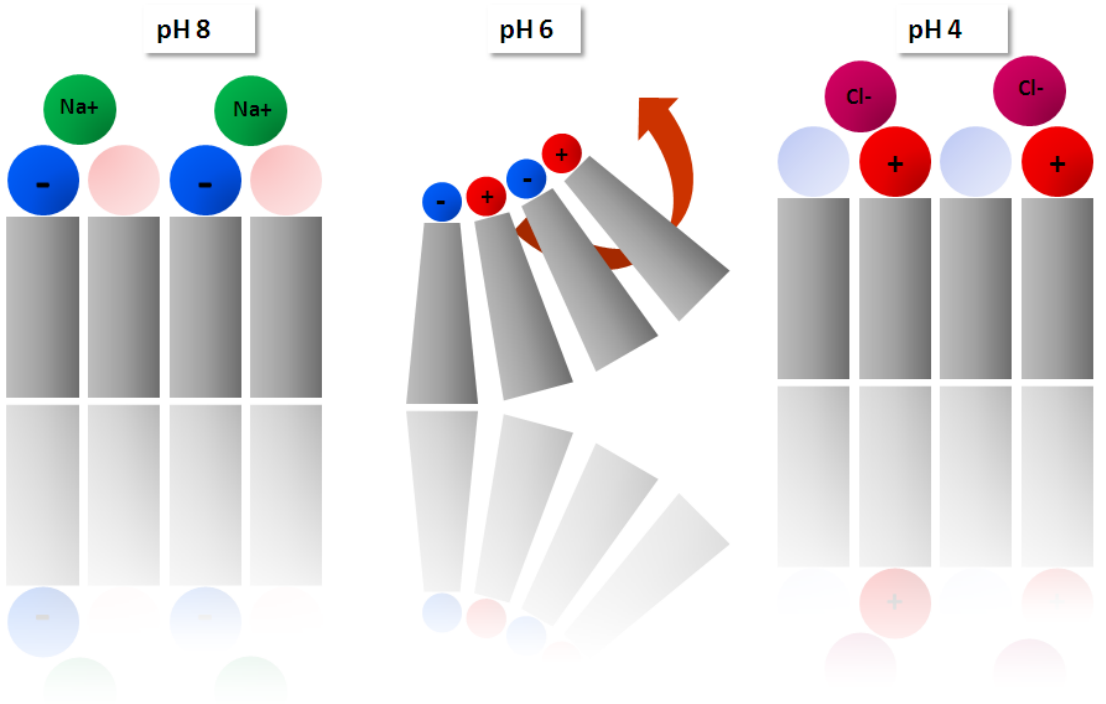

FIGURE 1.6: Schematic illustration of an amphoteric membrane at different pH values. At high pH, MoChol is protonated and becomes electrically neutral, whereas the charged CHEMS recruits its countercation from the solvent. A first drop of the pH at 6 produces the MoChol cation, which functions now as counterion to CHEMS thereby displacing the solvent counterion. Eventually, the full dissociation of MoChol creates an excess of this charged lipid over CHEMS and the free MoChol cation now recruits its counteranion from the solvent.

The algorithm is based on the parameter κ describing the phase behaviour of lipid bilayers. The parameter κ is the volume ratio between head group size (V_{head}) and tail group size (V_{apolar}). Therefore κ is given by $\kappa = V_{head} / V_{apolar}$. In the lipid salt the cationic amphiphile *(cat)* serves as a counterion to the anionic amphiphile *(an)* and vice versa, thus displacing the counterions from the headgroup. The lipid salt is net uncharged and its geometry is assumed to be the sum of both parts without the counterions. Salt formation is limited by the charged amphiphile that is present in the lowest concentration and κ_{salt} is being defined as $\kappa_{salt} = (V_{head}^{(cat)} + V_{head}^{(an)})/(V_{apolar}^{(cat)} + V_{apolar}^{(an)})$. The κ_{pH} of a specific mixture of charged lipid species can therefore be expressed as $\kappa_{pH} = (\kappa_{an^0} \cdot c_{an^0}) + (\kappa_{cat^0} \cdot c_{cat^0}) + (\kappa_{an^-} \cdot c_{an^-}) + (\kappa_{cat^+} \cdot c_{cat^+}) + (\kappa_{salt} \cdot c_{salt}) + \sum(\kappa_n \cdot c_n)$. Where: c is the concentration of the appropriate species and depends on the pK_α of the lipid and the pH of the medium; an^0 and cat^0 are the uncharged cationic and anionic species; an^- and cat^+ are the charged cationic and anionic species; n is the neutral lipid in the mixture.

Neutral lipids, such as PC, PE, sphingolipids or cholesterol, do not have pH-responsive elements that would react between pH 3 and 8 and no changes in the molecular geometry

occur in this range. Depending on the individual κ values of the neutral lipids, dilution of the bistable behaviour of the amphoteric lipid pair occurs and the steepness of **d(κ)/d(pH)** becomes smaller. In addition, the transition behaviour of the amphoteric membrane is shifted towards lower or higher values of κ, depending on the neutral lipid used for dilution of the charged lipids (Panzner et al., 2008-WO 08/043575).

1.7 Scope of this thesis

Oligonucleotides are sensitive, large and very polar molecules that are not taken up by cells in appreciable amounts. In recent years, lipid-mediated-gene transfer has become a versatile tool for cellular transfection, relevant to fundamental cell biological research and gene therapy alike. Cellular uptake of liposomes generally follows an endocytic pathway and through perturbation of the endosomal membrane, under acidic conditions, is expected to result in cytosolic translocation of the nucleic acid payload.

The present thesis is divided in two major parts: Part I addresses the biophysical parameters and the molecular mechanism that govern the fusion behaviour of amphoteric liposomes. In Part II, the findings from siRNA transfection and biophysical studies are correlated in an attempt to enhance the understanding of the structure-function relationship of amphoteric liposomes. The following specific objectives were investigated: (i) impact of counterion in lipid shape transition, (ii) fusion of amphoteric liposomes and their biphasic stability, (iii) impact of neutral and zwitterionics lipids in amphoteric membrane properties, (iv) *in vitro* siRNA transfection mediated by amphoteric liposomes and (v) the role of lipid shape parameter κ in the development of cellular transfectants.

The major scope of this study is to provide essential biophysical and biological information through experimental evidence, verifying the lipid shape theory and providing guidelines for an optimal design of an amphoteric mixture for efficient intracellular delivery of nucleic acids.

2. MATERIALS & METHODS

2.1 Chemicals and Reagents

2.1.1 Lipids

Lipids were purchased from following manufacturers:

Cholesterol (Chol) (Merck KGaA, Darmstadt, Germany); 1-Palmitoyl-2-oleoyl-sn-glycero-phosphatidylcholine (POPC), 1,2-Dioleoyl-sn-glycero-phosphatidylethanolamine (DOPE) (Lipoid, Ludwighafen, Germany); Cholesteryl hemissucinic acid (CHEMS), Sphingomyelin (SM); 3ß-[N-(N',N'-dimethylaminoethane)-carbamoyl]cholesterol hydrochloride (DC-Chol) and 3ß-[N-(N',N,N'-trimethylaminoethane)-carbamoyl]cholesterol hydrochloride (TC-Chol) (Sigma Aldrich, St. Louis, MO); N-[1-(2,3-Dioleoyloxy)propyl]-N,N,N trimethylammonium chloride (DOTAP) and 1,2-Dimyristoyl-sn-glycero-3-succinate (DMGS) (Merck Eprova AG Schaffhausen, Switzerland); 1,2-Di(cis-9-octadecenoyl)-sn-glycero-3-phosphate, sodium salt (DOPA), Dimethyldioctadecyl-ammonium bromide (DDAB), 1,2-Dioleoyl-sn-glycero-3-succinate (DOGS); 1,2-Dioleoyl-sn-glycero-phosphatidylcholine (DOPC) and N-[1-(2,3-Dioleoyloxy)propyl]-N,N-dimethylamine (DODAP) (Avanti Polar Lipids, Alabaster,AL); 1-Palmitoyl-2-oleoyl-sn-glycero-phospatidylglycerol (POPG) (Chemi, Cinisello Balsamo, Italy); N-(7-nitrobenz-2-oxa-1,3-diazol-4-yl)-1,2-dihexadecanoyl-sn-glycero-3-phosphoethanolamine, triethylammonium salt (NBD-PE) and Lissamine™ rhodamine B 1,2-dihexadecanoyl-sn-glycero-3-phosphoethanolamine, triethylammonium salt (*N*-Rh-PE) (Invitrogen-Molecular Probes, Karlsruhe, Germany).

The rest of the lipids used in this work are summarized in Appendix 2.9 and were purchased from ChiroBlock GmbH (Wolfen, Germany). Lipid synthesis details are available upon request from the corresponding author.

All other chemicals and reagents used were of analytical grade and they were used as received from the manufacturer.

2.1.2 SiRNA sequence

The siRNAs used in the present study were designed as described in (Haupenthal et al., 2007). All siRNAs were obtained as lyophilized duplex and they were resuspended in 50 mM NaCl. The sequences for the sense and antisense stands of siRNAs are as follows:

(i) Plk1 siRNA: (sence) 5´-agaccuaccuccggaucaa(dTdT)-3´
(antisense) 5´-uugauccggagguaggucu(dTdT)-3´

(ii) nonsilencing Plk1 siRNA as control: (sence) 5´-aacuggguaagcgggcgca(dTdT)-3´
(antisense) 5´-ugcgcccgcuuacccaguu(dTdT)-3´

The siRNAs contain two-base overhangs (dTdT) at the 3'-ends.

2.2 Fusion in response to pH

2.2.1 Preparation of particles

20 mM lipid stock solutions were prepared in isopropanol, split and individually supplied with 0.61 mol% either NBD-PE or *N*-Rh-PE. Due to limited solubility, all DOPA liposomes were prepared with an initial lipid concentration of 10 mM and the fluorescent lipid NBD-PE or *N*-Rh-PE was included at 1.2 mol%. For production of the liposomes, a liquid handling robot Multiprobe II Ex (Packard Bio Science now Perkin Elmer, Waltham, MA) was used. The preparation of liposomes was achieved by adding 360 µl of buffer (acetic acid 10 mM, phosphoric acid 10 mM, pH 7.5 adjusted with NaOH) to 50 µl alcoholic lipid mix, resulting in a lipid concentration of 1.95 mM (Batzri and Korn, 1973).

2.2.2 Lipid mixing – FRET assay

Lipid mixing of individually labelled liposomes was analyzed by fluorescence resonance energy transfer (FRET) (Struck et al., 1981). 100 µl of NBD-PE-labelled and 100 µl *N*-Rh-PE-labelled liposomes were combined immediately and 200 µl of buffer mentioned above was added to the mix. 50 µl of this mixed sample were transferred into the wells of a 96 well black micro-titer plate (BRAND GMBH, Wertheim, Germany) and brought to pH 2.5, pH 3.5, pH 4.6, pH 5.4, pH 6.6 and pH 7.5 with 50 µl of a buffer containing 50 mM acetic acid, 50 mM phosphoric acid

with required amounts of NaOH. The liposomes were incubated at 37°C for 2 h and subsequently FRET signals were measured. To discriminate between fusion and mere aggregation after the first FRET measurement the 100 µl suspension was neutralized to pH 7.5 with 50 µl of NaOH. Finally, a second FRET measurement and a size determination were carried out at a lipid concentration of 0.32 mM. A possible interference of the remaining alcohol content of < 3.1% on the fusion of the liposomes was excluded by pre-experiments.

The fusion in response to pH of 100% CHIM liposomes was demonstrated in a buffer system containing equal amounts of lysine, pyridine and imidazole. In this case, the liposomes were produced at pH 4 in 10 mM buffer (lysine/pyridine/imidazole) that was adjusted with HCl and brought to pH 3.8, pH 4.8, pH 5.7, pH 6.7, pH 7.3, pH 8.2 and pH 9 using a 50 mM buffer (lysine/pyridine/imidazole) with required amounts of HCl. After the first FRET measurement the liposome suspension was adjusted back to pH 3.8 with HCl.

2.3 Fusion after counterion discharge

2.3.1 Preparation of particles

0.57 mM liposomes, single modified with 1 mol% NBD-PE or *N*-Rh-PE, respectively, were prepared from pure CHEMS or CHIM by adding 10 ml of a buffer containing 50 mM acetic acid and 50 mM imidazole (~pH 6) to 0.32 ml alcoholic lipid mix.

2.3.2 Lipid mixing – FRET assay

The ion exchange resin Dowex® 50WX2 was freshly prepared in its hydrogen (H^+) form using 1N hydrochloric acid. Dowex® 1X2 was converted into its hydroxyl (OH^-) form using 1N sodium hydroxide (Ion exchange materials from Sigma Aldrich, St. Louis, MO). Upon charging, the ion exchange materials were extensively rinsed with water. The NBD-labelled and *N*-Rh-labelled liposomes were combined immediately in a volume ratio 1:1. The ion exchange resin Dowex® was added in portions to the liposome suspension and eventually aliquots were taken at different pHs, including pH 6, pH 5, pH 4, pH 3 (Dowex® 50WX2 H^+ form) or pH 7 and pH 8 (Dowex® 1X2 OH^- form). Then the liposomes were incubated at 37°C for 2 hours. Finally, required amounts of either acetic acid or imidazole were added to adjust the pH back to 6. FRET signals were measured before and after pH adjustment.

2.4 Counterion dependent fusion

2.4.1 Preparation of particles

30 mM lipid stock solutions were prepared in isopropanol and liposomes, single labelled with 1 mol% NBD-PE or *N*-Rh-PE, respectively, were prepared from mixtures of CHEMS/Chol (85:15 mol%) and CHIM/Chol (80:20 mol%). Liposomes were produced by adding 1 ml buffer pH 6 to 32 µl alcoholic lipid mix, resulting in a lipid concentration of 0.57 mM. The buffers, which have been used in each assay, are summarized in Table 2.1 below.

TABLE 2.1: Application and corresponding counterions used in this study.

ASSAY	CHEMS VS. COUNTERCATION	CHEMS VS. COUNTERANION	CHIM VS. COUNTERCATION	CHIM VS. COUNTERANION
Countercation*:	50 mM: K^+; Na^+; $Tris^+$; Arg^+; Li^+	Na^+	50 mM: K^+; Na^+; Li^+	$Imid^+$
Counteranion*:	Ac^-	50 mM: Ac^-; Ph^-; Glu^-	Ac^-	50 mM: Ac; Cl; Glu^-

*Abbreviation and name of acid/base: K^+ = pottasium hydroxid; Na^+ = sodium hydroxid; $Tris^+$ = tris-hydroxymethylaminomethan; Arg^+ = L-arginine; Li^+ = lithium hydroxid; $Imid^+$ = imidazole; Ac^- = acetic acid; Ph^- = phosphoric acid; Glu^- = glutamic acid.

2.4.2 Lipid mixing – FRET assay

The NBD-labelled and *N*-Rh-labelled liposomes mentioned above were combined immediately in a volume ratio 1:1. Finally, the liposomes were incubated at 37°C for several hours and FRET signals of 100 µl suspensions were measured at different points in time. The data in Figure 3.2 (see results) demonstrate fusion of CHIM and CHEMS liposomes after 2 and 48 hours incubation, respectively.

2.5 Fluorescence Resonance Energy Transfer (FRET) measurements

Samples were measured for FRET signals using a Packard FluoroCount™ Microplate Reader (Packard Bio Science now Perkin Elmer, Waltham, MA) with two sets of filters: NBD-PE/*N*-Rh-PE: Ex 460 nm/Em 590 nm and NBD-PE/NBD-PE: Ex 460 nm/Em 530 nm. The measurements were taken at one second per well read-length **s**etting with a PMT voltage of 907 volts. FRET as

a signal for membrane fusion was expressed as the ratio of the emission measurements of the two filter sets (Em 590 nm/Em 530 nm = E590/530). A background of 0.3 to 0.4 indicates background fluorescence and was therefore subtracted from the FRET signals. ∑FRET is expressed as the sum of all background corrected FRET signals (E590/530) in the matrix for Amphoter I systems (Ratio cation:anion (C:A) = 0.17, 0.33, 0.40, 0.50, 0.67 and 0.75) or Amphoter II systems (C:A = 0.33, 0.5, 0.67, 1, 1.5, 2 and 3) in response to pH. Pure anionic liposomes (C:A 0.00) were not considered for the analysis. Figure 2.1 shows an exemplary matrix for an Amphoter I system tested for fusion.

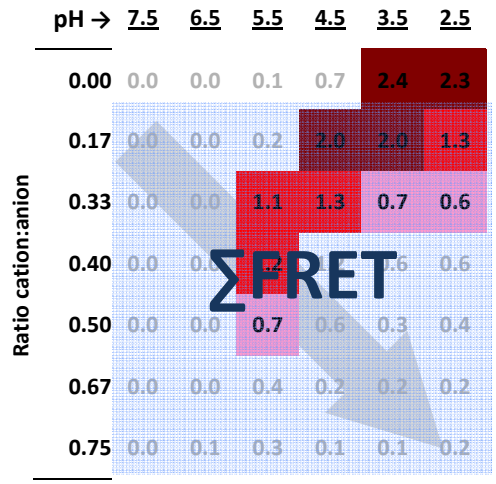

FIGURE 2.1: Fusion matrix of an Amhoter I system. Liposomes comprising DOTAP and CHEMS were produced at pH 7.5 and adjusted to acidic conditions to promote fusion. The cation:anion molar ratio was changed from 0 to 0.75. Intensity of fusion expressed as E590/530: less than 1 = pink; between 1 and 2 = red; more than 2 = dark red. The FRET signals (E590/530) in the matrix cation:anion ratio (0 to 0.75) of the different pH steps were summarized (∑FRET) to characterize the fusion properties of the system.

2.6 Size measurement

Particle properties were measured using a Zetasizer 3000 HSA (Malvern Instruments Ltd., Worcestershire, U.K.). Liposome size was measured at a final lipid concentration of 0.32 mM. Size values are recorded as $\bar{Z}$-average (mean particle size) and size distribution was calculated in the multimodal mode.

2.7 Fluorescence microscopy studies with fluorescently labelled lipid

2.7.1 Preparation of labelled MoChol/CHEMS liposomes

Stock solutions of MoChol, CHEMS and *N*-Rh-PE in chloroform were mixed in mol% ratio 33:66:0.5 and finally evaporated in a round bottom flask to dryness under vacuum. Lipid films were hydrated with PBS pH 7.5. The resulting lipid concentration was 20 mM. The suspensions

were hydrated for 45 minutes in a water bath at room temperature, sonicated for 5 minutes followed by three freeze/thaw cycles at -70°C. After thawing the liposomal suspensions were extruded 19 times through polycarbonate membranes with a pore size of 800/200/800 nm.

2.7.2 Fluorescence microscopy studies

The intracellular fate of liposomes was determined by monitoring the fate of FITC-Dextran (Sigma Aldrich, St. Louis, MO) and *N*-Rh-PE labelled liposomes by light and fluorescence microscopy (Axiovert S 100, Carl Zeiss Inc., Jena, Germany). HeLa cells were cultivated in DMEM (Invitrogen-Gibco®, Karlsruhe, Germany) supplemented with 10% fetal calf serum (FCS) at 37 ^{O}C under 5% CO_2. For transfection of the cells, cells were plated at a density of 2 x 10^4 cells/ml in 96-well plates and cultivated in 100 µl medium. After 16 h the growth medium was replaced by 100 µl Opti-MEM I (Invitrogen-Gibco®, Karlsruhe, Germany). The endosomal/lysosomal pathway in living HeLa cells was labelled with FITC-Dextran (MW 71,600; Sigma Aldrich, St. Louis, MO) by 4 h incubation with the probe at 2 mg/ml. Subsequently, the cells were washed and incubated with 200 µM *N*-Rh-PE labelled liposomes at 37 ^{O}C. Four hours after adding the liposomes to the cells, the transfection mixtures were replaced by growth medium. The cells were then further incubated for 24 hours.

2.8 Transfection of siRNA into HeLa and RAW264.7 cells

2.8.1 Preparation of particles

Individual lipids were dissolved in isopropanol in a final lipid concentration of 30 mM and mixed at desired molar ratios. A stock solution (50 mM NaCl) of the Plk1 or scrambled siRNA was diluted in a buffer system containing 20 mM sodium acetate and 300 mM sucrose adjusted at pH 4 with acetic acid. Liposomes were prepared by adding the siRNA solution to the alcoholic lipid mix in a volume ratio of 2.3:1, resulting in a final alcohol concentration of 30%. The ratio (N/P) between the cationic charged lipids and the anionic charges from the siRNA was set to 3 or 5, respectively, during the manufacturing at pH 4. The formed liposomal suspensions were shifted to pH 7.4 with twice the volume of 136 mM disodium hydrogen phosphate and 100 mM sodium chloride (pH 9), resulting in a final lipid concentration of 3 mM and a final isopropanol concentration of 10%.

The lipid combinations, which have been used for siRNA transfection into human cancer cells and macrophages, are summarized in Table 2.2. The amount of neutral lipid was set from 0% to 60% and the molar ratio of the charged lipids (cation:anion = C:A) from 0.33 to 3. The C:A ratio for Amphoter I systems was set to 0.33, 0.50, 0.67 and 0.82. For Amphoter II systems

TABLE 2.2: Amphoteric liposomes for siRNA delivery into HeLa and RAW264.7 cells.

Lipid combinations tested into **HeLa** cells

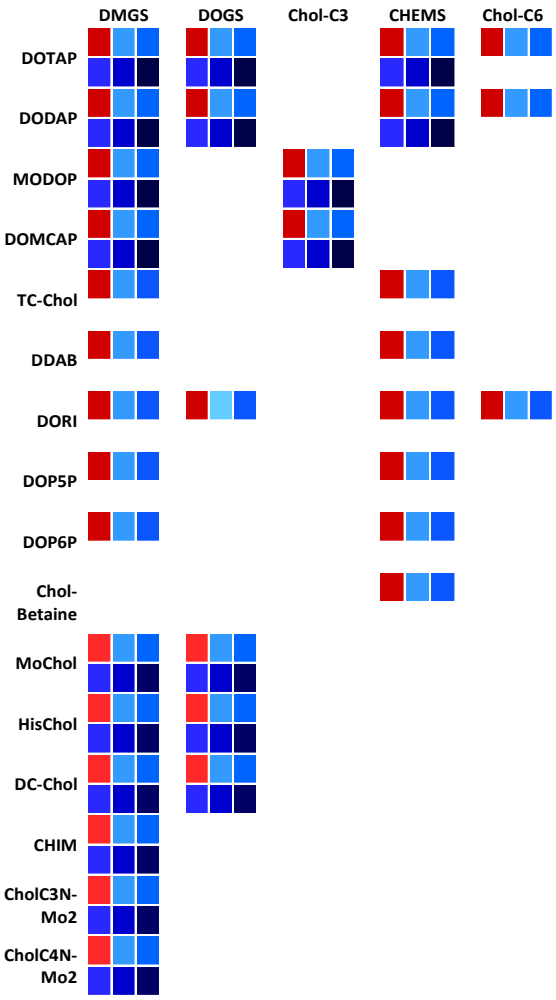

Lipid combinations tested into **RAW264.7** cells

Cation		Anion		Neutral 1		Neutral 2	
DOTAP	15%	DOGS	45%	Chol	40%	-	-
	27%		53%		20%	-	-
	28%	Chol-C1	42%	Chol	30%	-	-
	23%	Chol-C5	47%		30%	-	-
	25%		75%	-	-	-	-
	28%		42%	Chol	30%	-	-
	32%		48%		20%	-	-
	36%		44%		20%	-	-
	40%		60%	-	-	-	-
DODAP	36%	CHEMS	44%	Chol	20%	-	-
	45%		55%	-	-	-	-
MoChol	24%	DMGS	36%	Chol	40%	-	-
	27%		33%		40%	-	-
	20%		40%	Chol	27%	POPC	13%
	27%		53%		20%	-	-
HisChol	20%		60%		20%	-	-
	27%		53%		20%	-	-
CholC3N-Mo2	18%		52%		30%	-	-
	20%		40%		27%	POPC	13%
CholC4N-Mo2	20%		40%		40%	-	-
	20%		40%		27%	POPC	13%

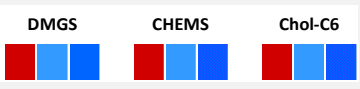

Molar ratio cation:anion 0.33; 0.50; 0.67; 0.82

Molar ratio cation:anion 0.33; 0.50; 1.00; 2.00

Charge only (0%)

Chol: 20%, 30%, 40%, 50%, 60%

Chol: 20%, 40%

POPC/Chol molar ratio 0.50: 20%, 40%, 60%

POPC/DOPE molar ratio 0.33: 20%, 30%, 40%

DOPE/Chol molar ratio 0.50: 20%, 40%, 60%

following ratios were used: 0.33, 0.50, 1 and 2. Neutral lipid has been either a single neutral lipid or a combination of two different neutral lipids. The liposomes were prepared with the following neutral lipids: Chol, POPC/Chol (ratio 0.50), POPC/DOPE (ratio 0.33) and Chol/DOPE (ratio 2).

2.8.2 Cell culture and transfection procedure

Human cervical carcinoma cells (HeLa) (DSMZ, Braunschweig, Germany) and murine leukemia monocyte/macrophage cells (RAW264.7) (ATCC, Manassas, VA) were maintained in Dulbecco's Modified Eagle Medium (DMEM) supplemented with 10% FCS, penicillin and streptomycin (Invitrogen-Gibco®, Karlsruhe, Germany) at 37°C under 5% CO_2. Twenty four hours prior to transfection, 3500 to 4500 HeLa cells or 4000 to 5000 RAW264.7 cells were seeded into each well of a 96 well plate.

After the cells reaching a confluence of approximately 30% the liposomes were added to the cells. One hour prior transfection the formulations were diluted to the desired siRNA concentration in the preparation buffer pH 7.4, a mixture of the two above-mentioned buffers used for the preparation of the particles, or in phosphate buffered saline (PBS) pH 7.4. A volume of 10 µl amphoteric liposomes encapsulating siRNA targeting the PLK1 message or a scrambled control were added to the cells, resulting to a final volume of 110 µl with 9.1% FCS. Cells treated with the preparation buffer or PBS served as untreated control. Each formulation was tested with 6 different siRNA concentrations ranging between 0.1-300 nM, and transfections were done in triplicates. Once transfected, the amphoteric liposomes were not removed from the cells. Cell culture dishes were incubated for 72 hours at 37°C under 5% CO2.

2.8.3 Cell proliferation assay

Cell proliferation was determined by using the CellTiter-Blue® Cell Viability Assay (Promega GmbH, Mannheim, Germany). In brief, 72 hours after transfection, 100 µl of DMEM/CellTiter Blue reagent, a mixture of 80 µl DMEM and 20 µl CellTiter-Blue reagent, were added to the wells. Following incubation at 37°C for 2.5 to 3 hours, 80 µl of the medium were transferred into the wells of a 96 well black micro-titer plate (BRAND GMBH, Wertheim, Germany). Fluorescence was recorded using a Packard FluoroCount™ Microplate Reader (Packard Bio

Science now Perkin Elmer, Waltham, MA) with one set of filters. The excitation filter was set to 460 nm and the emission was measured at a wavelength of 590 nm. The measurements were taken at one second per well read-length **s**etting with a PMT voltage of 907 volts. On each plate the following controls were included: i) wells without cells but with medium as control for culture medium background fluorescence and ii) wells with untreated cells as mock-transfected cells. For calculation, the mean fluorescence value of the culture medium background was subtracted from all mean (triplicates) values of experimental wells (transfected and mock-transfected cells). The fluorescence values from each transfection were normalized to the mean fluorescence value from mock-transfected cells, which were set as being 100%. The half maximal inhibitory concentration values (IC50) were calculated from truncated concentration-response curves. The IC50 values for formulations with an inhibition effect less than 50% were set to the maximum siRNA concentration tested in the transfection procedure (usually 100 nM for HeLa cells and 300 nM for RAW264.7 cells). Furthermore, values of a scrambled/Plk1 ratio higher than 2 were allowed for the formulation, lower values were not considered for the analysis, due to toxicity.

2.9 APPENDIX: Structures and physical properties of lipids used in this study

ABBREVIATION AND NAME	STRUCTURE	HEAD AND TAIL VOLUMES[5,6] [Å³]	pK_α[6]
POPC 1-Palmitoyl-2-oleoyl-sn-glycero-phosphatidylcholine	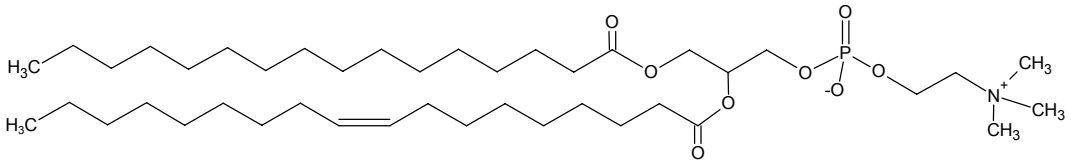	136.3 490.4	1.23[1] 15
DOPC 1,2-Dioleoyl-sn-glycero-phosphatidylcholine	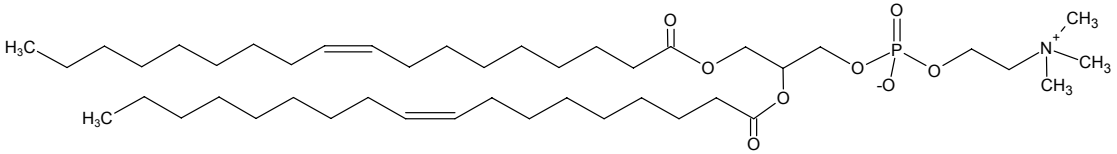	136.3 511.8	1.23[1] 15
DOPE 1,2-Dioleoyl-sn-glycero-phosphatidylethanolamine	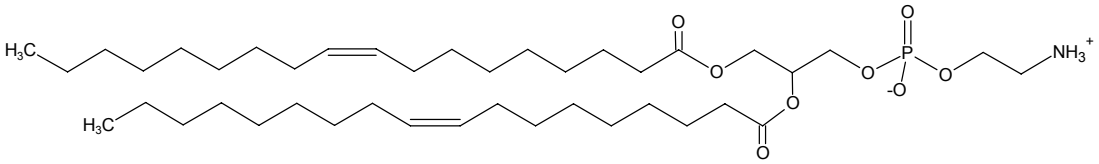	98.3 511.8	1.17[1] 8.02[1]
SM Sphingomyelin	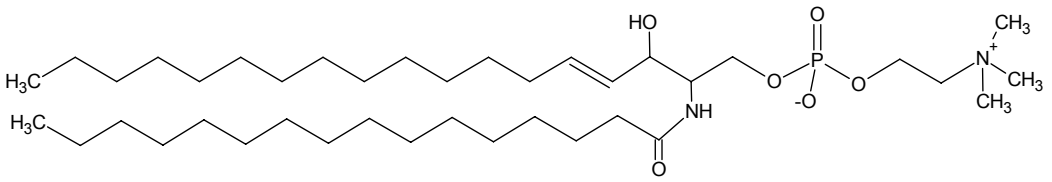	136.3 384.9	1.23[1] 15

Chol Cholesterol	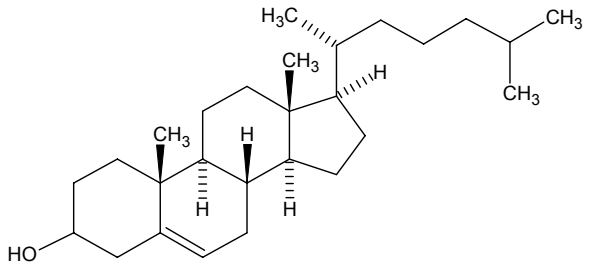	30 327	14.9[1]
POPG 1-Palmitoyl-2-oleoyl-sn-glycero-phospatidylglycerol	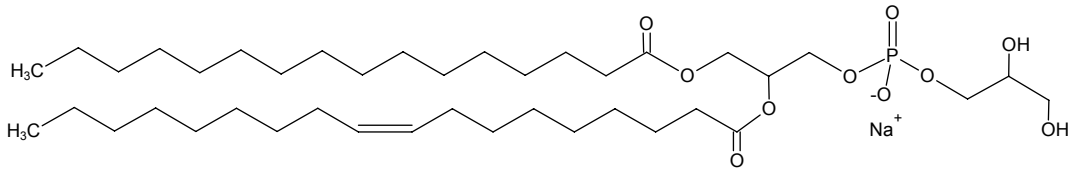	115.9 490.4	1.39[1]
DOPA 1,2-Dioleoyl-sn-glycero-3-phosphate, sodium salt	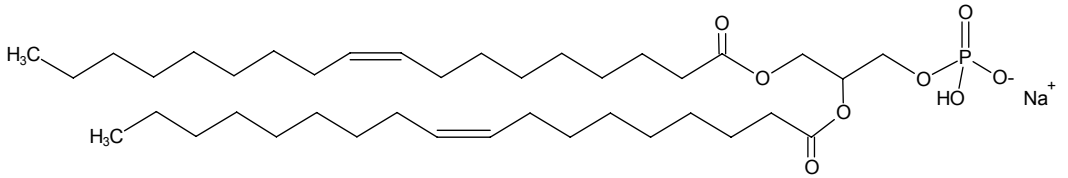	62.8 511.8	6.38[1] 1.83[1]
DMGS 1,2-Dimyristoyl-sn-glycero-3-succinate	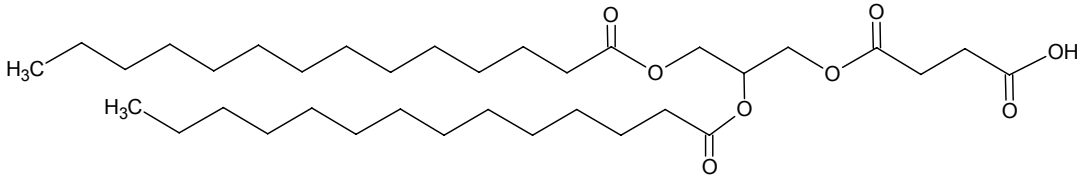	90.2 418.3	5.33[2]
DOGS 1,2-Dioleoyl-sn-glycero-3-succinate	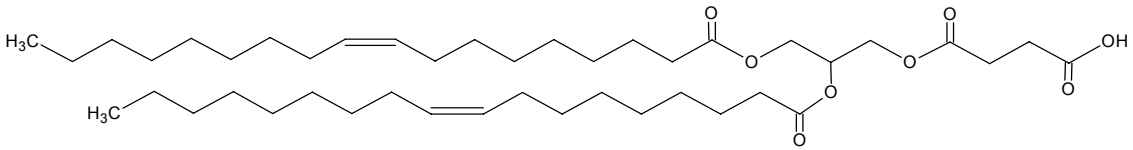	90.2 511.8	5.33[2]

Chol-C1 Cholesteryl-3-carboxylic acid	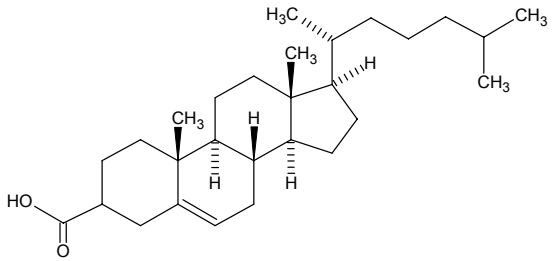	29.5 334	5.61[2]
Chol-C3 Cholesteryl hemimalonic acid	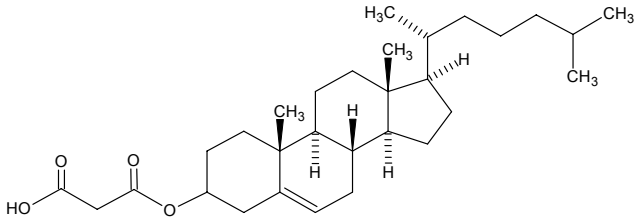	66.3 334	3.74[2]
Chol-C4 (CHEMS) Cholesteryl hemissucinic acid	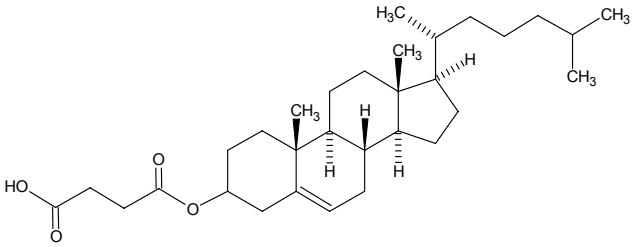	78.2 334	5.39[2] 5.53[3]
Chol-C5 Cholesteryl hemiglutaric acid	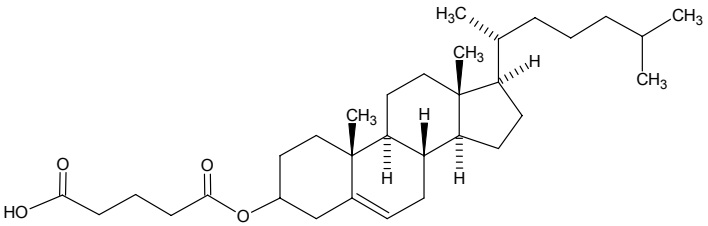	90.9 334	5.61[2]

Chol-C6 Cholesteryl hemiadipinic acid	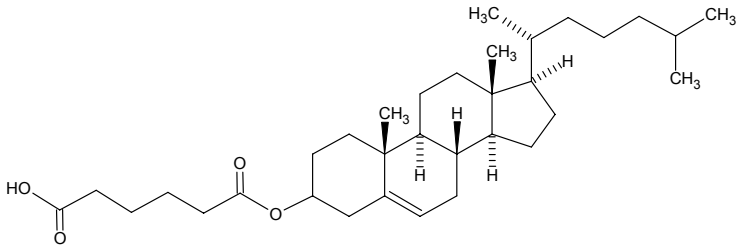	103.9 334	5.68[2] 5.68[3]
DDAB Dimethyldioctadecyl-ammonium bromide	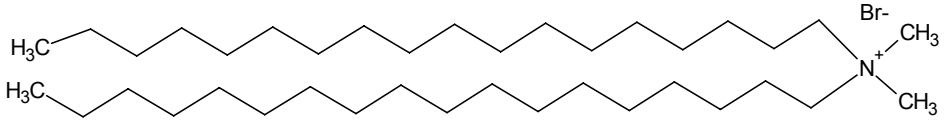	57.2 434.2	> 12
DODAP N-[1-(2,3-Dioleoyloxy)propyl]-N,N-dimethylamine	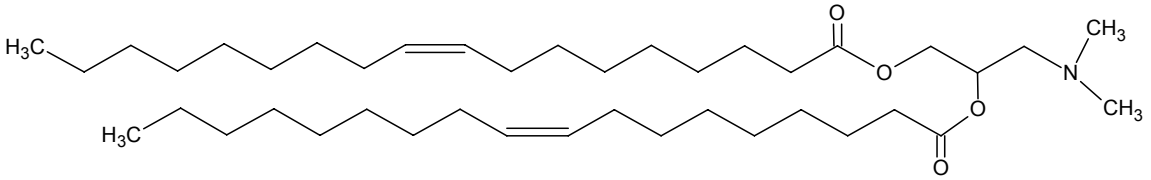	45.7 511.8	7.52[4]
DOTAP N-[1-(2,3-Dioleoyloxy)propyl]-N,N,N trimethylammonium chloride	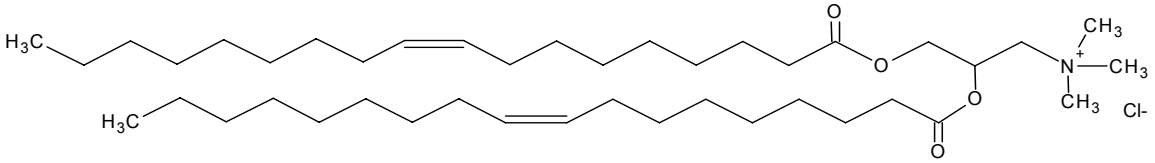	57.2 511.8	>12
DORI N-[1-(2,3-Dioleoyloxy)propyl]-(N,N-dimethyl,N-hydroxyethyl) ammonium chloride	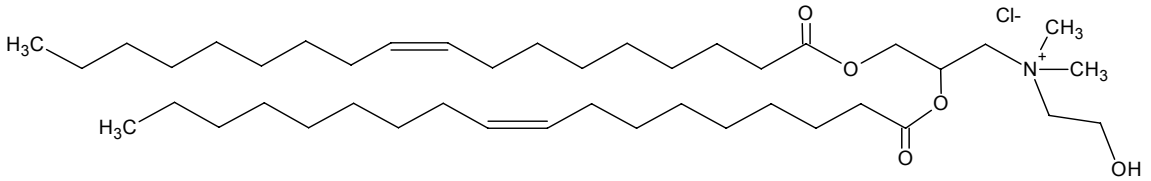	74.9 511.8	> 12

DOP5P
1,2-Dioleoyl-sn-glycero-3-N-pyrrolidine

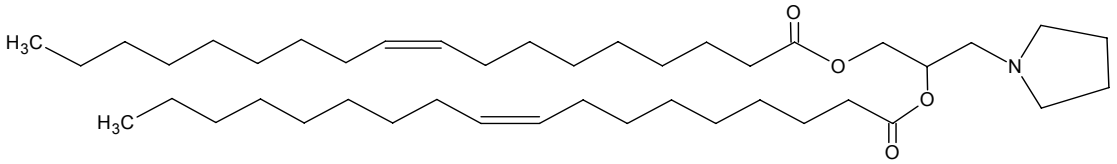

64.1
511.8

8.53[4]

DOP6P
1,2-Dioleoyl-sn-glycero-3-N-pyrridinium bromide

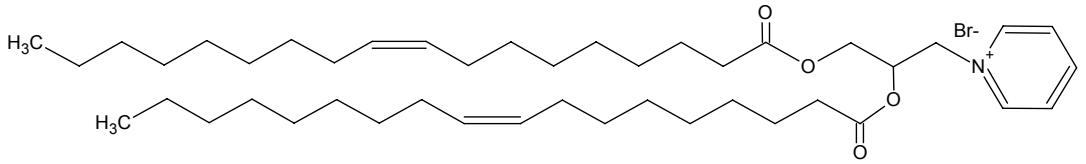

67.9
511.8

> 12

MODOP
1,2-Dioleoyl-sn-glycero-3-N-morpholine

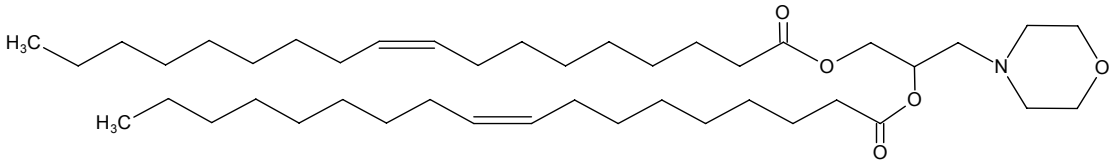

71.4
511.8

5.68[4]

DOMCAP
N-[1-(2,3-Dioleoyloxy)propyl]-(N-methyl,N-methoxycarbonyl-ethyl)-amine

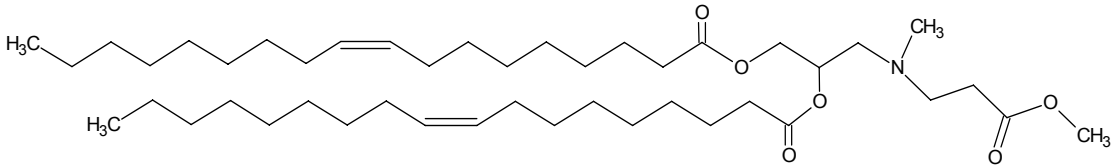

79.5
511.8

6.01[4]

Chol-Betaine
Cholesteryl-oxycarbonylmethyl-trimethyl-ammonium chloride

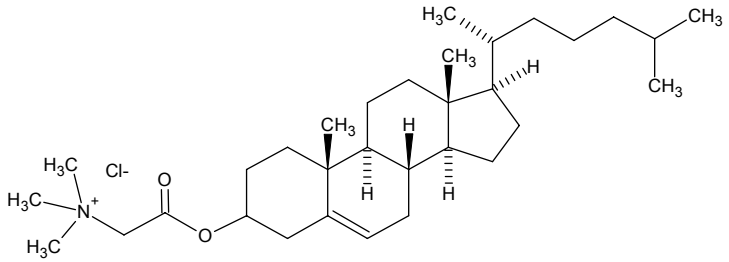

84.5
334

> 12

DC-Chol 3ß-[N-(N',N'-dimethylaminoethane)-carbamoyl]cholesterol hydrochloride	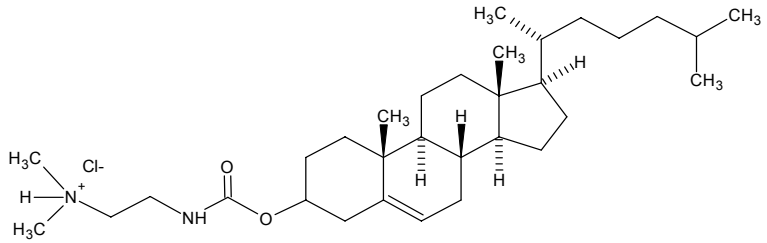	87.2 334	7.56[4]
TC-Chol 3ß-[N-(N',N, N'-trimethylaminoethane)-carbamoyl]cholesterol hydrochloride	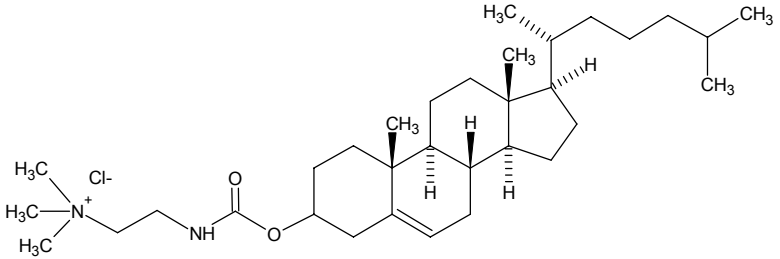	98.9 334	> 12
CHIM Cholesterol-(3-imidazol-1-yl propyl)-carbamate	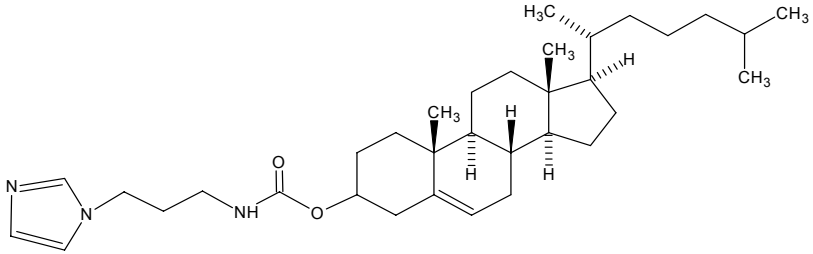	119.2 334	6.5[4]
HisChol (α-(3'O-cholesteryloxycarbonyl)-δ-(4-ethylimidazole)-succinamide)	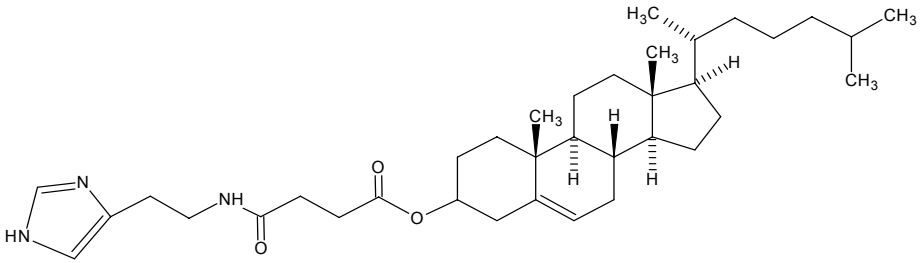	150.5 334	6.67[4]

Chol-C3Mo2
α-(3'O-cholesteryloxycarbonyl)-
γ-(N-ethylmorpholine)-
malonamide

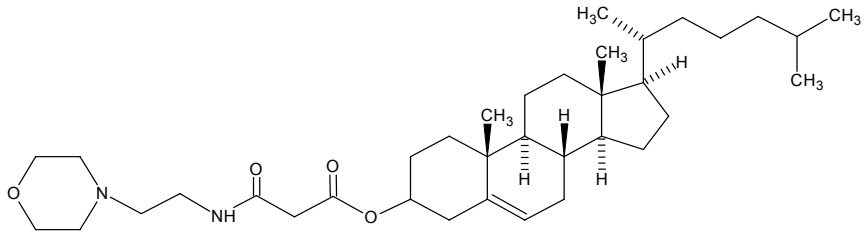

155.2
334

6.46[4]

Chol-C4Mo2 (MoChol)
α-(3'O-cholesteryloxycarbonyl)-
δ-(N-ethylmorpholine)-
succinamide

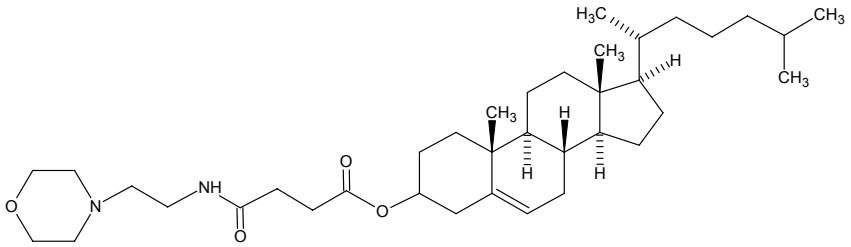

168.2
334

6.51[4]
6.50[3]

Chol-C5Mo2
α-(3'O-cholesteryloxycarbonyl)-
ε-(N-ethylmorpholine)-
glutaramide

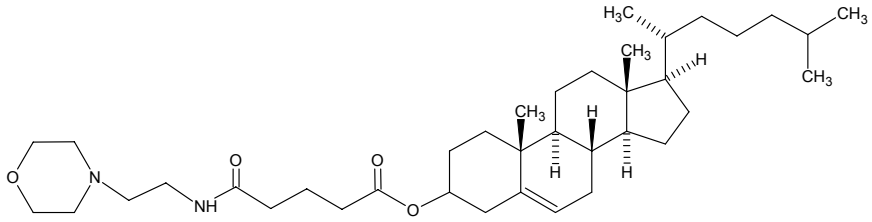

180.8
334

6.54[4]

Chol-C6Mo2
α-(3'O-cholesteryloxycarbonyl)-
z-(N-ethylmorpholine)-
adipinamide

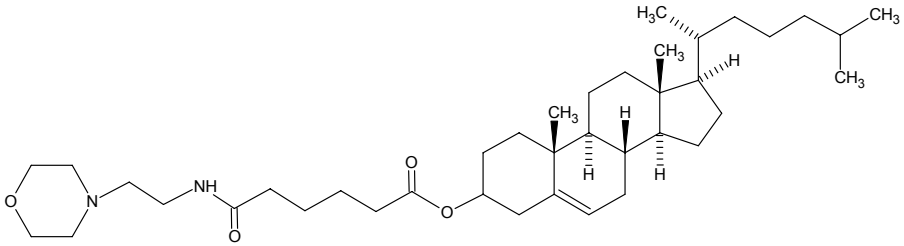

193.8
334

6.55[4]

Chol-C4N-Mo2 [(2-Morpholin-4-yl-ethylcarbamoyl)-ethyl]-carbamic acid cholesterylester	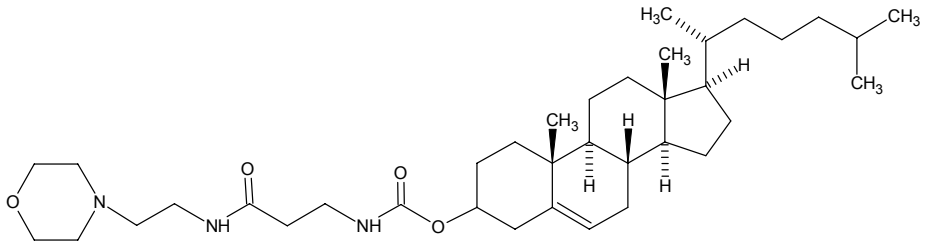	195.3 334	6.53[4]
Chol-C3N-Mo2 [(2-Morpholin-4-yl-ethylcarbamoyl)-methyl]-carbamic acid cholesterylester	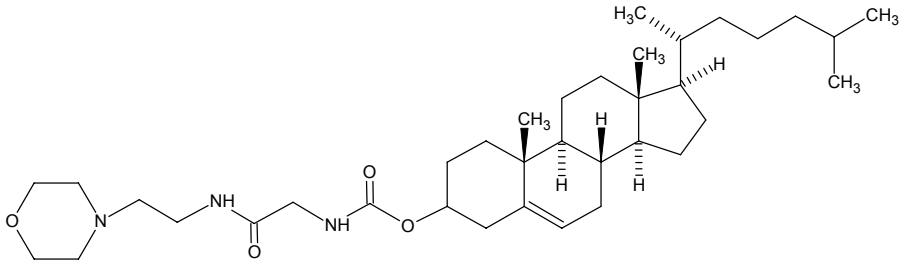	181.2 334	6.48[4]

[1] calculated by ACD/ pK_α DB (ACD Labs 7.00, Product Version 7.07).

[2] calculated pK_α +1, pK_α calculated by ACD/pK_α DB (ACD Labs 7.00, Product Version 7.07).

[3] experimentally determined in liposomes (Heyes et al., 2005).

[4] calculated pK_α -0.5, pK_α calculated by ACD/pK_α DB (ACD Labs 7.00, Product Version 7.0).

[5] all molecular volumes were determined using DS Viewer Pro5.0. For cholesterol, crystallographic data (1CRN of the Protein Data Bank) were used to ensure the proper conformation of the molecule.

[6] Panzner et al., 2008-WO 08/043575.

3. RESULTS

3.1 The role of counterions in the fusogenic behaviour of lipid bilayers

In the present study, the conceptual framework of the lipid shape theory has been used in order to explain the observations. The theory states that small polar lipid fragments relate to a fusogenic state, while larger headgroups relate to a lamellar, non-fusogenic phase (Israelachvili and Mitchell, 1975; Israelachvili et al., 1977; Israelachvili et al., 1980). In addition, the theory considers lipid-bound counterions as an integral and shape-determining portion of the charged, water exposed portion of a lipid (Li and Schick, 2001; Pandit et al., 2003; Mukhopadhyay et al., 2004).

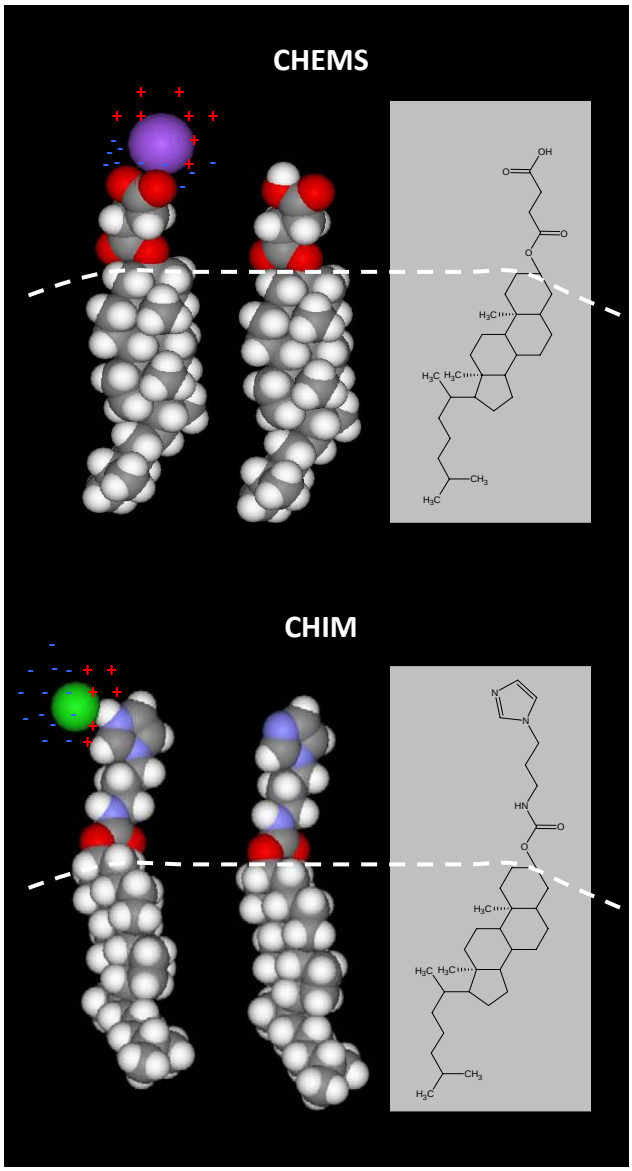

FIGURE 3.1: 3D schematic illustration of CHIM and CHEMS structures. The head/tail interface is set to carbon atom 3 of the cholesterol membrane anchor, this defines the head and tail groups in uncharged lipids. When charged, these lipids attract counterions, such as phosphate and sodium, which substantially increase head group volumes.

In order to deal with the unknown geometry of the lipid-ion complex, the cross sections of the lipid polar and apolar fragments were also replaced by their molecular volumes (Figure 3.1). This resulted in a volume of 78 Å³ for the polar headgroup of cholesterol hemissucinic acid (CHEMS), a value that more than doubled upon recruitment of a hydrated sodium ion. The radii of the sodium counterions in this case considerably vary; literature shows values between 2.25 and 3.59 Å (equal to a molecular

volume of between 65 and 200 Å³). Additional changes in hydration were reported during binding to a countercharge (Pandit et al., 2003; Pollack, 2001; Kielland, 1937; Conway 1981). Thus, a value of 100 Å³ was used as a reasonable estimation for a hydrated sodium cation in its bound state and it was assumed the same for a hydrated phosphate anion in association with cholesterol-(3-imidazol-1-yl propyl)-carbamate (CHIM).

Besides the binding of counterions, hydration of the charged headgroup or electrostatic repulsion between these moieties has been proposed to promote the lamellar phase of bilayers (Li and Schick, 2000 a,b,c). In order to test these assumptions, the charged bilayers were depleted from their counterions using ion exchange materials (Figure 3.2). Liposomes were prepared from pure CHEMS at pH 6 in the presence of charged imidazolium ions. As

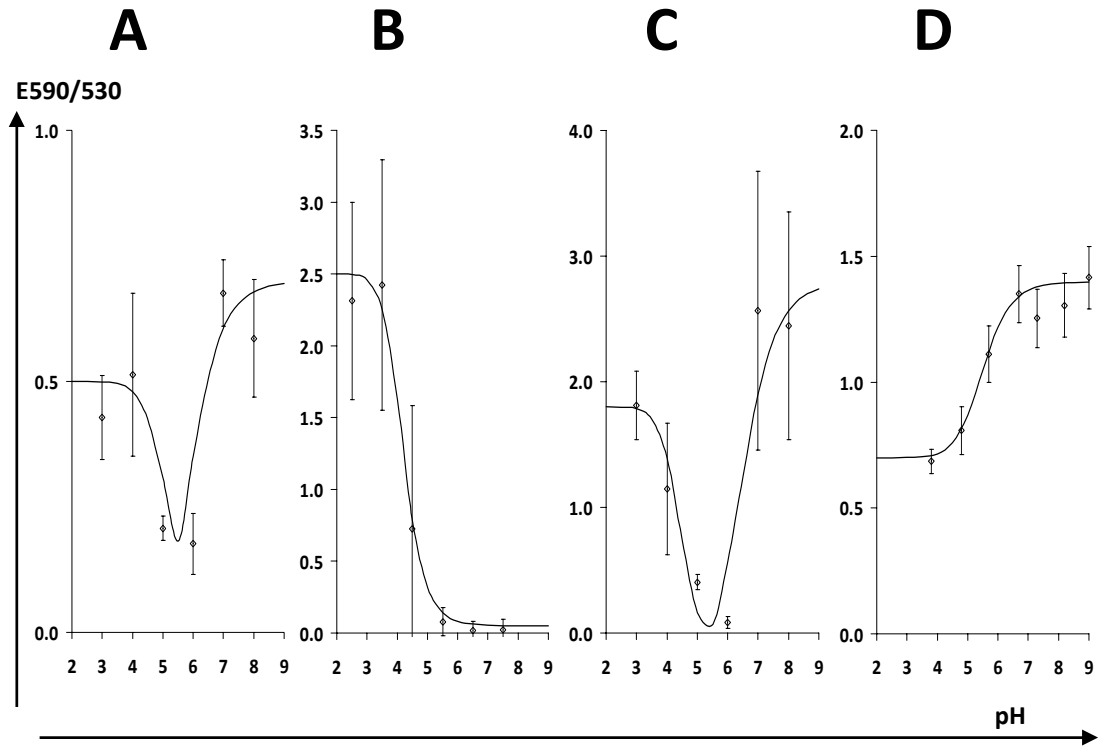

FIGURE 3.2: Counterion binding governs lipid fusion. (A) Liposomes from pure CHEMS were formed in imidazole buffer at pH 6 and the pH was adjusted by addition of ion exchange materials in their H^+ or OH^- form. Protonation of either the lipid head group at low pH or charge loss of the buffer ion at higher pH both resulted in fusion of the lipid materials. **(B)** Liposomes from pure CHEMS were produced in Na^+ buffer at pH 7.5 and exposed to the pH indicated using acetate/phosphate buffers. The fusion profile becomes single sided and no fusion is observed at high pH due to the presence of the constantly charged sodium ion. **(C)** Liposomes from pure CHIM were formed in acetate buffer at pH 6 and ion exchange materials were added as in (A). In analogy to the earlier experiment, charge loss of either the acetate ion at low pH or of the lipid head group at higher pH resulted in fusion of the liposomes. **(D)** Liposomes from pure CHIM were formed in lysine/morpholine/imidazole buffer that was adjusted to pH 4 using HCl. Upon exposure to higher values of pH, a single sided profile was obtained, wherein fusion was limited to conditions of the discharged head group. The error bars represent standard error of mean calculated from at least three separate experiments.

expected, the particles were stable and did not fuse. Adding small portions of the anion exchange resin Dowex® 1X2 in its OH^- form raised the pH of the system and neutralized the imidazolium ions, thereby generating a fully charged lipid assembly devoid of stabilizing ions. Instant fusion of the liposomes was observed. As expected, fusion was also observed in the CHEMS/imidazolium system upon addition of an ion exchange material in its H^+ form, which leads to protonation of CHEMS and loss of counterion binding, as presented in Figure 3.2 panel A. Conversely, liposomes made of the cationic, pH-sensitive lipid CHIM can be stabilized through the adsorption of acetate ions at pH 6, but fuse upon addition of the cation exchange resin Dowex® 50X2 in its H^+ form, which leads to protonation and concomitant loss of bilayer binding properties of the acetate ion. CHIM liposomes also fuse when the pH is raised by the addition of Dowex® 1X2 in its OH^- form, which was also expected (Figure 3.2, C).

Control reactions with constantly charged counterions, such as sodium or chloride, allowed only a single phase transition along with the protonation of the respective lipids (Figure 3.2 B and D). The results assign a dominant role for bound ions in the phase behaviour of lipid assemblies; electrostatic repulsion between or hydration of the charged lipid portions were both insufficient for the stabilization of a lamellar phase in the absence of counterions. The fusogenic potential created through the lipid shape appears to be strong, being able to even override the electrostatic repulsion between particles. According to the experimental data, lipid bilayers exhibit common phase behaviour independent of their chemistry. This can be explained by ion fluctuations at the bilayer and the induction of different molecular shape of the lipids involved.

If the counterion volume modulates the fusogenicity of a bilayer, one would expect a stabilizing role of larger ions and promotion of fusion in the presence of small ions. To test this hypothesis, liposomes from CHEMS and cholesterol (15:85 mol%) were labeled with either NBD-PE or *N*-Rh-PE. These were combined and the mixing of their bilayers was monitored over time in the otherwise undisturbed sample. Decreased lipid mixing was observed in the series of $arginine^+ > tris(hydroxymethylaminomethan)^+ > Li^+ > Na^+ > K^+$; that is larger cations inhibit the fusion of an anionic bilayer. On the contrary, buffers from sodium acetate, phosphate or glutamate did not substantially change the fusion of CHEMS/cholesterol liposomes (Figure. 3.3 A), since the different anions do not bind to the negatively charged membrane. Conversely, the fusion of pH-sensitive, cationic liposomes made from CHIM/cholesterol (20:80 mol%) was enhanced in the order of $Cl^- > acetate^- > glutamate^-$, but appeared unchanged in an acetate buffer comprising either potassium, sodium or lithium cations, as demonstrated in panel B Figure 3.3.

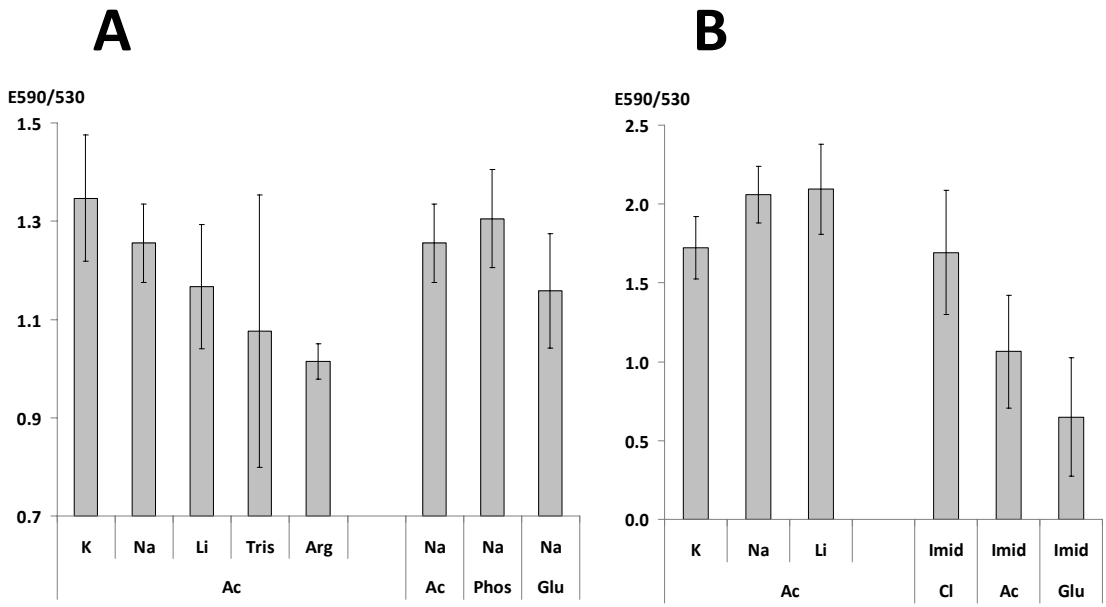

FIGURE 3.3: Counterions control lipid fusion. (A, B) FRET labelled liposomes from CHEMS and Chol (15:85 mol%, A) or CHIM and Chol (20:80 mol%, B) were formed at pH 6 in buffers containing the indicated ions. The appearance of a FRET signal was monitored over time without any external changes in pH or temperature. **(A)** Large countercations, such as tris-hydroxymethylaminomethan or arginine, suppress fusion, while counteranions do not affect the fusion properties of CHEMS/Chol, consistent with the idea of head group enlargement by the bound ions. **(B)** Conversely, the large anion glutamic acid (Glu), but not chloride does suppress fusion of CHIM/Chol liposomes; different countercations had no impact on fusion. The error bars represent standard error of mean calculated from at least three separate experiments.

In general, the results support a view wherein counterions are an integral part of all charged lipid headgroups; their volume contributes to the molecular shape of the respective lipids, which eventually determines the stability or fusogenicity of a bilayer. This finding has direct implications for the optimization of liposomes as carrier systems, but may also be relevant for the structure formation of biological membranes.

3.2 Amphoteric liposomes and their biphasic stability

The above-mentioned observations prompted to systematically probe the pH-dependent phase transition of amphoteric liposomes. For this purpose, mixtures comprising anionic and cationic lipids with at least one lipid being pH-sensitive were used. Three different charged-only systems were analyzed in this section: DOTAP/CHEMS (Amphoter I), CHIM/CHEMS (Amphoter II) and MoChol/DOPA (Amphoter III).

A membrane fusion assay, based on fluorescence resonance energy transfer (FRET) between two fluorescent lipid probes, was used to assess the fusion of the respective lipid mixtures in

response to pH (Struck et al., 1981). The systems were prepared as pairs of individually labelled liposomes using the isopropanol injection method. Liposomes were produced at neutral pH and incubated at lower values of pH for fusion. At intermediate pH, a fluorescence transfer was observed between the NBD and *N*-Rh label, resulting in an emission of light at 590 nm. Although FRET is widely used to monitor membrane fusion, the possibility of a mere aggregate formation at intermediate pH was considered. Therefore, in order to separate fusion from mere aggregate formation, the samples were neutralized with required amounts of sodium hydroxide and FRET signals were measured again. In the following sections, the FRET measurements recorded after neutralisation were used for data interpretation. Both signals, a decrease of the original emission of NBD at 530 nm and an increase at 590 nm, were measured. In some cases, an overall compression of the signal was observed. One explanation for such compression might be an aggregation of particles, which produces enhanced scattered light and decreases the intensity of the fluorescence signals. Further experimental details are provided in the MATERIALS & METHODS section 2.2.

3.2.1 Amphoter I system

To investigate the pH-dependent phase transition of the Amphoter I system, mixtures at a number of ratios comprising CHEMS and the stable cation DOTAP were used. Amphoter I systems need an excess of the pH-sensitive anion to achieve amphoteric character. As an example, a mixture of 30% DOTAP and 70% CHEMS has a net charge equal to 40% CHEMS at pH 7.5 or higher. The remainder being compensated from the DOTAP and salt formation occurs until all cationic lipids are consumed. Now, if the pH is lowered under the pK_α of CHEMS, the anion looses charge and the net surface charge of the membrane turns positive as the DOTAP prevails.

Experimental evidence is given in Figure 3.4 panels A and B. Lipid mixing was monitored as FRET signal and subsequently as size increment of the particles after recombination of individually labeled particles. Both were recorded at the end of the pH cycle. For all amphoteric mixtures, a stable phase at neutral and low pH was observed. Fusion was achieved as the pH was reduced toward the pK_α of the acidic lipid; a phenomenon that cannot longer be observed in cationic mixtures having an excess of the permanently charged cationic lipid DOTAP. Vesicles highly enriched with DOTAP display a size increment, presented as the ratio of the size at pH 7 and the size measurement at the end of the pH cycle, but do not fuse. This

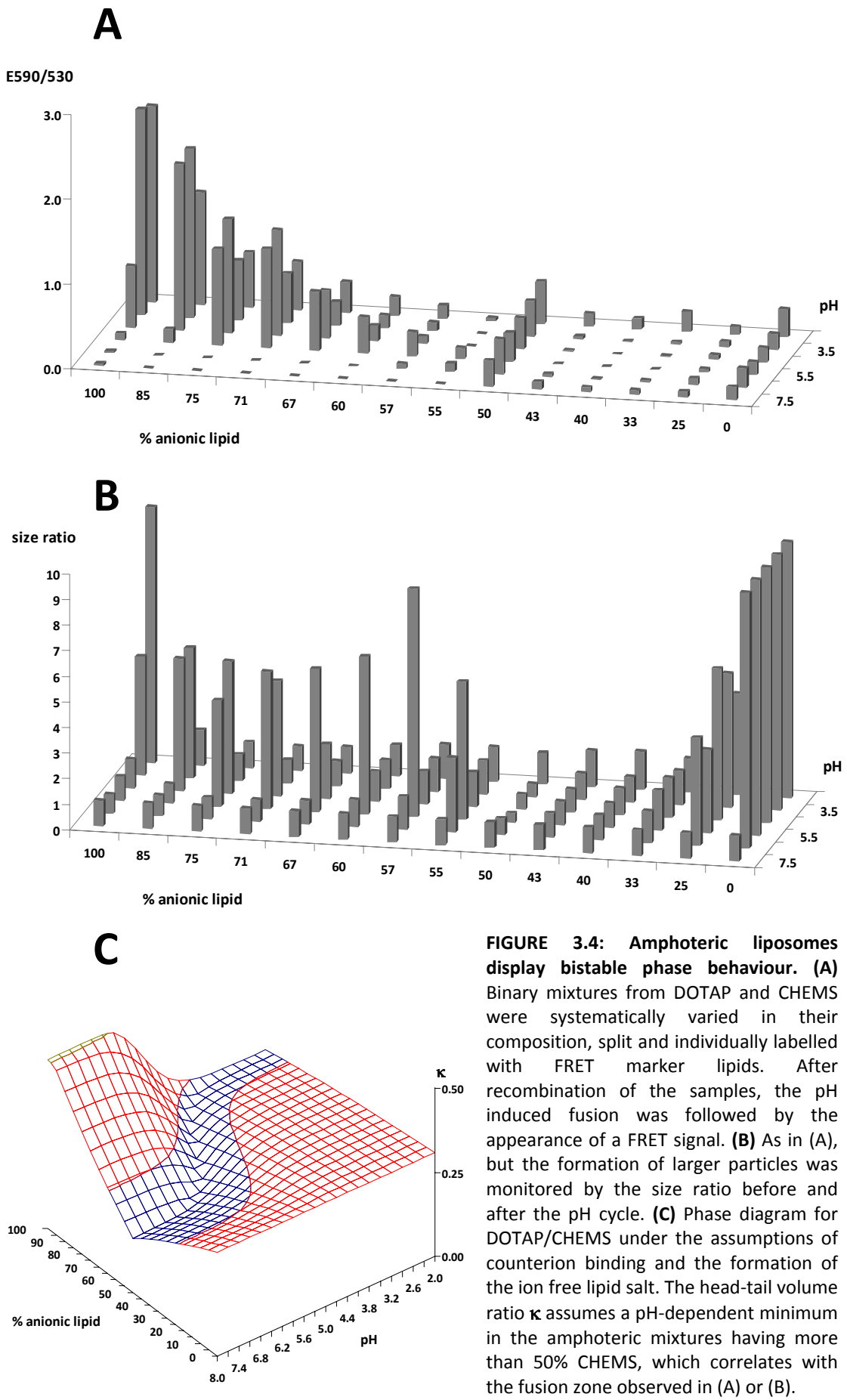

FIGURE 3.4: Amphoteric liposomes display bistable phase behaviour. (A) Binary mixtures from DOTAP and CHEMS were systematically varied in their composition, split and individually labelled with FRET marker lipids. After recombination of the samples, the pH induced fusion was followed by the appearance of a FRET signal. **(B)** As in (A), but the formation of larger particles was monitored by the size ratio before and after the pH cycle. **(C)** Phase diagram for DOTAP/CHEMS under the assumptions of counterion binding and the formation of the ion free lipid salt. The head-tail volume ratio κ assumes a pH-dependent minimum in the amphoteric mixtures having more than 50% CHEMS, which correlates with the fusion zone observed in (A) or (B).

phenomenon is attributed to cross linking of DOTAP liposomes in the presence of bivalent buffer ions, since the effect disappeared in the presence of monovalent buffers (data not shown).

The results correlated to a large extent with the predictions provided by the theory. The surface plot, presented in Figure 3.4 panel C, is calculated using the Panzner algorithm and represents the theoretical prediction of the fusogenicity in response to pH for the amphoteric mixture DOTAP/CHEMS. The blue zone reflects low values of κ indicating the point of strongest fusogenicity and the red zone reflects stable phases. Similar to the experimental findings (Figure 3.4 panels A and B), a valley of fusogenicity appears for DOTAP/CHEMS mixtures. Any amphoteric mixture having more than 50% and less than 90% CHEMS is expected to fuse under slightly acidic conditions but to be stable both at neutrality and under acidic conditions. Pure CHEMS have continuous fusion properties at low pH, no valley observed.

These findings extend the observations of Hafez and colleagues, who described pH-induced fusion of amphoteric lipid mixtures, but did not observe the lamellar phase at low pH (Hafez et al., 2000; Hafez and Cullis, 2004).

3.2.2 Amphoter II system

Liposomes in which both the cationic and anionic lipid are pH-sensitive have the distinct advantage to be amphoteric over the entire range of cation:anion (C:A) ratios. Thus, no charge overcompensation for the strong ion is needed, as it is the case in Amphoter I or Amphoter III systems.

The experimental data obtained using the Amphoter II system CHIM/CHEMS, demonstrate bistable phases that have a stable phase at low and neutral conditions, but undergo fusion at intermediate pHs, as demonstrated in Figure 3.5, panel A. This behaviour is most obvious for mixtures having not less than 30% of CHEMS. Mixtures having higher amounts of CHEMS are stable at neutral pH, but undergo fusion at intermediate and lower pHs. The offset of the biphasic stability is shifted to higher pH values with higher amounts of CHIM. For all liposomes, a fusion valley was obtained around their isoelectric point.

The above-mentioned experimental evidence strongly supports the salt bridge model. Panel B in Figure 3.5 shows a three-dimensional fusion profile calculated for the amphoteric lipid mixture CHIM/CHEMS. Low values for κ were calculated in areas (blue zone) where also lipid

mixing was observed experimentally. The biophysical model predicts a zone with stable states at pH 7.5 and pH 4, a pronounced valley of instability in between and increased valley type fusion for mixtures having no more than 80% of CHIM. Also, the pH of maximum fusion should be lower when higher amounts of the anionic lipids are used. All these predictions were fully confirmed by the experimental data.

Similar findings were observed in amphoteric mixtures comprising pH-sensitive lipids having acyl chains, such as the anionic lipids 1,2-Dioleoyl-sn-glycero-3-succinate (DOGS) and 1,2-Dimyristoyl-sn-glycero-3-succinate (DMGS) (data not shown) or the pH-sensitive cationic lipid MoChol (see Figure 3.8).

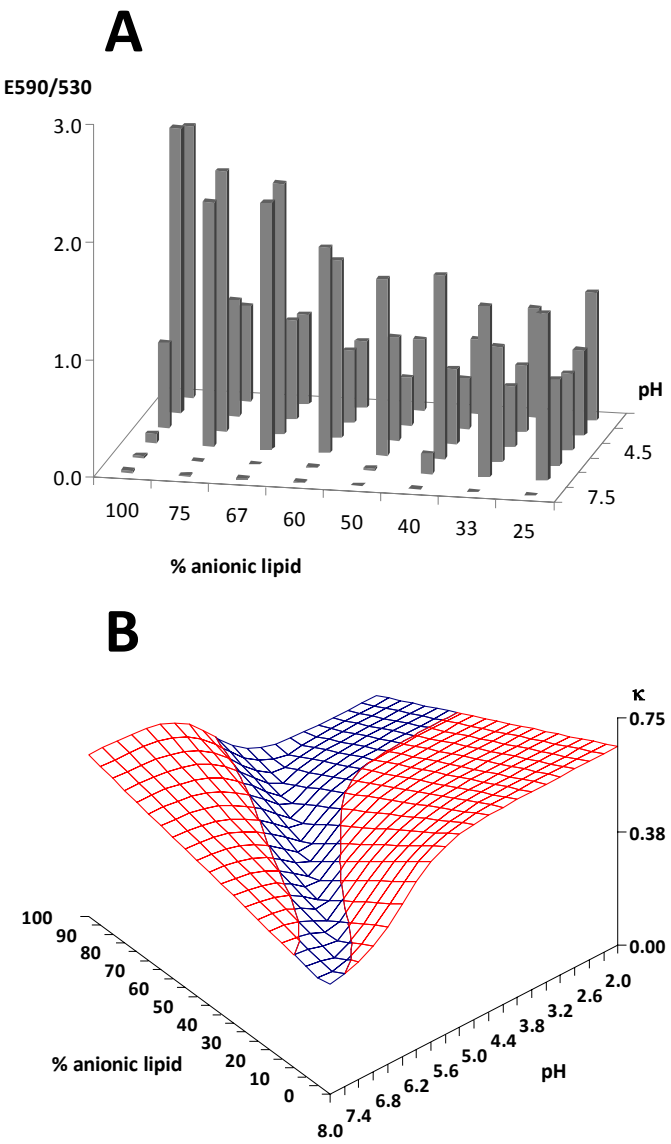

FIGURE 3.5: pH-dependent fusion properties of Amphoter II system. Liposomes from CHIM and CHEMS **(A)** were produced at pH 7.5, exposed to the pH indicated and neutralized after 2 hours. Fusion of the particles and lipid mixing was monitored by FRET at the end of the cycle; fusion maxima for amphoteric liposomes appeared at intermediate pH. **(B)** Phase diagram for amphoteric mixtures containing CHIM and CHEMS was calculated under the assumptions of ion binding to free, charged lipids and the formation of an ion-free lipid salt. For CHIM and CHEMS, a pH-dependent minimum of κ can be observed across a wide range of anionic lipid contents; all of these mixtures have amphoteric character.

3.2.3 Amphoter III system

The Amphoter III systems are composed of strong anionic lipids, such as DOPA, and an excess of pH-sensitive cationic lipids, behaving like the mirror image of Amphoter I systems. They provide a valley of fusogenicity as long as the weak cationic lipid is present in excess and over-compensates the constant charge on the opposite constantly

charged lipid. In contrast to Amphoter I systems, the pH for fusion locates higher than the pK_α of the pH-sensitive lipid.

Experimental evidence for the fusion valley of type III amphoteric mixtures is given in Figure 3.6 panel A. In this study, a series of Amphoter III liposomes were constructed from the stably charged anionic lipid DOPA, which exhibits pK_α values of ~3.0 and ~8.0 (Tocanne and Teissie´, 1990) and the pH-sensitive cationic lipid MoChol with a pK_α of ~5.8 (Andreakos et al., 2009).

As predicted by the mathematical model, illustrated in Figure 3.6 panel B, lipid mixing was observed and yielded a valley type fusion with the existence of a stable cationic phase only for MoChol/DOPA mixtures with an excess of MoChol. If an excess of DOPA is used, the fusion is shifted towards the low pH and was fully dominated by the behaviour of the stably charged DOPA.

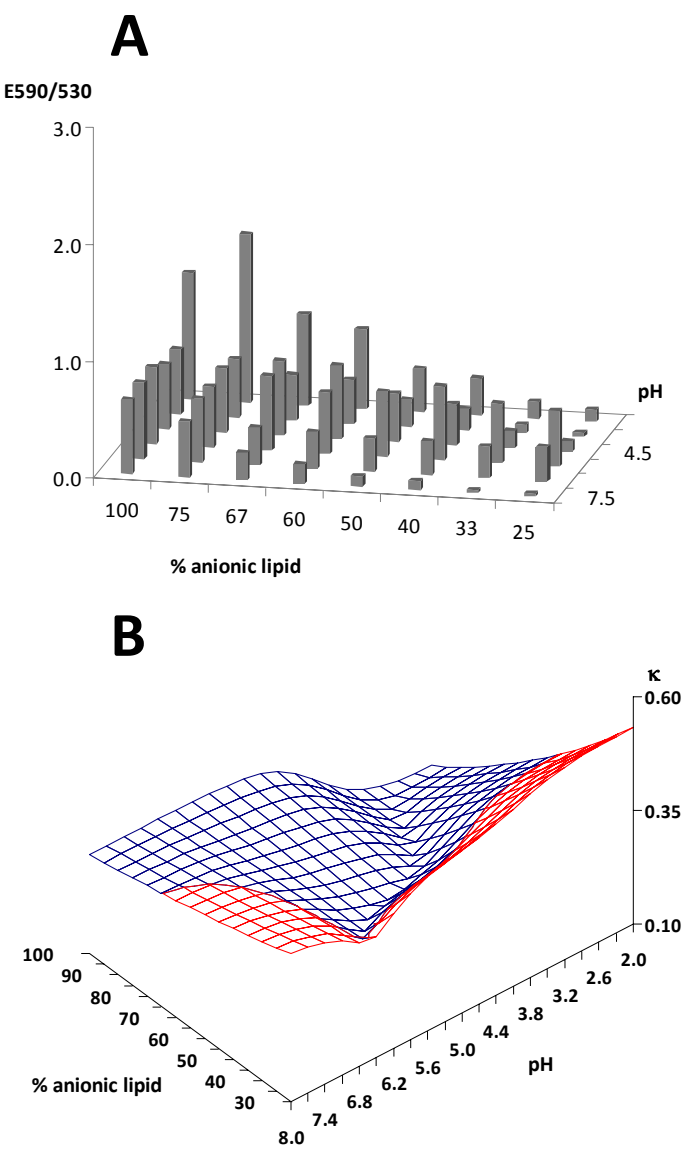

FIGURE 3.6: pH-dependent fusion properties of Amphoter III system. (A) Liposomes comprising the indicated amounts of the anionic lipid were produced from MoChol and DOPA and their pH-dependent lipid mixing was monitored by FRET at the end of the cycle; fusion maxima for amphoteric liposomes appeared at intermediate pH. **(B**) The phase diagram for MoChol/DOPA was calculated under the assumptions of ion binding to free, charged lipids and the formation of an ion-free lipid salt. Amphoteric mixtures of MoChol and DOPA require the molar fraction of the anionic lipid to lie in between 0.33 and 0.50 and biphasic stability is limited to this area.

Quite noticeable, the fusion between Amphoter III liposomes constructed from MoChol and POPG was greatly diminished in comparison to that of MoChol and DOPA (Figure 3.7 A), despite their almost identical lipid geometry. The only difference in the headgroup structure between the systems is the presence of an extra glycerol moiety that differentiates DOPA and POPG from each other.

Interestingly, the presence of this extra glycerol moiety in POPG largely inhibits the fusion behaviour. This may be due to steric hindrance of the lipid salt formation caused by the more bulky phosphoglycerol headgroup. A phase diagram calculated for the absence of lipid salt formation lacks the typical fusion valley (Figure 3.7 B).

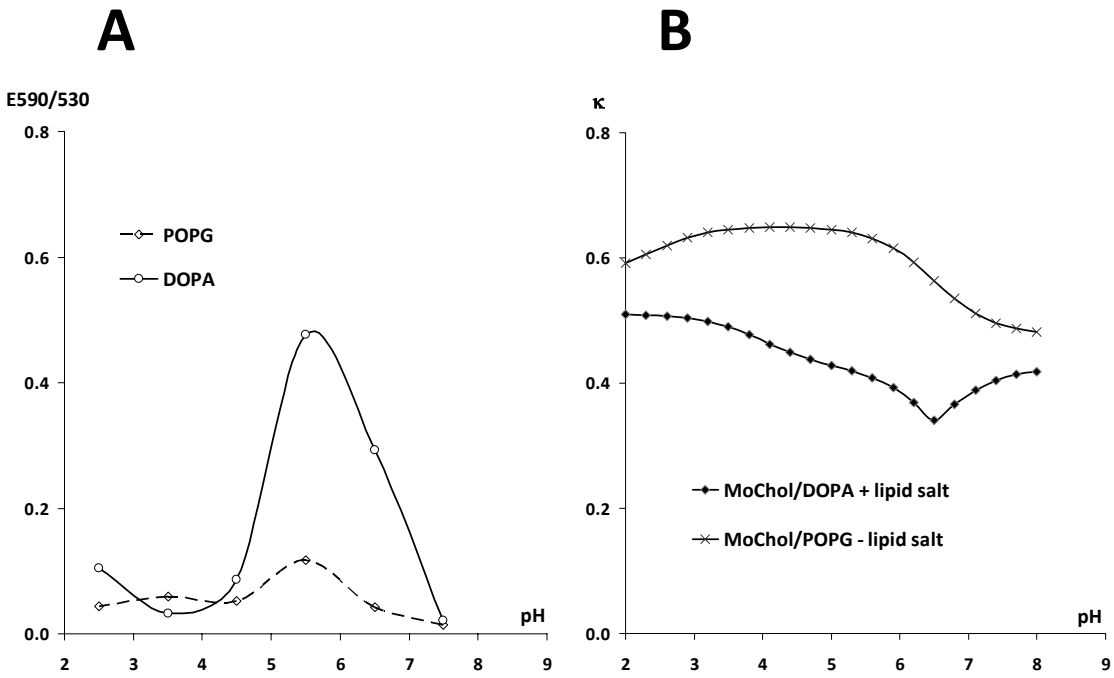

FIGURE 3.7: pH-dependent fusion properties of DOPA and POPG amphoteric liposomes. **(A)** shows an almost complete suppression of fusion in a system from MoChol and POPG (66:33 mol%). While contributing a strong anionic charge like DOPA, the extra glycerol moiety in POPG may prevent the charge interaction and lipid salt formation. Panel **(B)** shows the pH dependent values for κ for mixtures from MoChol/DOPA or MoChol/POPG (both 66:33 mol%), calculated with or without the assumption of a lipid salt formation. The non-fusogenic character of MoChol/POPG correlates with the abrogation of lipid salt formation in these mixtures.

To summarize, the predictions of the algorithm were confirmed to a great extend by the FRET experiments where the fusogenicity of the particles was analyzed. The proposed function for **κ** closely analyzes the interaction between oppositely charged lipids and describes the behavior of the Amphoter I, II and III systems tested; it reflects zones of stability at very low or neutral conditions and indicates a fusion valley at slightly acidic conditions.

3.3 High-Throughput Screen for lipid fusion

Relatively little is known concerning the structural properties of mixtures of bilayer-forming cationic and anionic lipids, which may be expected to exhibit bistable behaviour due to interactions between the positively and negatively charged headgroups. Based on the

collected results and considerations presented above, this screen sets out: (i) to investigate the fusion properties of amphoteric membranes comprising lipids with different or even common structural shapes and head/tail groups; (ii) to characterize the role of neutral/zwitterionic lipids in the amphoteric membrane by investigating their fusion properties; (iii) furthermore to develop new amphoteric lipid combinations with optimized parameters based on the lipid shape theory; which finally could potentially encapsulate oligonucleotides and fuse in response to intracellular acidic environments.

A screening of liposomal mixtures in a high throughput manner is designed to collect fusion data based on lipid mixing experiments for a wide range of amphoteric membranes. The screen was conducted using lipid combinations from all three amphoteric systems, comprising a wide range of stable and chargeable lipids, as well as neutral lipids included as a single lipid or a combination of different neutral lipids. An example is demonstrated in Figure 3.8, which

Date	Screen#	Plate	Cation	Anion	Neutral 1	Neutral 2
07.08.2007	75	5	MoChol	CHEMS	Chol	-

neutral lipid → 0%

Ratio cation:anion \ pH →	7.5	6.5	5.5	4.5	3.5	2.5
0.00	0.0	0.0	0.0	0.4	2.2	2.0
0.33	0.0	0.0	0.2	3.0	2.9	2.1
0.50	0.0	0.0	2.4	1.9	0.9	0.7
0.67	0.0	0.0	1.2	0.1	0.0	0.0
1.00	0.0	0.0	0.6	0.1	0.0	0.1
1.50	0.0	0.0	0.0	0.0	0.0	0.0
2.00	0.0	0.0	0.0	0.0	0.0	0.0
3.00	0.0	0.0	0.0	0.0	0.0	0.0

neutral lipid → 10%

Ratio cation:anion \ pH →	7.5	6.5	5.5	4.5	3.5	2.5
0.00	0.0	0.0	0.1	0.5	2.4	2.3
0.33	0.0	0.0	1.0	2.6	2.2	1.8
0.50	0.0	0.0	2.1	2.1	1.0	0.7
0.67	0.0	0.0	1.7	0.5	0.2	0.2
1.00	0.0	0.0	0.9	0.1	0.0	0.0
1.50	0.0	0.0	0.0	0.0	0.0	0.0
2.00	0.0	0.0	0.0	0.0	0.0	0.0
3.00	0.0	0.0	0.0	0.0	0.0	0.0

neutral lipid → 20%

Ratio cation:anion \ pH →	7.5	6.5	5.5	4.5	3.5	2.5
0.00	0.0	0.0	0.1	0.5	2.3	2.3
0.33	0.0	0.0	1.0	2.5	2.2	1.6
0.50	0.0	0.0	2.3	2.3	1.6	1.1
0.67	0.0	0.0	2.1	1.4	0.6	0.4
1.00	0.0	0.0	1.6	0.1	0.1	0.1
1.50	0.0	0.0	0.1	0.0	0.0	0.0
2.00	0.0	0.0	0.0	0.0	0.0	0.0
3.00	0.0	0.0	0.0	0.0	0.0	0.0

neutral lipid → 30%

Ratio cation:anion \ pH →	7.5	6.5	5.5	4.5	3.5	2.5
0.00	0.0	0.0	0.1	0.5	2.3	2.5
0.33	0.0	0.0	1.1	2.5	2.1	1.5
0.50	0.0	0.0	2.1	2.3	1.5	1.3
0.67	0.0	0.0	1.9	1.7	0.9	0.8
1.00	0.0	0.0	1.6	0.2	0.1	0.1
1.50	0.0	0.0	0.7	0.0	0.0	0.1
2.00	0.0	0.0	0.1	0.0	0.0	0.0
3.00	0.0	0.1	0.0	0.0	0.0	0.0

neutral lipid → 40%

Ratio cation:anion \ pH →	7.5	6.5	5.5	4.5	3.5	2.5
0.00	0.0	0.0	0.1	0.5	2.7	2.7
0.33	0.0	0.0	1.2	2.7	2.4	1.6
0.50	0.0	0.0	2.3	2.4	1.7	1.4
0.67	0.0	0.0	2.0	2.3	1.3	1.2
1.00	0.0	0.0	1.9	0.4	0.3	0.4
1.50	0.0	0.1	0.6	0.1	0.1	0.2
2.00	0.0	0.1	0.1	0.0	0.1	0.3
3.00	0.0	0.3	0.0	0.0	0.1	0.1

neutral lipid → 50%

Ratio cation:anion \ pH →	7.5	6.5	5.5	4.5	3.5	2.5
0.00	0.1	0.1	0.1	0.6	2.6	2.7
0.33	0.1	0.0	1.6	3.0	2.6	2.1
0.50	0.0	0.1	2.6	2.6	1.9	1.7
0.67	0.0	0.0	2.1	2.1	1.3	1.1
1.00	0.0	0.0	1.9	1.2	0.5	0.4
1.50	0.0	0.2	1.4	0.6	0.2	0.6
2.00	0.0	0.4	0.5	0.3	0.3	0.5
3.00	0.0	0.8	0.1	0.2	0.2	0.3

FIGURE 3.8: Fusion matrix of amphoteric liposomes obtained by HTS. Liposomes comprising MoChol, CHEMS and Chol as neutral lipid were produced at pH 7.5 and adjusted to acidic conditions to promote fusion. The cation:anion molar ratio was changed from 0 to 3 and the amount of neutral lipid from 0% to 50%. Intensity of fusion expressed as E590/530: less than 1 = pink; between 1 and 2 = red; more than 2 = dark red.

shows data obtained from an Amphoter II system. The amphoteric mixtures were prepared from MoChol, CHEMS and the neutral lipid cholesterol. By changing the amount of neutral lipids from 0% to 50% and using eight different ratios of the charged lipids, a total of 48 specific combinations were produced and the fusion effect was tested. The liposome solutions were shifted to different acidic pHs ranging from 2.5 to 7.5 and FRET signals were measured. The experimental procedure is based on our first experiments, as been described in section 3.2.1. Experimental details are provided in the MATERIALS & METHODS section 2.2.

The results show that these amphoteric liposomes are characterized by a biphasic stability, which depends on the molar ratio of cationic to anionic lipid. For all cation to anion molar ratios, a fusion valley was shown around their isoelectric point. Clearly, in comparison to the carriers with 1.5 to 3 molar ratios, the liposomes prepared with molar ratios from 0.0 to 1.0 were more fusogenic. In general, the fusogenicity of amphoteric liposomes comprising MoChol and CHEMS decreases with an increasing molar ratio. It was also clearly found that in all ratios the addition of the helper lipid cholesterol significantly improves the fusion behaviour of the amphoteric liposomes. The data obtained from this screen also provides specific optimal ratios between the charged lipids depending on the amounts of neutral lipid being used. As an example, an optimum of cation to anion molar ratio of 1.5 has been found for liposomes having 30% to 50% cholesterol in comparison to that with lower amounts of cholesterol. Finally, it has been found that the addition of cholesterol to the amphoteric lipid mixture MoChol/CHEMS does not have any impact on its isoelectric point (fusion valley).

3.3.1 Charge only systems-Size of headgroup can modulate amphoteric membrane fusion

The Panzner algorithm predicts reduced fusogenicity for liposomes from charged amphiphiles with larger polar headgroups. This prediction was confirmed by using homologues of either CHEMS or MoChol in an Amphoter II system or homologues of CHEMS in combination with DOTAP in an Amphoter I system.

As shown in the diagrams of Figure 3.9, enlargement of the lipid headgroups results in reduced fusion of the entire amphoteric system. Said reduction in fusogenicity could be triggered both from the anionic or cationic lipid, consistent with the thesis that the anionic and the cationic headgroup form a lipid salt. Although both large lipid headgroups and large counterions reduce the fusogenicity of the bilayer, they differ in their profile for such stabilization. Polar headgroups are an integral part of the lipid bilayer and stabilize the membrane irrespective of

its charged state, including the fusion zone. The counterions, being displaceable upon lipid salt formation, selectively stabilize the charged states of the bilayer, but have no impact on the fusion itself. This recommends large counterions for the specific stabilization of fusogenic lipid membranes at neutral pH without compromising the fusion properties of these materials.

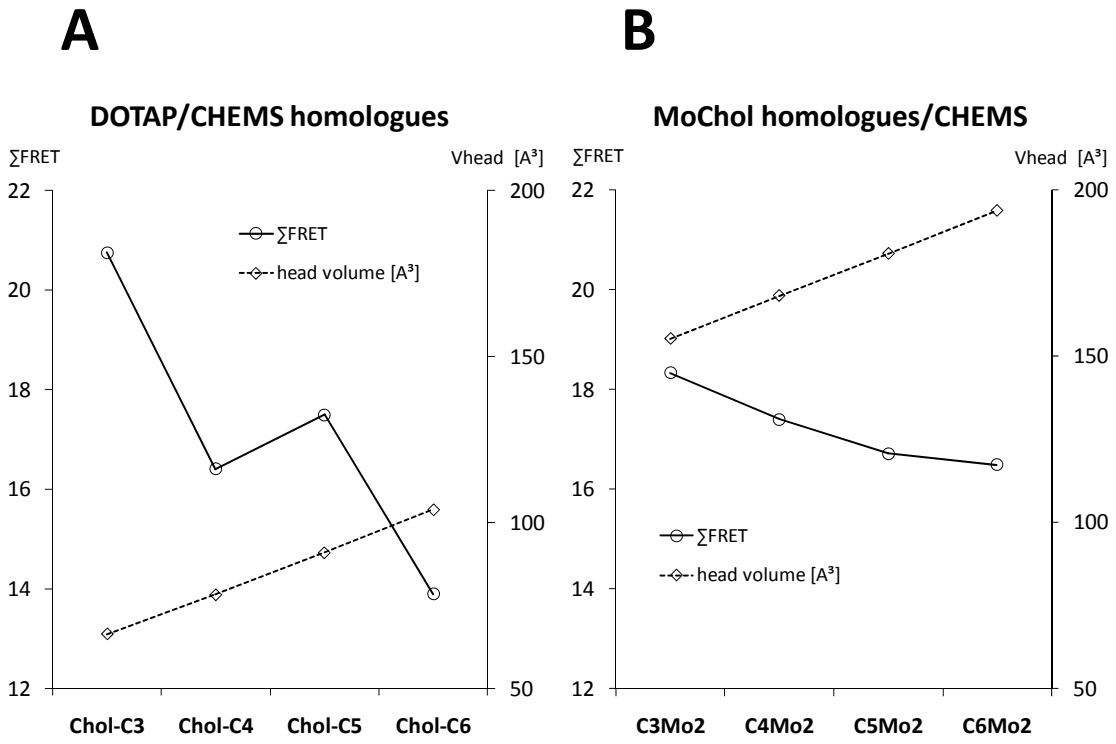

FIGURE 3.9: For charged lipids, liposome fusion correlates with the head group volumes. (A) The cationic lipid DOTAP was combined with CHEMS homologues having the indicated numbers of carbon atoms in their polar head group. For each of the combinations, a series of liposomes having cation:anion ratios between 0.17 and 0.75 were tested for their pH induced fusion; the summarized FRET signal is plotted here. Elongation of the anionic head group and increase of its volume continuously diminishes the fusion tendency for these systems. **(B)** Homologues of MoChol were tested for their fusion propensity with CHEMS as in (A), but using cation:anion ratios between 0.33 and 3; a decrease of fusion was associated with larger headgroups.

3.3.2 Fine tuning of amphoteric membrane fusion by the addition of neutral or zwitterionic lipids

In a second step, a screen was set up to determine whether the addition of lipids without any pH-responsive elements would result in changes in the fusion behaviour of the amphoteric membrane. The following experiments therefore elucidate the influence of increasing amounts of neutral/zwitterionic lipids, such as phosphatidylcholine, on the pH-dependent fusion properties of amphoteric mixtures, which were selected from all three Amphoter systems.

The anions used in this part include CHEMS, DMGS, DOGS and DOPA. CHEMS and DMGS are widely used for liposomal formulations, having the identical anionic group but a different lipid anchor. The pH-sensitive lipid DOGS is structurally related to DMGS and according to their molecular volumes (small headgroup) both could easily adopt the inverted hexagonal phase in a pH-dependent manner, therefore being considered as fusogenic lipids. The fourth anionic lipid chosen was the stable anion DOPA. For the construction of the three Amphoter systems (I, II, and III) two different cationic lipids were used. The pH-sensitive cation MoChol was used for the preparation of Amphoter II and III systems and the stable cation DOTAP for the Amphoter I system.

TABLE 3.1: Amphoteric mixtures in combination with neutral lipids tested in the second step.

AMPHOTERIC MIXTURE	NEUTRAL SYSTEM		
(1) DOTAP/DMGS	DOPC	DOPC/Chol 2:1	POPC/DOPE 3:1
(2) DOTAP/DOGS	POPC	DOPC/Chol 2:1	POPC/DOPE 1:1
(3) MoChol/DOGS	Chol	DOPC/Chol 1:2	POPC/DOPE 1:3
(4) MoChol/CHEMS	DOPE		
(5) MoChol/DOPA		POPC/Chol 2:1	DOPE/Chol 2:1
		POPC/Chol 1:1	DOPE/Chol 1:1
		POPC/Chol 1:2	DOPE/Chol 1:2

The amphoteric mixtures were prepared by addition of 0-50% of different neutral or zwitterionic lipids or mixtures thereof. Lipids such as POPC, which prefers the lamellar phase, or DOPE, which easily adopts the hexagonal phase and therefore may lead to fusogenic liposomes even at high neutral lipid content, were used. Table 3.1 summarizes the amphoteric mixtures and the lipid combinations tested in this step of the screen. Fusion was measured for a series of liposomes having different cation to anion molar ratios. The effect of the neutral lipids was analyzed using the sum of all such measurements in the entire matrix over the series lipids was analyzed using the sum of all such measurements in the entire matrix over the series of the six different pHs. Values are expressed as ∑Fret. Experimental details are provided in the MATERIALS & METHODS section.

The results obtained from this part of the screen are summarized in Figure 3.10. It is apparent that lipids having acyl chains with a cylindrical shape, such as POPC or DOPC, decrease the fusogenicity of all amphoteric mixtures. Especially in the Amphoter II system MoChol/CHEMS and Amphoter III system MoChol/DOPA (Panel 3/5 A, B and C), the fusion is being completely dismissed upon addition of 30% POPC or DOPC. Similar results were observed when the two lipids were combined either with DOPE or cholesterol. The experimental evidence in panel 4 B

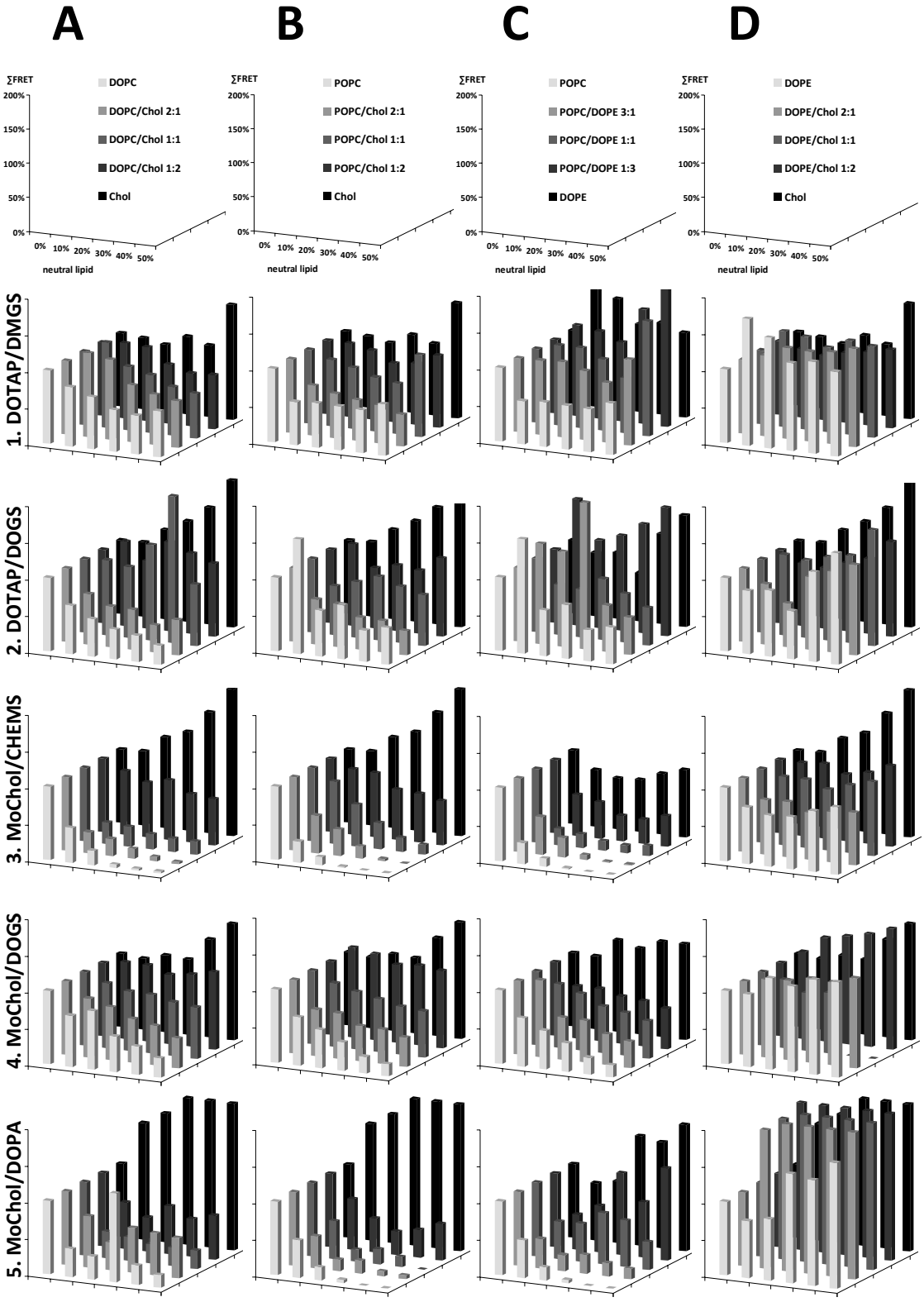

FIGURE 3.10: Impact of neutral and zwitterionic lipids on the fusion properties of amphoteric liposomes. Amphoteric mixtures (1-5) were prepared containing increasing amounts (0-50%) of a single neutral lipid, zwiterionic lipid or a combination thereof (A = DOPC/Chol; B = POPC/Chol; C = POPC/DOPE; D = DOPE/Chol). Intensity of fusion is expressed as % ∑FRET in the matrix cation:anion (C:A) ratio over a series of the different pH steps; C:A = 0.17, 0.33, 0.40, 0.50, 0.67, 0.75 for DOTAP/DMGS; 0.33, 0.50, 0.67 for DOTAP/DOGS; 0.33, 0.50, 0.67, 1, 2, 3 for MoChol/CHEMS and MoChol/DOGS; 1.5, 2, 3 for MoChol/DOPA. The ∑FRET for 0% neutral is set to 100%.

demonstrates that increasing amounts of a mixture containing POPC and cholesterol in a molar ratio 2:1 diminishes the fusogenicity of MoChol/DOGS liposomes.

As shown in panel 4 A, increasing molar ratios of DOPC and cholesterol mixtures also reduce the fusogenicity of the system. It is also clear that the impact factor on the fusogenicity of amphoteric lipid systems depends on the ratios of the two lipids. The higher the molar ratio, the lower the fusogenicity of the amphoteric liposomes. It has also been found that in case of both DOTAP/DMGS and DOTAP/DOGS, addition of POPC/DOPE mixture in a molar ratio of 1:3 even leads to an improvement of fusogenicity at higher amounts. As expected, the presence of DOPE and cholesterol in the membrane of the amphoteric liposomes does not affect the fusogenicity and may even lead to a significant improvement. Mixtures comprising the two lipids demonstrate a similar behaviour.

It becomes apparent that amphoteric lipid systems having a low fusogenicity can be clearly improved by the addition of neutral or zwitterionic lipids. Furthermore, the results indicate that neutral or zwitterionic lipids may have also an impact on the range of fusogenicity. This means that the range of cation to anion ratios can be broadened or narrowed depending on the neutral or zwitterionic lipid used in the mixtures. It is of course possible to use mixtures of different neutral lipids to optimize the balance between fusogenicity and stability of such systems.

3.3.3 Algorithm predicts impact of neutral lipid

The model also applies to amphoteric lipid mixtures further comprising neutral lipids. Another point of interest is to which extent the addition of neutral or zwitterionic lipids correlates with the fusion of amphoteric liposomes as predicted by the algorithm.

For a theoretical prediction we used κ of 0.1 for cholesterol, 0.19 for DOPE and 0.55 for POPC, a reasonable assumption in the light of the different headgroup structures for POPC and DOPE suggested by molecular dynamics simulations (Pandit et al., 2003; Suits et al., 2005; Murzyn et al., 2006). The reported betaine structure for the PE headgroup excludes additional ion adsorption, while the open conformation of PC facilitates ion recruitment to its phosphate and, to a lesser extent, its ammonium group and concomitant headgroup enlargement. Since fusion of DOTAP/CHEMS and MoChol/CHEMS liposomes is observed when κ for the entire system falls below 0.25 and 0.4 respectively, the first two lipids, but not POPC were expected

to improve the fusogenic properties of the amphoteric mixtures. The calculated propensity for liposome fusion was expressed as κ_{MIN}, the minimum for κ_{pH} observed at the isoelectric point of a given system.

This correlation was investigated using mixtures of DOTAP/CHEMS and MoChol/CHEMS at a molar ratio 0.5 and 0.67 respectively, containing increasing amounts (0 to 50%) of the neutral

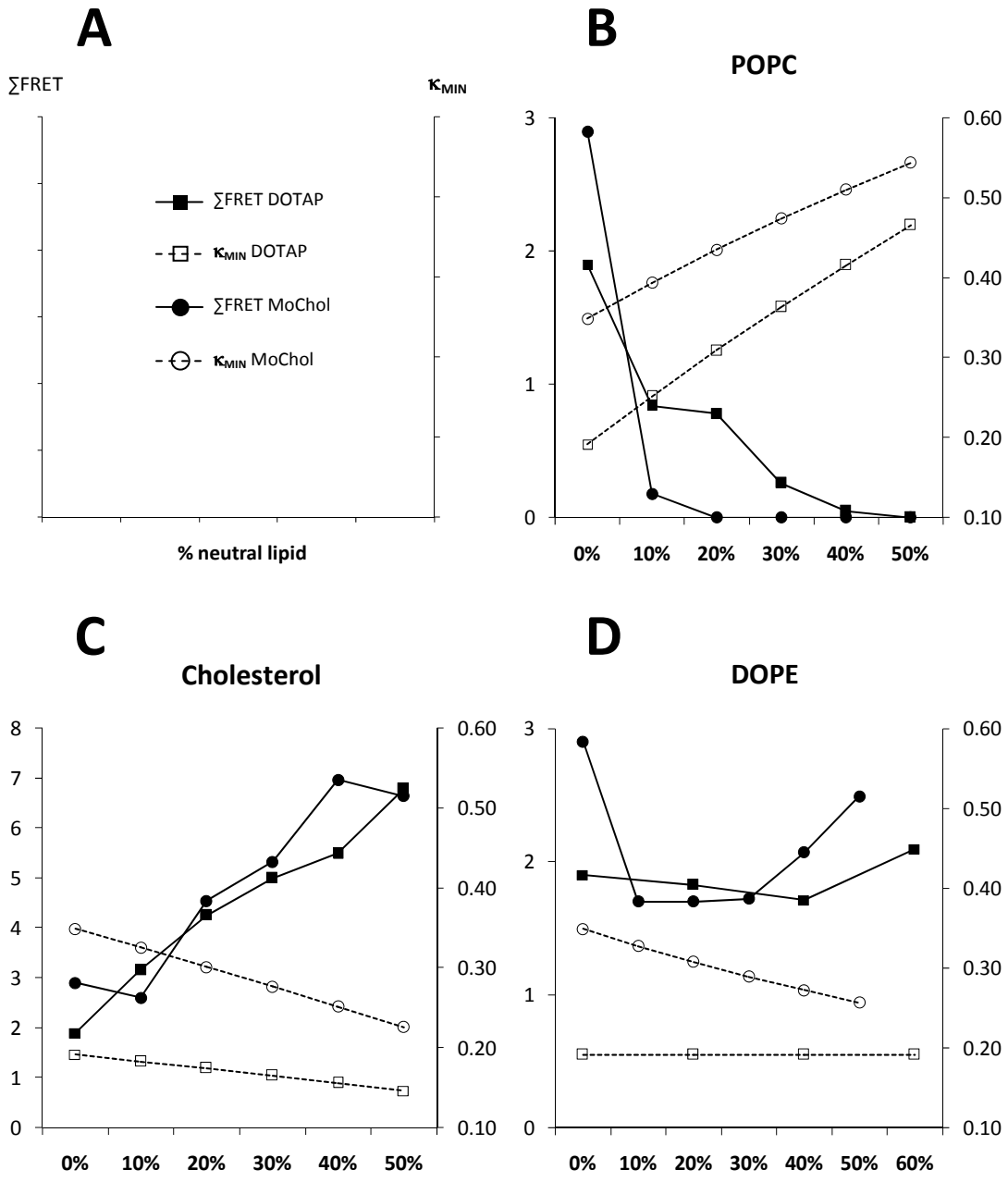

FIGURE 3.11: For neutral lipids, liposome fusion correlates with the headgroup volumes. (A) displays legends and axes for all subsequent figures, **(B-D)** The impact on the fusion of DOTAP/CHEMS (33:67 mol%) or MoChol/CHEMS (40:60 mol%) liposomes was analyzed upon admixture of 0% to 50% POPC (B), cholesterol (C) or DOPE. Lipid mixing was expressed as the summarized FRET signal over a series of different pH steps; the second axis shows the minimum of κ_{pH} for each system.

lipids mentioned above. Panel B in Figure 3.11 demonstrates the rapid loss of the pH-induced fusion upon admixture of POPC and its inverse correlation with higher values of κ_{MIN}, while panel C shows increased fusogenicity upon addition of cholesterol and concomitantly lower values κ_{MIN}. It was also found that an admixture of DOPE to a system of DOTAP/CHEMS does not change κ_{MIN} and has little or no effect on the fusion. Addition of 10% DOPE to MoChol/CHEMS diminishes fusion, while higher amounts re-establish lipid mixing, as predicted by the decrease of κ_{MIN} (Figure. 3.11 D).

These findings correlate strongly with the results shown in Figure 3.11. The experimental evidence obtained in the second step of the HTS (see section 3.3.2) confirmed improved fusogenicity upon the addition of neutral or zwitterionic lipids having lower κ values than those of the amphoteric mixtures and a reduced or abolished fusion when adding lipids with higher values.

In summary, the performed High-Throughput Screen based on FRET measurements has shown to be a valuable tool for the broad selection of lipids in order to improve and characterize the fusion ability of liposomal carriers. Additionally, the data presented in this section again verify the predictions of the model. While the pH-induced binding or loss of counterions provides a sufficient explanation for the phase transition observed in fusion competent bilayers of one charge, the data support an additional lipid salt formation in membranes comprising oppositely charged lipids. The fusogenicity of amphoteric liposomes critically depends on lipid salt formation and can be modulated by headgroup size or through the addition of neutral lipids. In contrast to these factors, ions do not modulate the fusion characteristics of amphoteric liposomes, but large counterions can be instrumental in stabilizing their charged state.

3.4 Fusion studies with vesicular models of the cell membrane

Since it is an essential process for cell survival, membrane fusion has been widely studied using artificial membranes. Therefore, in order to promote fusion between two different vesicular membranes, it is important to facilitate closer membrane proximity and transition into non-lamellar phases. In the case of liposomes, the two contacting membranes are the outer monolayer of the vesicle and the inner monolayer of the endosomal membrane. The fusion behaviour of amphoteric liposomes with different models of cellular membranes was investigated in the following experiment.

The organisation of lipid molecules in most biological membranes is that of a bimolecular layer of lipid molecules, or bilayer (Gruner et al., 1985). The lipid constituents of the most biological membranes can be classified as sphingamine, glycerol and sterol. The inner lipid layer of most eukaryotic membranes is composed of phosphatidylserine and phosphatidylethanolamine, while the outer monolayer harbours most of the phosphatidylcholine, sphingomyelin and cholesterol (Jaaskelainen et al., 1998; Tamaddon et al., 2007). The models were developed based on the lipid composition of the cellular membranes. Therefore, it was decided to develop models of plasma and endosomal membranes in a way that their fusion with liposomes during the internalization into cells is probable. The models were designed based on the physicochemical properties of the mentioned membranes.

As models for the simulation of possible cellular membranes, NBD-PE marked liposomes were prepared using the lipids cholesterol, DOPE, POPC and sphingomyelin. Anionic phosphatidylserine lipids were excluded from the models in order to create target membranes with neutral surface to avoid any physicochemical artefacts. The experiment was performed using three basic membrane simulation models: (i) POPC and Cholesterol, (ii) POPC and DOPE and (iii) a mixture of cholesterol, POPC and sphingomyelin. The liposomes were prepared using different amounts of each lipid. The lipid compositions of the above-mentioned models are shown in Table 3.2. These represent approximate early/late stage endosomal membranes.

TABLE 3.2: Lipid composition of model cellular membranes

	Lipid composition in mol%		
	A. POPC/Chol	B. POPC/DOPE	C. POPC/SM/Chol
1.	15:85	18:82	0:50:50
2.	23:77	33:67	33.3:22.2:44.4
3.	37:63	50:50	33.3:33.3:33.3
4.	50:50	65:35	33.3:44.4:22.2
5.	100:0		66:17:17
6.			50:50:0

As the carrier membrane, amphoteric liposomes were first prepared containing the lipids DOTAP and DMGS. The amphoteric particles were modified with *N*-Rh-PE and prepared using different cation to anion molar ratios. The liposomes were incubated with the simulated vesicular models and FRET signals were measured.

Figure 3.12 shows the results obtained in this experiment. The incubation of the DMGS liposomes with the POPC/Chol vesicular models of the cell membrane resulted in a very significant decrease of the fusion measurements. As expected, the sum of FRET (∑FRET) signals decreased upon admixture increasing amounts of phosphatidylcholine. Similar results were

found for the vesicular models POPC/DOPE and POPC/SM/Chol. The data support that the presence of POPC and sphingomyelin dominates the fusion behaviour independent of the helper lipid cholesterol or even DOPE. These results proposed that the fusion of the two non-identical membranes at least partially depends on the fusion character of the model membrane, which is dominated by the amount of PC lipids. As a matter of fact, early and late stage of endosomes exhibit different lipid compositions, which makes it difficult to determine their fusion behaviour. Therefore, the question is whether the properties of the carrier membrane can be designed in a way to improve fusion behaviour.

In the next step, the model membranes were target using an amphoteric mixture with enhanced fusion properties as predicted by the algorithm. Liposomes comprising DOGS were tested. DOGS and DMGS have an identical polar headgroup but different hydrophobic parts. The DOGS hydrocarbon chain contains two double bonds and four additional carbon atoms than that of DMGS. In this case the shape parameter κ is smaller than the κ calculated for DMGS, resulting to a highly fusogenic membrane. Indeed, when mixtures of DOGS were incubated with the model membranes, an overall increase of FRET signals upon acidification

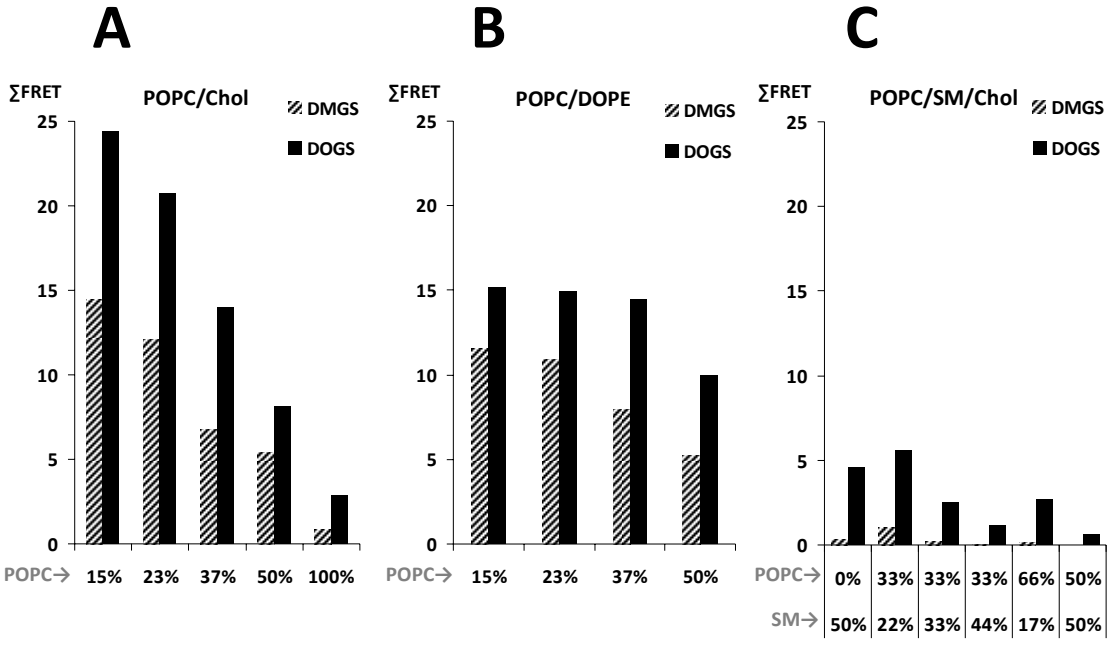

FIGURE 3.12: pH-dependent fusion properties of amphoteric membranes upon incubation with model cellular membranes. Mixtures composed of DOTAP/DMGS and DOTAP/DOGS were incubated with three different vesicular membranes. Data are presented for mixtures in several molar ratios of **(A)** POPC/Chol, **(B)** POPC/DOPE and **(C)** POPC/SM/Chol. All liposomes prepared at pH 7.5 were then incubated in buffers with the low pH values. Fusion and lipid mixing were monitored, as described in Materials and Methods. Lipid fusion presented in the y axis; is expressed as the summarized FRET signal over a series of different pH steps for the following cation to anion molar ratios: 0.17, 0.4, 0.33, 0.5, 0.67 and 0.75.

was observed. The data implies that the amphoteric membrane due to its optimized design was able to significantly improve the fusion level independent of the type of the target membrane.

Conclusively, the data implies that amphoteric membranes could fuse with the endosomal membranes at acidic pH while the liposomes are stable at neutral conditions and therefore could not fuse with plasma membrane. These models also can serve as a screening tool to predict and improve the fusogenic behaviour of a liposomal membrane in cellular studies. Subsequently, they could be useful for studying the fusion dynamic between the endosomal and the liposomal membrane.

3.5 Intracellular delivery of siRNA mediated by amphoteric liposomes

In recent years, lipid-mediated-gene transfer has become a versatile tool for cellular transfection, relevant to fundamental cell biological research and gene therapy alike. The above-presented lipid mixing experiments demonstrated that amphoteric liposomes can be produced in their stable cationic state which facilitates efficient loading with oligonucleotides; they adopt a second stable state at neutral pH and transit into a fusogenic state when exposed to the slightly acidic conditions.

Previous works suggested that pH-sensitive liposomes follow an endocytic pathway and exhibit strong membrane fusion in acidic environments, such as those inside the endosomal compartments, and are expected to result in cytosolic/cytoplasmatic translocation of the nucleic acid payload (Budker et al., 1996; Zhang et al., 2006; Chiu et al., 2004). To this end, an example is demonstrated in Figure 3.13, which shows the intracellular localization of an

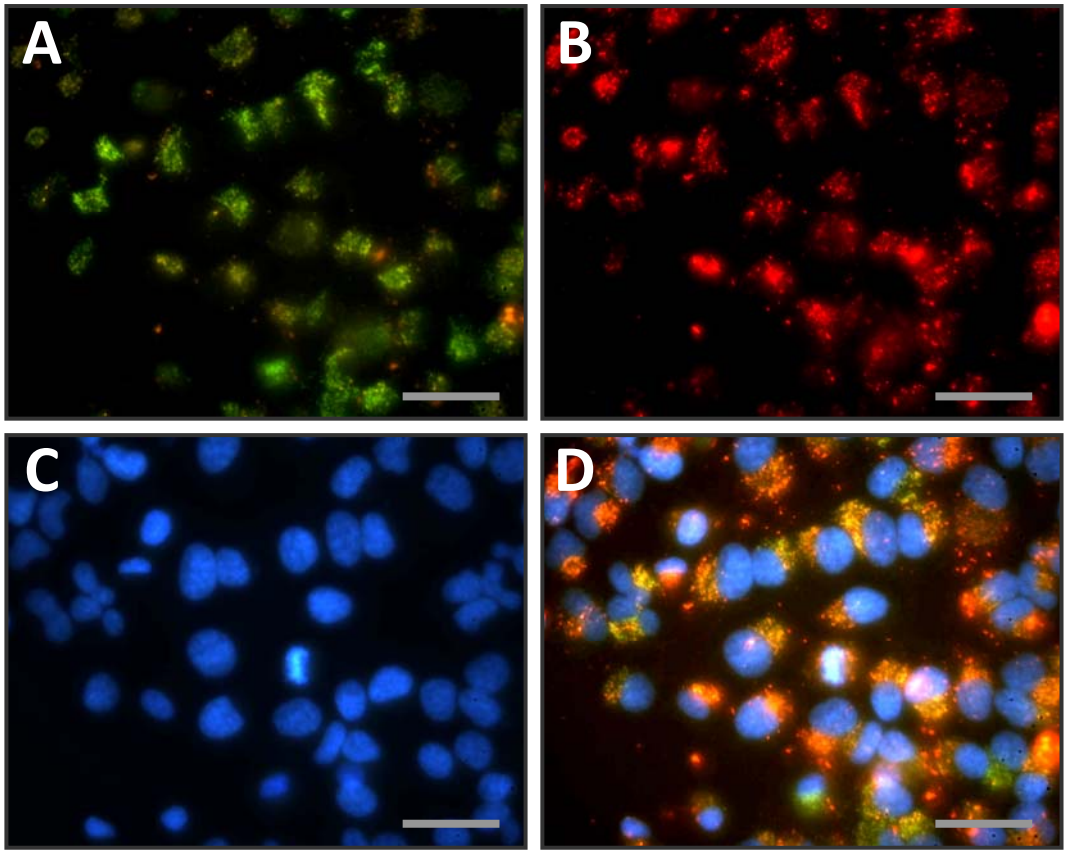

FIGURE 3.13: Intracellular localisation of MoChol/CHEMS liposomes. (A) HeLa cells were preincubated with 200 µg FITC-dextran to mark the endosomal/lysosomal pathway. **(B)** After washing, the cells were incubated for 24 hours with 200 µM empty 0,5 % N-Rh-PE labelled amphoteric liposomes (red) that had been prepared from MoChol and CHEMS in a molar ratio 1:2. **(C)** The nuclei were stained with 1µg/ml Hoechst dye **(D)** Overlay; Note that the liposomes are mostly colocalized with dextran at the perinuclear region. (40x Objectiv; Exposure 1500 ms).

amphoteric liposome comprising MoChol and CHEMS (33:67 mol%) examined by fluorescence microscopy. Human cancer cells were incubated with the amphoteric mixture, marked by *N*-Rh-PE labelling (red), and the endosomal marker FITC-dextran (Shi et al., 2002; Shurety et al., 1998). The internalized labelled liposomes can be discerned as a fine-punctuated fluorescence, which primarily localizes at perinuclear regions of the cells. The perinuclear localisation reflects the presence of carriers in the endosomal-lysosomal pathway, as demonstrated by a colocalisation of FITC-dextran, presented in the merged picture (D).

Therefore, the next step was the evaluation of carrier ability to transport siRNA into the cytosol of the target cell. Furthermore, the correlation of their activity in a biological system with their structure expressed by the shape parameter κ was analyzed and validated. For that, wide arrays of carriers were systematically screened for their ability to mediate RNAi in various cell types.

3.5.1 Screen design for siRNA *in vitro* application

In this set of experiments, the potential of different amphoteric liposomes to transfect Plk1 siRNA *in vitro* using human cancer cells was assessed. The screen includes liposomes comprising different lipids which were selected according to their fusion properties characterized in the FRET experiments described above. Anionic lipids; such as the ionisable acidic DMGS, or cholesterol conjugates, such as CHEMS and derivates thereof, were mixed with permanently charged cationic lipids, such as DODAP (N-[1-(2,3-Dioleoyloxy)propyl]-N,N-dimethylamine) or DOTAP, or ionisable cationic lipids, such as cholesterylimidazol (CHIM) or morpholinocholesterols (MoChol and derivatives thereof). All amphoteric mixtures were at least prepared with increasing amounts of the helper lipid cholesterol, which has been identified in the fusions screen to act as an enhancer of the amphoteric fusions properties. Other neutral lipids used were mixtures prepared from DOPE and POPC, POPC or DOPE with cholesterol.

The Plk1 gene was chosen as a target for mediated down-regulation due to its ubiquitous expression at relatively constant levels and the simplicity to monitor Plk1 knockdown using a cell viability assay kit (Haupenthal et al., 2007). Plk1 is a serine/threonine kinase that performs several important functions throughout the M phase of the cell cycle, including the regulation of centrosome maturation and spindle assembly (Golsteyn et al., 1995; Lane and Nigg, 1996). A reduction of Plk1 induces mitotic arrest and apoptosis in proliferating tumor cell culture (Wolf

et al., 1997; Takai et al., 2005). Thus, cell viability can be used as a read-out for siRNA transfection. In addition, cell proliferation also serves as a marker for identifying cellular toxicity resulting from transfection.

Small-scale hand-batches of amphoteric liposomes were loaded with Plk1 and scrambled siRNA using an advanced loading procedure, as described in the MATERIALS & METHODS section 2.8. The final concentration of the encapsulated siRNA molecules was calculated assuming a 60% encapsulation efficacy. Each formulation was tested in a dose response manner using 6 different concentrations ranging between 0.1-200 nM, each point was calculated as the mean value from a physical triplicate. Once added to the culture medium, the amphoteric liposomes were not removed from the cells. To circumvent variations between different culture plates, both the Plk1 and the control siRNA formulations were manufactured in parallel and transfected in one single culture plate. 72 hours post transfection, cell viability was determined and IC50 values were derived from the data.

The toxicity to a given cell line can be identified by transfecting cells with a negative control siRNA; also referred to as scrambled siRNA (SCR). Therefore, two values were used to evaluate the results of the assay. One is the effect of the control siRNA and the other the Plk1 siRNA treated cells in comparison to the control (Figure 3.14). The mean fluorescence values derived from the triplicate of transfected cells were related to the mean fluorescence value determined from the untreated cells; also referred as buffer treated cells (10 wells in each plate); which was defined as 100% cell viability. In addition, wells without cells but

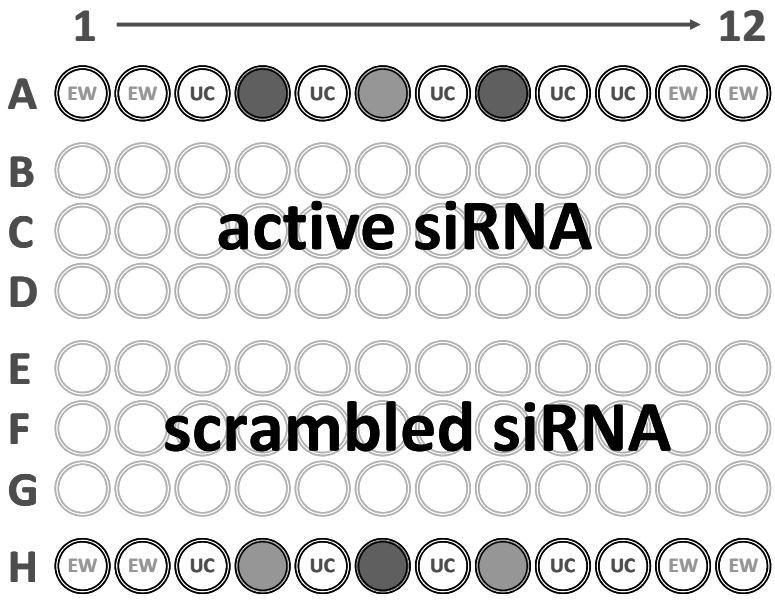

FIGURE 3.14: Schematic illustration of a 96 well transfection plate. Each plate contains two different amphoteric mixtures; each loaded with Plk1 and scrambled siRNA. The wells B1-D12 contain the Plk1 oligo formulations; the wells E1-G12 the scrambled oligo formulations. Transfections were performed in triplicate wells and siRNA concentration was used in a dose dependent manner (6). The wells in row A and H are used for the transfection procedure controls; UC: untreated cells, equivalent to 100 % survival; EW: empty wells, mediums background fluorescence; dark grey wells: Plk1 control formulation; light grey wells: scrambled control formulation;

containing only medium, the so-called empty wells, were used for an assessment of the background fluorescence. Further experimental details are provided in the MATERIALS & METHODS section.

A reference sample from 24% DODAP, 36% DMGS and 40% cholesterol was freshly prepared on each day to positively control production and transfection, this control formulation was established in pre experiments. As shown in Figure 3.14, all controls were placed on every MTP in row A and H. The liposomes encapsulating the two siRNAs (Plk1 and scrambled siRNA) were added in the rows B-D and E-G, respectively.

An example of data obtained from the cell screen is shown in Figure 3.15. Amphoteric liposomes comprising DODAP, CHEMS and increasing amounts of cholesterol were loaded with siRNA targeting Plk1 and a scrambled siRNA. The *in vitro* analysis revealed several trends in amphoteric liposomes capable of delivering siRNA to HeLa cells. These results show that amphoteric liposomes in general are relatively non cytotoxic at the concentration ranges in which they are efficacious. Clearly, the transfection efficiency depends on the molar ratio of cationic to anionic lipid. In comparison to the carriers with 0.33 or 0.82 molar ratios, liposomes prepared with molar ratios 0.50 or 0.67 were more effective in delivering siRNA.

It was also clearly found that in all four ratios the addition of the helper lipid cholesterol improves significantly the transfection efficiency of the amphoteric liposomes. Plk1 siRNA delivered in the absence of cholesterol did not cause a significant inhibition of the cell proliferation. On the contrary, addition of 20% cholesterol improved the delivery potential at least 3fold and blocked the cell proliferation almost completely. The data obtained from this screen provide specific optima of the neutral lipid content depending on the ratio of the charged lipids used. As an example, an optimum of 50% cholesterol has been found for liposomes having a cation to anion molar ratio of 0.33. For 0.50 molar ratios, 30% or 40% cholesterol is necessary to enhance transfection efficiency.

Date	Screen#	Cation	Anion	Neutral 1	Neutral 2
08.06.2008	75	DODAP	DMGS	Chol	-

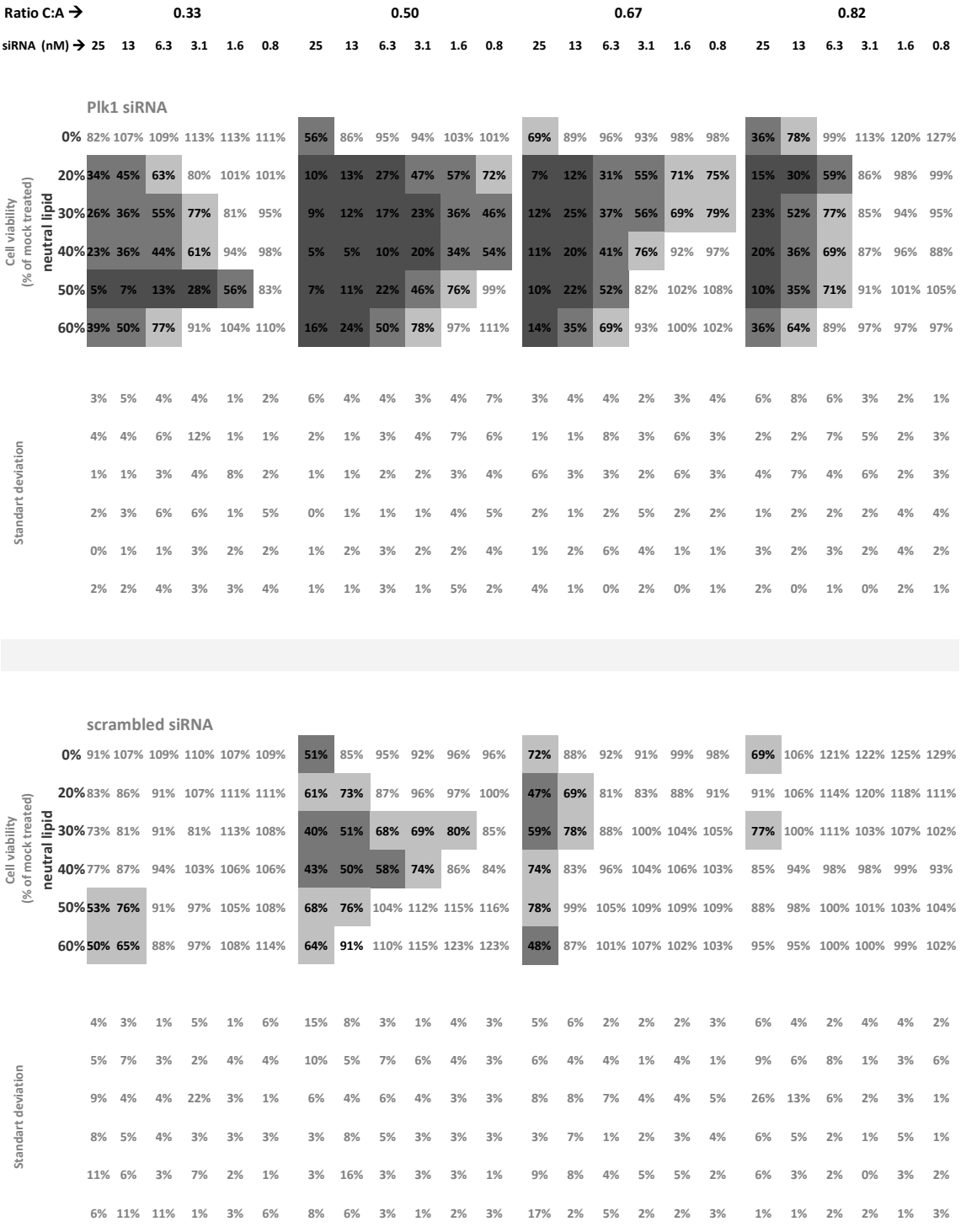

FIGURE 3.15: *In vitro* screen of amphoteric liposomes for siRNA delivery. HeLa cells were treated for 72 hours with Plk1 siRNA and scrambled siRNA loaded in amphoteric mixtures comprising DODAP, DMGS and Chol as neutral lipid. The cation to anion (C:A) molar ratio was changed from 0.33 to 0.82 and the amount of neutral lipid from 0% to 60%. Data show siRNA-mediated inhibition of cell proliferation in a dose dependent manner. Mean viability and standard deviation were calculated from triplicates cultures relative to the PBS treated cells: dark grey= less than 30%; grey = between 30% and 60%; light grey more than 60%.

3.5.2 Transfection efficiency based on the molecular shape theory

The algorithm presented above provides a structure-activity relationship between lipid chemistry and pH-induced membrane fusion summarized in the dominant shape parameter κ. A further, more implicit question and also the main focus of this work was to investigate a possible correlation between the transfection efficiency of amphoteric liposomes through endosome escape and the above-described algorithm which allows a theoretical calculation of the phase behaviour of amphoteric lipid mixtures. Proof of such a correlation will facilitate practical use of the theoretical algorithm for carrier optimization.

One of the goals of this work was to decipher the rules concerning the manner in which transfection efficiency is determined by lipid molecular structure. A first example is demonstrated in Figure 3.16. We here compare the transfection efficiency of amphoteric liposomes prepared using the transfection lipid DOTAP and three different anions: DOGS, DMGS and CHEMS. Increasing amounts of cholesterol were also added in the amphoteric membrane and the preparations were tested using the Plk1/scrambled siRNA system and HeLa cells.

For CHEMS, the dynamic shape theory predicts better fusogenicity for higher C:A ratios; in practical terms, this would apply to particles having a C:A of 0.82. For DMGS and DOGS, the minimum value of κ is less correlated with the C:A ratio; therefore the transfection activity is also not expected to correlate with the C:A ratio.

As shown in Figure 3.16, the experimental evidence supports these predictions. Panel B shows the in vitro results obtained from the siRNA transfected with DOGS carriers. It is evident, that the cation to anion molar ratios 0.33 and 0.5 present stronger transfection efficiency than the cation rich molar ratios 0.67 and 0.82. DMGS carriers, while still being very active at low C:A ratios also show activity in the presence of higher amounts of the cationic lipid. Still, the DMGS/DOTAP mixtures with low amounts of cationic lipid demonstrated strong transfection efficiency at very low siRNA concentrations. Similar results were obtained for molar ratio 0.67, while the effect of the siRNA seems to disappear when using liposomes with molar ratio 0.82. In contrast to the DOGS and DMGS mixtures, CHEMS liposomes delivered siRNA only when they prepared at the molar ratios 0.67 and 0.82.

The addition of cholesterol enhanced the fusogenicity of the mixture, a finding that was often confirmed by the transfection efficiencies. At higher amounts, a deterioration of transfection performance of the liposomal carries was observed, probably due to insufficient stability of

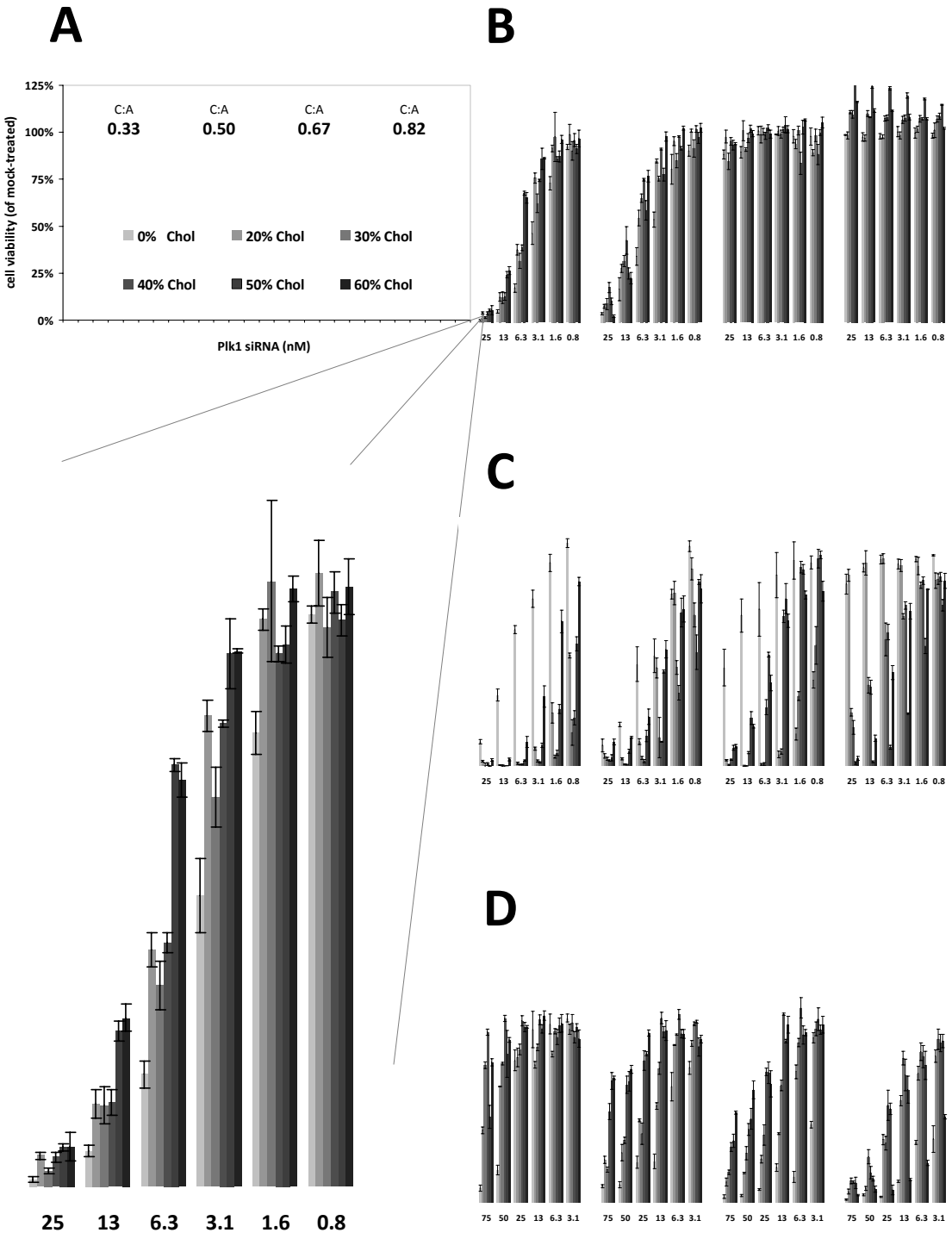

FIGURE 3.16: The shape parameter κ determinate cation to anion ratio for transfection efficiency. (A) displays legends and axes for all subsequent figures. Cell viability was determined at 72h. Values are expressed as percentage of cell viability relative to PBS treated cells. The error bars represent standard error of mean calculated from triplicate transfections. Values higher than 2 of a scrambled/Plk1 ratio were allowed for the formulation, lower values were not considered for the analysis, due to toxicity (data not shown). **(B-D)** In vitro activity screen comparing pH-sensitive anionic lipids DOGS (B), DMGS (C) and CHEMS (D). Decreased cell viability is associated with cation:anion (C:A) molar ratios 0.33 and 0.50 for DOGS liposomes; 0.33, 0.50 and 0.67 for DMGS liposomes; 0.82 for CHEMS liposomes. All amphoteric liposomes were prepared using the cationic lipid DOTAP and with increasing amounts cholesterol (enlarged graphic: 0-60%; white bars to black bars, respectively).

materials. Cholesterol drops the κ of the membrane at the isoelectric point but also at neutral pH, which may lead to premature fusion or mere aggregation of the particle.

3.5.3 The shape parameter κ_{MIN} dictates cellular transfection potency

Eventually, the predictive power of the theory was challenged by correlating κ_{MIN}, the value that κ_{pH} adopts at the isoelectric point, with the efficacy of RNAi mediated by amphoteric liposomes, a process that is thought to be strictly dependent on a membrane fusion event between the carrier and cellular membranes.

More than 2000 chemically distinct amphoteric liposomes comprising neutral and charged lipids with different structural shapes and head/tail groups were loaded with siRNA targeting polo-like kinase (Plk1). The viability of human carcinoma cells was challenged with these materials and then analyzed. Matching liposomes were loaded with an unrelated siRNA and transfected in parallel to exclude lipid/siRNA mediated effects. The efficacy of transfection was expressed as IC50, the concentration of siRNA needed to inhibit cell proliferation by 50% and correlated with κ_{MIN}, the fusion determinant. Lipid combinations and experimental details are provided in the MATERIALS & METHODS section 2.8 (see Table 2.2).

The experimental data in Figure 3.17 reveal κ_{MIN} as the guiding factor of cellular transfection, since the frequency of potent transfectants, but also the efficacy of the vectors increased with low values of the fusion determinant. Carriers with extreme fusogenicity are less successful and an optimum is formed around κ_{MIN} ~0.16. It was found that liposomes with $\kappa_{MIN} < 0.16$ were at least 100fold more effective than those with κ_{MIN} values higher than 0.3. Selected carriers were also loaded with Plk1 siRNA and tested for their ability to mediate knockdown of Plk1 in macrophage cell line RAW264.7.

As with HeLa cells, a similar relation was observed between the efficacy of inhibiting the viability of these cells and κ_{MIN}. Low values of κ_{MIN} between 0.14 and 0.18 are required for optimized cellular transfection and no appreciable inhibition of cell proliferation is observed for $\kappa_{MIN} > 0.20$. In both cases, carriers with extreme fusogenicity indicated by κ_{MIN} values lower than 0.14 were less successful, probably due to insufficient stability of these materials. The above-presented data provide a link between pH-dependent fusogenicity (κ_{MIN}) and functionality (IC50) for the cellular delivery.

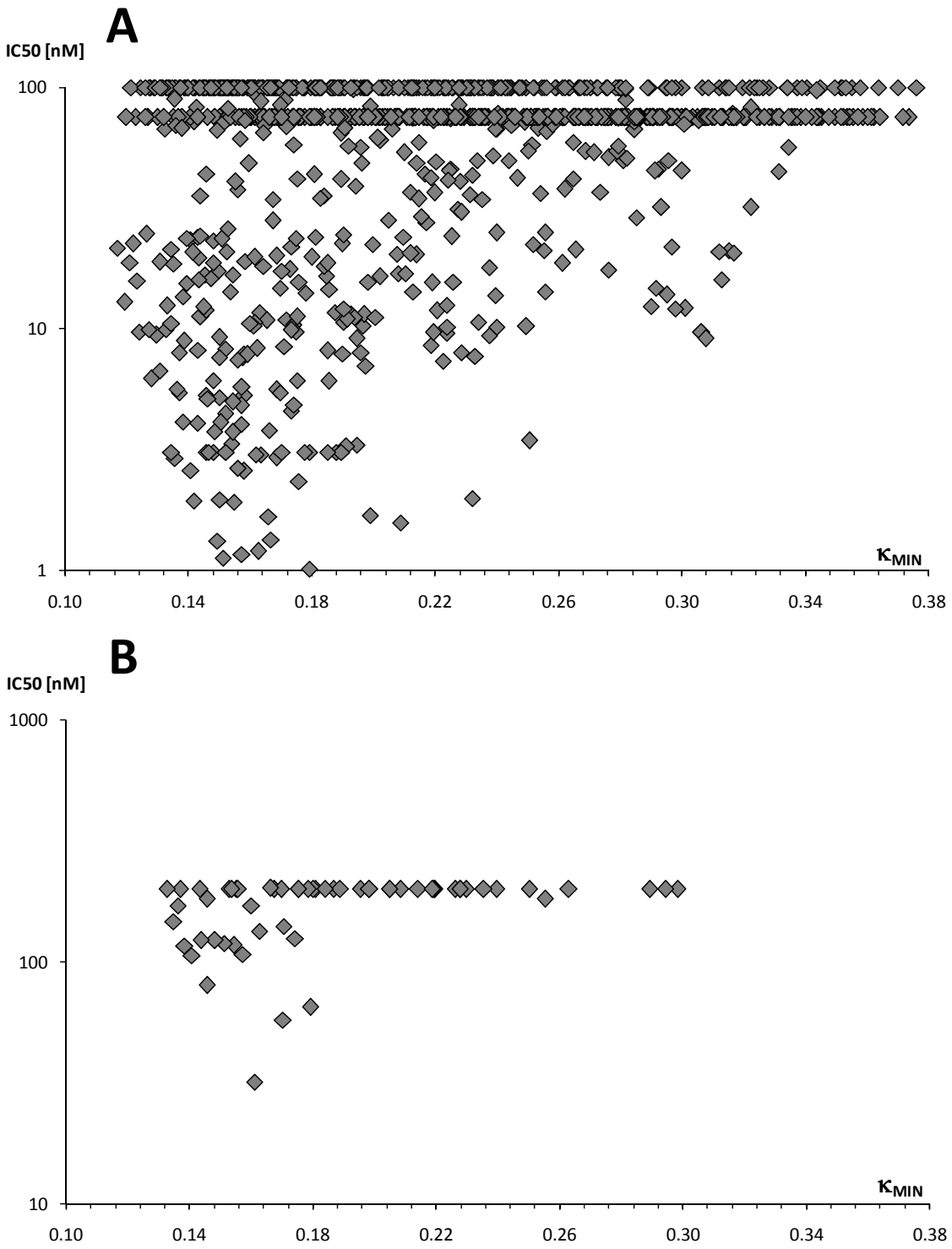

FIGURE 3.17: The fusion determinant κ_{MIN} governs the siRNA transfection into HeLa or macrophages cells with amphoteric liposomes. (A) More than 2000 chemically distinct amphoteric liposomes were loaded with siRNA targeting polo-like kinase 1 and tested for the inhibition of cell proliferation of HeLa cells. The efficacy of transfection was expressed as IC50 from dose response between 1 and 100nM with all liposomes. The transfection of the cells was limited by κ_{MIN} and low values of about 0.16 were required for optimized cellular transfection. No appreciable cellular transfection was observed for κ_{MIN} > 0.30. **(B)** Potency of carrier on RAW264.7 cells. As in panel (A) potency correlates strongly with fusogenicity of these carriers and no cellular transfection was observed for carriers with κ_{MIN} > 0.20 within the limits of this experiment (highest dose tested: 300 nM). (A and B) Background, positive and negative controls were used on each plate and IC50 were deduced for samples showing a specific proliferation inhibition of a Plk1/SCR ratio higher than 2. Values of a Plk1/SCR ratio lower than 2, indicating toxicity, were not included in the analysis (data not shown).

In contrast to κ_{MIN}, the efficacy of carriers was unpredicted by κ_{pH8}. The data in Figure 3.18 demonstrate that no correlation was observed between κ_{pH8} and the frequency of transfection competent carrier in a liposome matrix normalized to a certain κ_{MIN}.

In this analysis, the frequency of transfection competent carriers, indicated by IC50 values lower than 50 nM, was analyzed in liposome samples that are chemically divers, but normalized for κ_{MIN} to be between 0.14 and 0.18. When analyzed with respect to κ_{pH8}, the head to tail volume ratio at neutral conditions, frequencies of transfection competent carriers were randomly distributed over the sample, which renders this parameter less predictive for cellular delivery. However, such relationship can be observed for the reverse correlation between the frequency of competent liposomes with κ_{MIN} for liposomes selected for a common κ_{pH8}. Panel B in Figure 3.18 illustrates the frequency of carriers having an IC50 below 50nM and sharing a κ_{pH8} between 0.28 and 0.32, but have different values of the fusion determinant κ_{MIN}. The

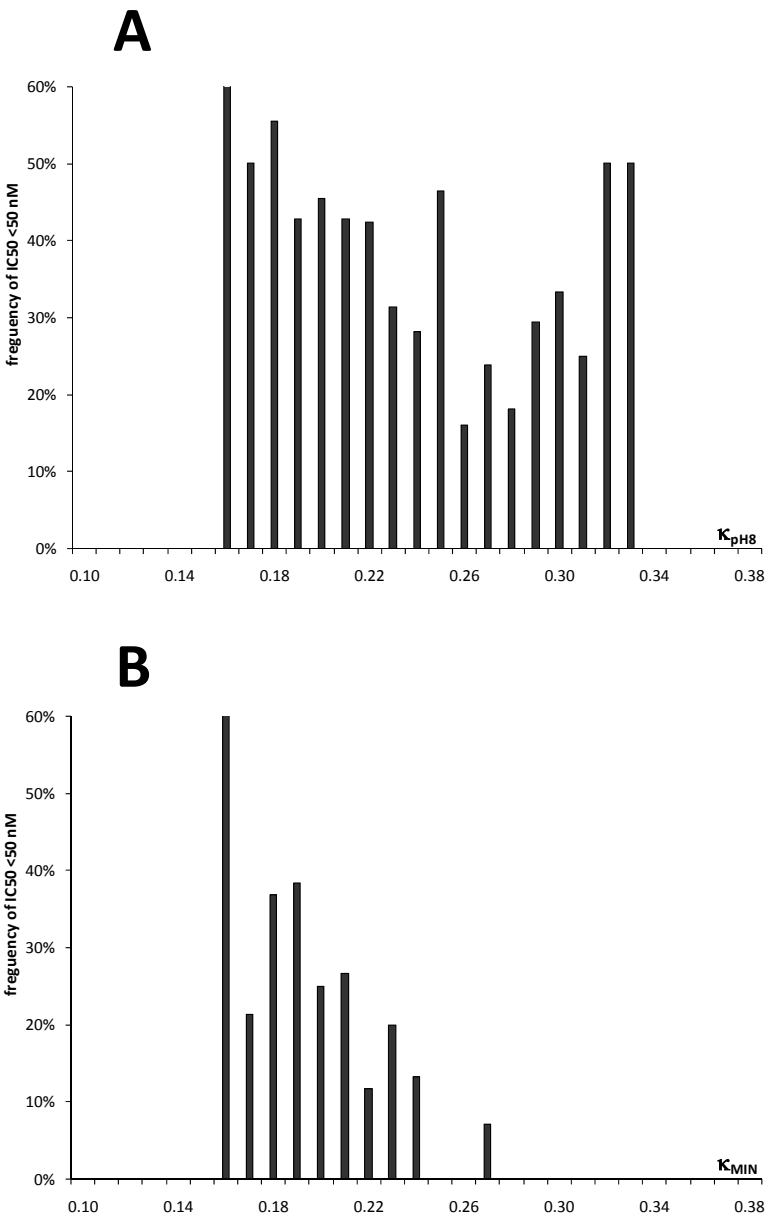

FIGURE 3.18: κ_{MIN}, but not κ_{pH8} governs the transfection of cells with amphoteric liposomes. (A) Liposomes with κ_{MIN} between 0.14 and 0.18 were analysed for IC50 values lower than 50 nM versus κ_{pH8}. No correlation was observed between transfection potency and κ_{pH8}. **(B)** In contrast, when the IC50 values were analyzed for liposomes with a common κ_{pH8} (0.28 to 0.32) the frequency of active carriers is correlated with lower κ_{MIN} values.

frequency of active carriers is negatively correlated with high values of κ_{MIN}. For low values of κ_{MIN} the frequency of transfection competent carriers reaches up to 60%.

In summary, the extensive screening of carriers using *in vitro* transfection of human and mouse cell lines have established a quantitative relationship between the shape parameter κ_{MIN} and the cellular transfection potency IC50, since the efficacy of the vectors, but also the frequency of potent transfectants increased with low values of the fusion determinant. In contrast, no correlation was observed between κ_{pH8}, the parameter characterizing ion stabilized states of the membrane at neutral conditions, and the frequency of transfection competent carrier in a liposome sample normalized to a certain κ_{MIN}. Therefore, κ_{MIN} limits the efficacy of transfection.

Conclusively, these results provide a strong link between the acidification in subcellular compartments and the induction of fusion of amphoteric liposomes. This is related to structural features of these carriers, thereby establishing a structure-activity relationship for transfectants.

4. DISCUSSION

Liposomal vectors have become a useful tool in pharmaceutical applications, especially for the intracellular delivery of oligonucleotides. The use of liposomal carriers to enhance oligonucleotide uptake and presentation to the cytoplasm is essential for functional cellular studies. After the uptake of a liposome into a cell by endocytosis the release of the nucleic acids from the endosome is a crucial step for their delivery into the cytosol of cells. The pH within the endosome is getting slightly acidic and pH-sensitive liposomes can fuse with the endosomal membrane, allowing the release of the drug from the endosome (Budker et al., 1996). This means that the endosomes escape can be facilitated by destabilization of the endosomal lipid phase due to enhanced carrier fusogenicity resulting in the intracellular delivery of oligonucleotides.

Based on experimental data, the present work unravels and confirms the mechanism of how pH-sensitive lipid materials can display unique biphasic stability as proposed by Panzner and colleagues (Panzner et al., 2002-WO 02/066012). The fusion properties of amphoteric liposomal particles were demonstrated through lipid mixing experiments using matching pairs of labeled liposomes in a FRET assay. The counterion fluctuations between the bilayer and the bulk solvent were identified as the driving force behind the biphasic stability of the amphoteric mixtures. The results obtained from monocharged liposomes predict additive stabilization in bilayers from mixed charged amphiphiles. Indeed, valley type fusion was observed in such structures by size increase and lipid mixing and thus confirmed the explanations of Panzners algorithm (Panzner et al., 2008-WO 08/043575). The formation of intrabilayer lipid salts in the amphoteric lipid systems, proposed in this mathematical model, could explain this contradiction. The pH-dependent processes that involve both the actual bilayer, but also the solvent were integrated into a model that expands beyond the framework of the original lipid shape theory. Key variables in the new theory are the molecular volumes, ion adsorption and the pK_α values of the lipid species. These key regulators were confirmed by the experimental data obtained in this work.

Finally, a further experimental approach as an aid in identifying and developing functional mixtures of amphoteric liposome formulations, as predicted by the algorithm, includes the transfection of cells using different amphoteric liposome formulations. In this context, amphoteric carriers were systematically screened for their ability to mediate RNAi in human

cancer cells and murine macrophages. A strong correlation was observed between fusogenicity and cellular efficacy, allowing further use of the theoretical algorithm for carrier optimization. Enhanced fusion properties resulting in promising siRNA release *in vitro* could translate into increased *in vivo* efficacy. This thesis demonstrates the development of a library of amphoteric materials, which represents an important expansion of the diversity and collection of liposomal vehicles for siRNA intracellular delivery.

4.1 Counterion binding causes shape transition

The lipid molecular shape concept was first introduced by Israelachvili and colleagues. The theory assumes that the overall form of lipid molecules determines the structure of the hydrated lipid membrane (Israelachvili and Mitchell, 1975). This means that the lipid geometry and more specifically the size ratio between the polar headgroup and the hydrophobic membrane anchor is the key parameter determining the lipid phase (Israelachvili, et al., 1977). The original theory however does not consider counterions being a steric part of the polar headgroup. This was contributed by the work of Li and Schick. In their description of the DODAC/CHEMS system, the sodium countercation enlarges the headgroup of CHEMS at neutral pH, but dissociates as the pH drops, thus minimising the headgroup volume and promoting a hexagonal phase (H_{II}). DODAC as a strong cation is assumed to be in constant association with its respective counteranion, irrespective of the pH (Li and Schick, 2001).

In this work, bilayer destabilization and lipid mixing was observed upon depletion of the charged counterions acetate and imidazole in 100% CHIM and CHEMS liposomes respectively. CHIM liposomes undergo fusion either upon discharge of the buffer ion at low pH or the lipid headgroup at pH 8. Conversely, CHEMS bilayers fuse upon discharge of the either the imidazole ion at pH 8 or the lipid headgroup at pH 4. The results from the buffer discharge experiment indicate that electrostatic repulsion or hydration of charged lipids may not suffice for bilayer stabilization. For liposome fusion the loss of counterions is necessary and not the charge status of a bilayer.

In addition, for fusion of competent anionic (CHEMS/Chol) and cationic liposomes (CHIM/Chol) this study provided evidence that the counterion volume modulates their fusion properties. When CHEMS and CHIM liposomes were prepared using different counterions, bilayer stabilization has been achieved over time only when large counterions are used, such as arginine and glutamic acid respectively. The fusion of CHEMS liposomes made in the presence

of various countercations enhanced in the series of $K^+ > Na^+ > Li^+ > Tris^+ > arginine^+$ and for the CHIM liposomes in the counteranion order of $Cl^- > acetate^- > glutamate^-$.

According to the results obtained in the course of this work, the proposed contribution to the lipid shape theory involves multiple approaches. The first observation in section 3.1 is that counterions must be considered an integral part of most, if not all charged lipid bilayers. The volume of a bound ion modulates the molecular shape of the respective lipid which in turn affects the stability of the lipid assemblies. Counterion binding provides a sufficient explanation for the stabilization of fusion competent, single-charged anionic or cationic bilayers at neutral or low pH, respectively. Finally, counterions modulate the stability of the bilayer on the charge state, but do not influence fusion properties in its non-ionized state.

4.2 Amphoteric lipid membranes present pH-guided, biphasic stability

Amphoteric liposomes belong to the larger group of pH-sensitive liposomes that were introduced first by Straubinger (DOPE/CHEMS liposomes) and co-workers (Straubinger et al., 1985). In contrast to zwitterionic structures, the advantage of amphoteric liposomes is that they exhibit an isoelectric point, the net charge of the particles is zero, where the fusion process occurs (Panzner et al., 2008-WO 02/066012, Andreakos et al., 2009).

Such pH-sensitive mixtures present amphoteric properties in the sense that they exist in a cationic state at low pH and as anionic particles at physiological pH. In this study, amphoteric systems comprising CHEMS as anionic lipids in combination with DOTAP (Amphoter I system) and CHIM (Amphoter II system) were tested. Strong, valley type fusion and generation of a second stable phase at low pH is predicted and confirmed by experimental data for compositions bearing an excess of the anionic lipid. The typical fusion maximum was observed at intermediate pH for all amphoteric mixtures. Amphoter I systems were only fusogenic in the fluorescent assay when high amounts of CHEMS were present in the mixture, whereas the Amphoter II system CHIM/CHEMS was fusogenic in both, cationic and anionic state. Also, the FRET signals observed at the different pH values was largely stable against neutralization in the presence of high amounts of lipid anion. The Amphoter III systems are composed of permanently charged anionic lipids in combination with pH-sensitive cationic lipids. Fusion was observed as predicted by theory and yielded only a valley type fusion with the existence of a bistable phase in an excess of MoChol.

The results presented in this work provide information on a new class of pH-sensitive liposomal systems composed of mixtures of cationic and anionic lipids. There are several major points of interest, which can be summarized as follows:

(a) Amphoteric liposomes can be generated from mixtures of cationic and anionic lipids when either the cationic or anionic lipid species is in excess and has a pK_α in the range of between 4 and 8.

(b) The fusion process of amphoteric liposomes is a consequence of non-bilayer "inverted" lipid phase structures when the surface charge is zero.

(c) By varying the ratios of the cationic and anionic lipids the pH/isoelectric point at which this fusion occurs can be modulated, depending on the pK_α values of the anionic and cationic lipids.

(d) Lamellar amphoteric systems can be prepared at acidic pH under the existence of a cationic state. This solves the problem of poor oligonucleotide encapsulation in anionic pH-sensitive carriers.

(e) Finally, lipid salt formation can occur within an existing amphoteric bilayer and the process is pH-dependent, rapid and reversible.

4.3 Influencing fusogenicity through the addition of neutral/zwitterionic lipids

Amphoteric liposomes are complex structures and comprise at least one complementary pair of charged lipids. The inclusion of one or more neutral or/and zwitterionic lipids can significantly add to the complexity of the mixture, especially since the amounts of the individual components may vary. Therefore, one of the scopes of this work was to simplify the addition of a third component to amphoteric mixtures by providing information about its impact in the biophysical properties of the system.

The observations presented in sections 3.3.2 and 3.3.3 describe the influence of POPC, DOPC, DOPE and cholesterol as single lipids or in combination thereof, on the fusogenicity of amphoteric lipid mixtures. Lipid combinations from the three amphoteric systems (Amphoter I, II, and III) were tested for their fusogenicity upon addition of these lipids. It is apparent that neutral lipids having a high κ value, such as POPC or DOPC, decrease the fusogenicity of the

amphoteric liposomes, whereas the lipids having a lower κ value, such as DOPE or cholesterol, have little impact on the fusogenicity or may even improve the fusion. Additionally, mixtures of POPC and DOPE and mixtures of POPC or DOPC and cholesterol may have little impact or decrease the fusion ability, depending on the ratios of the neutral/zwitterionic lipid combination.

An important finding, presented in Figure 3.8, is that the addition of neutral lipid cholesterol to amphoteric charged mixture does not affect the isoelectric point of amphoteric liposomes. The former makes the design of an amphoteric mixture upon addition of neutral lipid less complicated. In these results, although the Amphoter II system MoChol/CHEMS presented biphasic stability, the mixture was not fusogenic with less than 50% CHEMS, in contrast to the CHIM/CHEMS mixture presented in Figure 3.5. Addition of further fusion promoting lipids like cholesterol with an extraordinary low κ, has created a κ_{MIN} low enough to promote fusion at MoChol mixtures with less than 50% CHEMS without shifting the isoelectric point of the mixture. Although more systems would meet κ_{MIN}, the other parameter **d(κ)/d(pH)** becomes in this case critical and thus could affect the stability and integrity of the nucleic acid liposomal formulation at neutral/storage condition.

Some cases clearly indicate that the choice of the neutral lipid is critical for the fusion properties of the amphoteric membrane. Depending on the field of application, *in vitro* or *in vivo*, the selection of the third component must be done taking into consideration the fusogenicity of the carrier in its final state. For *in vitro* nucleic acid transfection, the most commonly used lipid is DOPE in combination with cationic lipids (Felgner et al., 1987). In this case, the stability of the particle is not an issue since the preparation and transfection process is rapid and efficient. On the other hand, for *in vivo* application, the carriers comprised cholesterol (Zimmermann et al., 2006) and additional lipids which prefer the lamellar phase, such as DOPC and POPC, could enhance the stability of these particles hence facilitating longer circulation and improved biodistribution. Still, the addition of lamellar adopting lipids should be done carefully to avoid any negative consequence on the fusion properties of the liposomal carrier.

The presented results in combination with the previous scientific work of Hafez and Li provide some guidance on how to select lipid mixtures with amphoteric properties and more specifically how to define their isoelectric point and onset of fusion (Hafez et al., 2000; Li and Schick, 2001). Neutral lipids modulate both fusion and stability of the charged state through a constant adjustment of κ and a dilution of the system amplitude. Nevertheless, the plethora of

possible combinations of charged and neutral/zwitterionic lipids represents a practical hurdle towards a more rapid optimization of amphoteric liposomes for systemic administration. However, there remains a need for a systematic method of predicting or analysing which mixtures of lipids form satisfactorily stable lamellar phases at high and low pH, whilst forming a fusogenic, hexagonal phase at an intermediate pH.

4.4 Algorithm – Rational optimization of liposome design

The data obtained in the present study coincide with the predictions from the model calculation. Therefore, the algorithm represents a quantitative structure-activity relationship between lipid chemistry and stability/fusogenicity of the resulting membrane, particularly in response to the pH of the environment. However, there are still several questions that need to be answered, in order to further develop and expand the new molecular shape theory. For example, the algorithm fails to reflect steric fit or misfit of the components. It also does not take into account phase transition temperatures and the associated molecular movements which might occur in isolated cases, resulting to a different dynamic and orientation of lipids in the bilayer as would be expected. Likewise, the vertical position of lipids in the bilayer may change with their protonation state or with the headgroup size. The theory in its current form can not differentiate between cholesterol derivatives, saturated or unsaturated diacylglycerols. The model also uses general assumptions about counterion size, hydration and the extent of the lipid salt formation.

In more details, the stable anionic lipid POPG, as a structure related lipid to DOPA, was tested and modelled in combination with MoChol. Surprisingly, impaired fusion behaviour occurred in the FRET protocol as described in section 3.3. This is probably due to inaccessibility of the bulkier POPG headgroup as a counterion in a salt bridge model, an effect that can not be predicted by the model. Further examples are the fusion behaviour of the Amphoter II systems; e.g. CHIM/CHEMS and MoChol/CHEMS (Figures 3.5 and 3.8); which starts at a relatively high value of κ compared to DOTAP/CHEMS (Figure 3.5), or the enhanced fusion behaviour of Chol-C5 (a CHEMS homologue) in mixtures with DOTAP as demonstrated in Figure 3.9. A possible explanation for both cases could be a deeper or shallower membrane insertion of Chol-C5 or MoChol, resulting in lower or higher κ values for each membrane compared to the mathematical calculations and assumptions provided by the algorithm.

However, despite these few drawbacks and without any further assumptions or concerns, this model is sufficient to describe a biphasic stability of amphoteric bilayers in response to the pH of the medium and establishes amphoteric character as a necessary condition. Moreover, the newly extended lipid shape theory proposed by Panzner deduces the lipid phase behaviour from the molecular volumes and pK_α values of its components. It is therefore independent of the chemical representation of the respective lipids. Collectively, the algorithm can be applied beyond amphoteric lipid membranes facilitating also the analysis of neutral, zwitterionic or monocharged lipid membranes.

4.5 The fusion determinant κ_{MIN} guides activity of amphoteric liposomes

Despite encouraging progress, there are significant obstacles on the way to the application of siRNA molecules *in vivo*. These obstacles include difficulties regarding delivery, biostability, pharmacokinetics and off target effects. One of these, the functional delivery of siRNA molecules can be viewed as a sequel of events, which includes loading of siRNA into the delivery system, administration into the systemic circulation, cellular distribution and endosomal maturation resulting to escape of siRNA from this sub cellular compartment.

The observations from the fusion experiment, using the model membranes, suggest that the fusion - although it is a process of two membranes - can be controlled by the optimal design of the delivery membrane. Such models, when optimized, can be used as excellent alternatives or compliments for *in vitro* studies, providing great opportunities for studying the individual variables of liposome-cell interactions.

Eventually, the link between the fusion potential of liposomes and their ability to transfect cells of different origin was investigated. As a result, a quantitative structure-activity relationship between the liposome and solvent components and the fusogenicity of such systems was established. This will facilitate a description of the chemical space for the lipids used in transfection systems and the rational optimization of transfection systems. The predictive power of the algorithm was challenged by correlating κ_{MIN}, the fusion determinant, with the efficacy of RNAi mediated by amphoteric liposomes, a process that is thought to be strictly dependent on a membrane fusion event between the carrier and cellular membranes. For that, wide arrays of chemically distinct amphoteric liposomes were loaded with siRNA targeting polo-like kinase 1 and analyzed the viability of HeLa cells upon exposure to the materials. The results revealed κ_{MIN} as the guiding factor of cellular transfection, since the

frequency of potent cellular transfectants, but also the efficacy of the vectors increased with low values of the fusion determinant. Similar correlations were obtained when inhibiting the viability of the macrophage cell line RAW264.7 as well as upon targeting the mRNA for ApoB in primary mouse hepatocytes (Dissertation by Christian Reinsch).

The general correlation between the efficacy of cell transfection and κ_{MIN} points towards a common, pH-dependent fusion event between the carrier liposomes and cellular membranes in the different cell types. No correlation was observed between κ_{pH8} and the frequency of transfection competent carrier in a liposome sample normalized to a certain κ_{MIN}, but such relationship can be observed for the reverse correlation between the frequency of competent liposomes with κ_{MIN} for a sample of liposomes selected for a common κ_{pH8}. It is thus clear, that κ_{MIN} is the fusion determinant of a given liposome and not its stability at pH 8, which predicts the efficacy of cell transfection. This relationship underlines the need for a structural transition of a liposomal carrier between a stable state, which is necessary for storage and biodistribution, and a fusogenic state that is induced upon cellular uptake.

Acidification within the endosomal compartment provides ubiquitous and functional trigger. While being a necessary parameter, the low value of κ_{MIN} is not sufficient for the functionality of liposomes, since a large number of carriers is less active in transfection than predicted. Stability in cell culture medium, binding of the carriers to the cell surface or uptake via different routes of endocytosis may all contribute to a lack of activity and more detailed analysis is needed to elucidate the structure-activity relationships of these processes. A more implicit conclusion can be drawn with respect to the actual cellular binding and uptake. There is no specific binding of some carriers to the cell surface, since any such binding would lead to better-than predicted potency. No such carriers were observed, which leaves the potential for further enhancement through ligands.

To summarize, amphoteric liposomes have been found to exhibit excellent biodistribution and to be well tolerated in animals. They can encapsulate active agents, including nucleic acid molecules, with high efficiency and more importantly, they can confer oligonucleotides protection, an issue really essential. Moreover, their anionic surface at neutral conditions repulses oligonucleotides from binding to the membrane surface, thus avoiding any possible immunostimulatory responses (Andreakos et al., 2009). All these in combination with the findings of this study are promising insight for the development of oligonucleotide therapeutic applications. The present study supports the concept that the correct design of a delivery vehicle is the key for the effective delivery of siRNAs. Moreover, the algorithm can predict both

fusogenic or non-fusogenic liposomal mixtures and their fusogenicity can be improved or impaired upon addition of neutral/zwitterionic lipids. Fusogenic liposomes can be used for transfecting cells with siRNA molecules and non-fusogenic for endosomal delivering of immunostimulatory oligonucleotides. Collectively, the model in its current form allows a mechanistic insight into the process of lipid fusion and its surprising relationship to counterion binding, thus facilitating the development of liposomal carriers. The newly extended shape theory therefore is a novel design algorithm for the rational tuning of liposomal formulations for different delivery applications.

REFERENCES

- **Aberle, A.M., Bennett M.J., Malone R.W., and Nantz, M.H. 1996.** The counterion influence on cationic lipid–mediated transfection of plasmid DNA. *Biochim. Biophys. Acta.* **1299**:281–283.

- **Ahn, T. and Yun, C. H. 1999.** Phase properties of liquid-crystalline phosphatidylcholine and phosphatidylethanolamine bilayers revealed by fluorescent probes. *Arch. Biochem. Biophys.* **369**:288–294.

- **Andreakos, E., Rauchhaus, U., Stavropoulos, A., Endert, G., Wendisch, V., Benahmed, A.S., Giaglis, S., Karras, J., Lee, S., Gaus, H., Bennett, C.F., Williams, R.O., Sideras, P., and Panzner, S. 2009.** Amphoteric liposomes enable systemic antigen-presenting cell-directed delivery of CD40 antisense and are therapeutically effective in experimental arthritis. *Arthritis Rheum.* **60**:994–1005.

- **Batzri, S. and Korn, E.D. 1973.** Single bilayer liposomes prepared without sonication. *Biochim. Biophys. Acta.* **298**:1015–1019.

- **Behlke, M.A. 2006.** Progress towards in vivo use of siRNAs. *Mol. Ther.* **13**:644–670.

- **Bennett, C.F., Chiang, M.Y., Chan, H., Shoemaker, J.E., and Mirabelli, C.K. 1992.** Cationic lipids enhance cellular uptake and activity of phosphorothioate antisense oligonucleotides. *Mol. Pharmacol.* **41**:1023–1033.

- **Bennett, C.F. and Swayze, E.E. 2010.** RNA targeting Therapeutics: Molecular Mechanisms of Antisense Oligonucleotides as aTherapeutic Platform. *Annu. Rev. Pharmacol. Toxicol.* **50**:259–93.

- **Bennett, M.J., Aberle, A.M., Balasubramaniam, R.P., Malone, J.G., Malone, R.W., and Nantz, M.H. 1997.** Cationic lipid-mediated gene delivery to murine lung: correlation of lipid hydration with *in vivo* transfection activity. *J. Med. Chem.* **40**:4069–4078.

- **Bennett, M.J., Nantz, M.H., Balasubramaniam, R.P., Gruenert, D.C., and Malone, R.W. 1995.** Cholesterol enhances cationic liposome-mediated DNA transfection of human respiratory epithelial cells. *Bioscience Reports.* **15**:47–53.

- **Bonfils, E., Depierreux, C., Midoux, P., Thuong, N.T., Monsigny, M., and Roche, A.C. 1992.** Drug targeting: synthesis and endocytosis of oligonucleotide-neoglycoprotein conjugates. *Nucleic Acids Res.* **20**:4621–4629.

- **Budker, V., Gurevich, V., Hagstrom, J.E., Bortzov, F., and Wolff, J.A. 1996.** pH-sensitive, cationic liposomes: A new synthetic virus-like vector. *Nat. Biotechnol.* **14**:760–764.

- **Campbell., J.M., Bacon, T.A., and Wickstrom, E. 1990.** Oligodeoxynucleoside phosphorothioate stability in subcellular extracts, culture media, sera and cerebrospinal fluid. *J. Biochem. Biophys. Methods.* **20**:259–267.

- **Gao, X. and Hui, L. 1991.** A novel cationic liposome reagent for efficient transfection of mammalian cells. Biochem. *Biophyhs. Res. Comm.* **179**:280–285.

- **Cerritelli, S.M. and Crouch, R.J. 2009.** Ribonucelase H: the enzymes in eukaryotes. *FEBS J*. **276**:1494–505.

- **Chiu, Y.L., Ali, A., Chu, C.Y., Cao, H., and Rana, T.M. 2004.** Visualizing a correlation between siRNA localization, cellular uptake, and RNAi in living cells. *Chem. Biol.* **11**:1165–1175.

- **Citro, G., Perrotti, D., Cucco, C., D'Agnano, I., Sacchi, A., Zupi, G., and Calabretta, B. 1992.** Inhibition of leukemia cell proliferation by receptor-mediated uptake of c-myb antisense oligodeoxynucleotides. *Proc. Natl. Acad. Sci. U. S. A.* **89**:7031–7035.

- **Citro, G., Szczylik, C., Ginobbi, P., Zupi, G., and Calabretta, B. 1994.** Inhibition of leukaemia cell proliferation by folic acid-polylysine-mediated introduction of c-myb antisense oligodeoxynucleotides into HL-60 cells. *Br. J. Cancer*. **69**:463–467.

- **Conway, B. E. 1981.** Ionic hydration in chemistry and biophysics. *Elsevie.* **Chap. 4**, pp. 59-72.

- **Crooke, R.M., Graham, M.J., Lemonidis, K.M., Whipple, C.P., Koo, S., and Perera, R.J. 2005.** An apolipoprotein B antisense oligonucleotide lowers LDL cholesterol in hyperlipidemic mice without causing hepatic steatosis. *J. Lipid Res.* **46**: 872–884.

- **Cullis, P.R. and de Kruijff, B. 1978.** The polymorphic phase behavior of phosphatidylethanolamines of natural and synthetic origin. A ^{31}P NMR study. *Biochim. Biophys. Acta.* **513**:31– 42.

- **Cullis, P.R. and de Kruijff, B. 1979**. Lipid polymorphism and the functional roles of lipids in biological membranes. *Biochim. Biophys. Acta.* **559**:399–420.

- **Cullis, P.R., Hope, M.J., and Tilcock, C.P. 1986**. Lipid polymorphism and the roles of lipids in membranes. *Chem. Phys. Lipids.* **40**:127–144.

- **Daleke, D.L., Hong, K., and Papahadjopoulos, D. 1990.** Endocytosis of liposomes by macrophages: binding, acidification and leakage of liposomes monitored by a new fluorescence assay. *Biochim. Biophys. Acta.* **1024**:352–366.

- **de Fougerolles, A., Vornlocher, H.P., Maraganore, J., and Lieberman, J. 2007.** Interfering with disease: a progress report on siRNA-based therapeutics. *Nat. Rev. Drug Discov.* **6**:443–453.

- **de Kruijff, B. and Cullis, P.R. 1980.** The influence of poly(L-lysine) on phospholipid polymorphism. Evidence that electrostatic polypeptide-phospholipid interactions can modulate bilayer/non–bilayer transitions. *Biochim. Biophys. Acta.* **601**:235–240

- **Dickey, A. and Faller, R. 2008.** Examining the Contributions of Lipid Shape and Headgroup Charge on Bilayer Behavior. *Biophys. J.* **95**:2636–2646.

- **Donis-Keller, H. 1979.** Site specific enzymatic cleavage of RNA. *Nucleic Acids Res.* **7**:179-192.

- **Duxbury, M.S., Matros, E., Ito, H., Zinner, M.J., Ashley, S.W., and Whang, E.E. 2004.** Systemic siRNA-mediated gene silencing: a new approach to targeted therapy of cancer. *Annals of Surgery.* **240**:667–674.

- **Duzgunes, N., Straubinger, R.M., Baldwin, P.A., Friend, D.S., and Papahadjopoulos, D. 1985.** Proton-induced fusion of oleic acid– phosphatidylethanolamine liposomes. *Biochemistry.* **24**:3091–3098.

- **Elbashir, S., Harborth, J., Lendeckel, W., Yalcin, A., Weber, K., and Tuschl, T. 2001.** "Duplexes of 21-nucleotide RNAs mediate RNA interference in cultured mammalian cells". *Nature.* **411**:494–8.

- **Ellens, H., Bentz, J., and Szoka, F.C. 1984.** pH-induced destabilization of phosphatidylethanolamine-containing liposomes: role of bilayer contact. *Biochemistry.* **23**:1532–1538.

- **Ellens, H., Bentz, J., and Szoka, F.C. 1985.** H1- and Ca21-induced fusion and destabilization of liposomes. *Biochemistry*. **24**:3099–3106.

- **Ellens, H., Siegel, D.P., Alford, D., Yeagle, P.L., Boni, L., Lis, L.J., Quinn, P.J., and Bentz, J. 1989.** Membrane fusion and inverted phases. *Biochemistry.* **28**:3692–3703.

- **Farhood, H., Serbina, N., and Huang, L. 1995.** The role of dioleoylphosphatidylethanolamine in cationic liposome mediated gene transfer. *Biochim. Biophys. Acta.* **1235**:289–295.

- **Fattal, E., Couvreur, P., and Dubernet, C. 2004.** "Smart" delivery of antisense oligonucleotides by anionic pH-sensitive liposomes. *Adv. Drug Del. Rev*. **56**:931–46.

- **Feinberg, E.H. and Hunter, C.P. 2003.** Transport of dsRNA into cells by the transmembrane protein SID-1. *Science.* **301**:1545–1547.

- **Felgner, J.H., Kumar, R., Sridhar, C.N., Wheeler, C.J., Tsai, Y.J., Border, R., Ramsey, P., Martin, M., and Felgner, P.L. 1994.** Enhanced gene delivery and mechanism studies with a novel series of cationic lipid formulations. *J. Biol. Chem.* **269**:2550–2561:

- **Felgner, P.L., Gadek, T.R., Holm, M., Roman, R., Chan, H.W., Wenz, M., Northrop, J.P., Ringold, G.M. and Danielsen, M. 1987**. Lipofectin: a highly efficient, lipid-mediated DNA-transfection procedure. *Proc. Natl. Acad. Sci.* **84**:7413–7417.

- **Fire, A., Xu, S., Montgomery, M., Kostas, S., Driver, S., and Mello, C. 1998.** "Potent and specific genetic interference by double-stranded RNA in *Caenorhabditis elegans*". *Nature.* **391**:806–11.

- **Gao, H. and Hui, K.M. 2001**. Synthesis of a novel series of cationic lipids that can act as efficient gene delivery vehicles through systematic heterocyclic substitution of cholesterol derivatives. *Gene Ther.* **8**:855–863.

- **Golsteyn, R.M., Mundt, K.E., Fry, A.M., and Nigg, E.A. 1995.** Cell cycle regulation of the activity and subcellular localization of PLK1, a human protein kinase implicated in mitotic spindle function. *J. Cell Biol.* **129**:1617–1628.

- **Graham, M.J., Crooke, S.T., Monteith, D.K., Cooper, S.R., Lemonidis, K.M., Stecker, K.K., Martin M.J., and Crooke, R.M. 1998.** In vivo distribution and metabolism of a phosphorothioate oligonucleotide within rat liver after intravenous administration. *J. Pharmacol. Exp. Ther.* **286**:447–458.

- **Gruner, S.M., Cullis, P.R., Hope, M.J., and Tilcock, C.P. 1985.** Lipid polymorphism: the molecular basis of nonbilayer phases. *Annu. Rev. Biophys. Biophys. Chem.* **14**:211–238.

- **Hafez, I.M. and Cullis, P.R. 2000.** Cholesteryl hemisuccinate exhibits pH sensitive polymorphic phase behavior. *Biochim. Biophys. Acta.* **1463**:107–114.

- **Hafez, I.M. and Cullis, P.R. 2004.** Tunable pH-sensitive liposomes. *Methods in enzymology.* **387**:113–134.

- **Hafez, I.M., Ansell, S., and Cullis, P.R. 2000.** Tunable pH-sensitive liposomes composed of mixtures of cationic and anionic lipids. *Biophys. J.* **79**:1438–1446.

- **Hafez, I.M., Maurer, N., and Cullis, P.R. 2001.** On the mechanism whereby cationic lipids promote intracellular delivery of polynucleic acids. *Gene Ther.* **8**:1188–1196.

- **Halder, J., Kamat, A.A., Landen Jr., C.N., Han, L.Y., Lutgendorf, S.K. Lin, Y.G., Merritt, W.M., Jennings, N.B., Chavez–Reyes, A., Coleman, R.L., Gershenson, D.M., Schmandt, R., Cole, S.W., Lopez–Berestein, G., and Sood, A.K. 2006.** Focal adhesion kinase targeting using in vivo short interfering RNA delivery in neutral liposomes for ovarian carcinoma therapy. *Clin. Cancer Res.* **12**:4916–4924.

- **Hannon, G.J., and Rossi, J.J. 2004.** Unlocking the potential of the human genome with RNA interference. *Nature.* **431**:371–378.

- **Haupenthal J., Bähr C., Zeuzem S., and Piiper, A. 2007.** RNAse A-like enzymes in serum inhibit the anti-neoplastic activity of siRNA targeting polo-like kinase 1. *Int. J. Cancer.* **121**:206–210.

- **Hawley-Nelson, P., Ciccarone, V., Geheyehu, G., Jessee, J., and Felgner, P.L. 1993** LipofectAMINE reagent: a new, higher efficiency polycationic liposome transfection reagent. *Focus*. **15**:73–83.

- **Heyes, J., Palmer, L., Bremner, K., and MacLachlan, I. 2005.** Cationic lipid saturation influences intracellular delivery of encapsulated nucleic acids. *Control Release.* **107**:276–287.

- **Hope, M.J., Walker, D.C., and Cullis, P.R. 1983.** Ca^{2+} and pH induced fusion of small unilamellar vesicles consisting of phosphatidylethanolamine and negatively charged phospholipids: a freeze fracture study. *Biochem. Biophys. Res. Commun.* **110**:15–22.

- **Hu, Q., Bally, M.B., and Madden, T.D. 2002.** Subcellular trafficking of antisense oligonucleotides and down–regulation of bcl-2 gene expression in human melanoma cells using a fusogenic liposome delivery system. *Nucleic. Acids Res.* **30**:3632–3641.

- **Huang, Y. Y. and Pieter, R. C. 2000.** "Transfection of BHK Cell by Serum- Stabilized Cationic Liposome-DNA Particles". *Biomedical Engineering: Appln. Basis, Communi.* **12**:281–287.

- **Hudziak, R., Summerton, J., Weller, D., and Iversen, P. 2000.** Antiproliferative effects of steric blocking phosphorodiamidate morpholino antisense agents directed against *c-myc. Antisense Nucleic Acid Drug Dev.* **10**:163–176.

- **Hui, S. W., Stewart, T. P., Boni, L. T., and Yeagle, P. L. 1981.** Membrane fusion through point defects in bilayers. *Science*. **212**:921–923.

- **Hui, S.W., Langner, M., Zhao, Y.L., Ross, P., Hurley, E., and Chan, K. 1996.** The role of helper lipids in cationic liposome-mediated gene transfer. *Biophys. J.* **71**:590–599.

- **Israelachvili, J.N., Marcelja, S., and Horn, R.G. 1980.** Physical principles of membrane organization. *Q. Rev. Biophys.* **13**:121–200.

- **Israelachvili, J.N. and Mitchell, D.J. 1975.** A model for the packing of lipids in bilayer membranes. *Biochim. Biophys. Acta.* **389**:13–19.

- **Israelachvili, J.N., Mitchell, D.J., and Ninham, B.W. 1977.** Theory of self-assembly of lipid bilayers and vesicles. *Biochim. Biophys. Acta.* **470**:185–201.

- **Jaaskelainen, I., Sternberg, B., Monkkonen, J., and Urtti, A. 1998.** Physicochemical and morphological properties of complexes made of cationic liposomes and oligonucleotides. *Int J Pharm.* **167**:191–203.

- **Jeffs, L.B., Palmer, L.R., Ambegia, E.G., Giesbrecht, C., Ewanick, S. and MacLachlan, I. 2005.** A scalable, extrusion-free method for efficient liposomal encapsulation of plasmid DNA. *Pharm. Res.* **22**:362–72.

- **Kasireddy, K., Ali, S.M., Ahmad, M.U., Choudhury, S., Chien, P.Y., Sheikh, S., and Ahmad, I. 2005.** Synthesis of cationic cardiolipin analogues. *Bioorg. Chem.* **33**:345–362.

- **Kielland, J. 1937.** Individual activity coefficients of ions in aqueous solutions. *J. Am. Chem. Soc.* **59**:1675–1678.

- **Kim, K., Lee, Y.S. and Carthew, R.W. 2007.** Conversion of pre-RISC to halo-RISC by Ago2 during assembly of RNAi complexes. *RNA*. **13**:22–29

- **Klimuk, S.K., Semple, S.C., Nahirney, P.N., Mullen, M.C., Bennett, C.F., Scherrer, P., and Hope, M.J. 2000.** Enhanced anti–inflammatory activity of a liposomal intercellular adhesion molecule-1 antisense oligodeoxynucleotide in an acute model of contact hypersensitivity. *J. Pharm. Exp. Ther.* **292**:480–488.

- **Koltover, I., Salditt, T., Rädler, J.O., and Safinya, C.R. 1998.** An inverted hexagonal phase of cationic liposome-DNA complexes related to DNA release and delivery. *Science.* **281**:78–81.

- **Kooijman, E.E., Chupin, V., Fuller, N.L., Kozlov, M.M., de Kruijif, B., Burger, K.N.J. and Rand, P.R. 2005.** Spontaneous curvature of phosphatidic acid and lysophosphatidic acid. *Biochemistry*. **44**:2097–2102.

- **Kooijman, E.E., Chupin, V., de Kruijif, B., and Burger, K.N.J. 2003.** Modulation of membrane curvature by phosphatidic acid and lysophosphatidic acid. *Traffic*. **4**:162–74.

- **Kozlovsky, *Y.,* Chernomordik, L.V.*, and* Kozlov, M.M. 2002.** Lipid intermediates in membrane fusion: Formation, structure, and decay of hemifusion diaphragm. *Biophys. J.* **83**:2634–2651.

- **Kurreck, J. 2009.** RNA Interference: From Basic Research to Therapeutic Applications. *Angew. Chem. Int. Ed.* **48**:1378–1398.

- **Lai, M.Z., Vail, W.J., and Szoka F.C. 1985.** Acid- and calcium-induced structural changes in phosphatidylethanolamine membranes stabilized by cholesteryl hemisuccinate. *Biochemistry.* **24**:1654–1661.

- **Landen Jr., C.N., Chavez–Reyes, A., Bucana, C., Schmandt, R., Deavers, M.T., Lopez–Berestein, G., and Sood, A.K. 2005.** Therapeutic EphA2 gene targeting in vivo using neutral liposomal small interfering RNA delivery. *Cancer Res.* **65**:6910–6918.

- **Lane, H.A. and Nigg, E.A. 1996.** Antibody microinjection reveals an essential role for human polo-like kinase 1 (Plk1) in the functional maturation of mitotic centrosomes. *J. Cell Biol.* **135**:1701–1713.

- **Lee, A.G. 2004.** How lipids affect the activities of integral membrane proteins. *Biochim. Biophys. Acta.* **1666**:62–87.

- **Lee, E.R., Marshall, J., Siegel, C.S., Jiang, C., Yew, N.S., Nichols, M.R., Nietupski, J.B., Ziegler, R.J., Lane, M.B., Wang K.X., Wan, N.C., Scheule, R.K., Harris, D.J., Smith, A.E., and Cheng, S.H. 1996.** Detailed analysis of structures and formulations of cationic lipids for efficient gene transfer to the lung. *Hum. Gene Ther.* **7**:1701–1717.

- **Lentz, B. R., Malinin, V., Haque, M.E., and Evans, K. 2000.** Protein machines and lipid assemblies: current views of cell membrane fusion. *Curr. Opin. Struct. Biol.* **10**:607–615.

- **Leventis, R. and Silvius, J.R. 1990.** Interactions of mammalian cells with lipid dispersions containing novel metabolizable cationic amphiphiles. *Biochim. Biophys. Acta*. **1023**:124–132.

- **Lewis, D.L., Hagstrom, J.E., Loomis, A.G., Wolff, J.A., and Herweijer, H. 2002**. Efficient delivery of siRNA for inhibition of gene expression in postnatal mice. *Nat. Genet.* **32**:107–108.

- **Li, B., Hughes, J.A., and Phillips, M.I. 1997.** Uptake and efflux of intact antisense phosphorothioate deoxyoligonucleotide directed against angiotensin receptors in bovine adrenal cells. *Neurochem. Int.* **31**:393–403.

- **Li, X.-J., and Schick, M. 2000a.** Theory of lipid polymorphism: application to phosphatidylethanolamine and phosphatidylserine. *Biophys. J.* **78**:34–46.

- **Li, X.-J., and Schick, M. 2000b.** Distribution of lipids in nonlamellar phases of their mixtures. *J. Chem. Phys.* **112**:6063–6072.

- **Li, X.-J., and Schick, M. 2000c.** Fluctuations in mixtures of lameller- and nonlameller-forming lipids. *J. Chem. Phys.* **112**:10599–10607.

- **Li, X.-J., and Schick, M. 2001.** Theory of Tunable pH-Sensitive Vesicles of Anionic and Cationic Lipids or Anionic and Neutral Lipids. *Biophys. J.* **80**:1703–1711.

- **Liang, W. W., Shi, X., Deshpande, D., Malanga, C. J., and Rojanasakul, Y. 1996.** Oligonucleotide targeting to alveolar macrophages by mannose receptor–mediated endocytosis. *Biochim. Biophys. Acta.* **1279**:227–234.

- **Liu, D. and Huang, L. 1989.** Role of cholesterol in the stability of pH sensitive large unilalellar liposomes prepared by the detergent dialysis method. *Biochim. Biophys. Acta*. **981**:254–260.

- **Lindau, M. and Almers, W. 1995.** Structure and function of fusion pores in exocytosis and ectoplasmic membrane fusion. *Curr. Opin. Cell Biol.* **7**:509–517.

- **Lindblom, G. and Rilfors, L. 1992.** Nonlamellar phases formed by membrane Lipids. *Adv. Colloid Interface Sci.* **41**:101–125.

- **Loke, S.L., Stein, C., Zhang, H., Cohen, J.S., and Neckers, M. 1989.** Characterization of oligonucleotide transport into living cells. *Proc. Natl. Acad. Sci. U. S .A.* **86**:3474–3478.

- **Lubrich, B., van Calker, D., and Peschka–Suss, R. 2000.** Inhibition of inositol uptake in astrocytes by antisense oligonucleotides delivered by pH–sensitive liposomes. *Eur. J. Biochem.* **267**:2432–2438.

- **Matranga, C., Tomari, Y., Shin, C., Bartel, D., Zamore, P. 2005.** "Passenger-strand cleavage facilitates assembly of siRNA into Ago2-containing RNAi enzyme complexes". *Cell*. **123**:607–20.

- **Markin, V.S., Kozlov, M.M., and Borovjagin, V.L. 1984.** On the theory of membrane fusion. The stalk mechanism. *Gen. Physiol. Biophys.* **3**:361–377.

- **Marcusson, E.G., Bhat, B., Manoharan, M., Bennett, C.F. and Dean, N.M. 1998.** Phosphorothioate oligodeoxyribonucleotides dissociate from cationic lipids before entering the nucleus. *Nucleic Acids. Res.* **26**:2016–2023.

- **McCaffrey, A.P., Meuse, L., Pham, T.T., Conklin, D.S., Hannon, G.J. and Kay, M.A. 2002.** RNA interference in adult mice. *Nature*. **418**:38–39.

- **Meekel, A.A.P., Wagenaar, A., Smisterova, J., Kroeze, J.E., Haadsma, P. Bosgraaf, B., Stuart, M.C.A., Brisson, A., Ruiters, M.H.J., Hoekstra, D., and Engberts, J.B.F.N. 2000.** Synthesis of pyridinium amphiphiles used for transfection and some characteristics of amphiphile/DNA complex formation. *Eur. J. Org. Chem.* **4**:665–673.

- **Mislick, K.A. and Baldeschwieler, J.D. 1996.** Evidence for the role of proteoglycans in cation–mediated gene transfer. *Proc. Natl. Acad. Sci. U S A.* **93**:12349–12354.

- **Mok, K. W. and Cullis, P. R. 1997.** Structural and fusogenic properties of cationic liposomes in the presence of plasmid DNA. *Biophys. J.* **73**:2534–2545.

- **Morrissey, D.V., Lockridge, J.A., Shaw, L., Blanchard, K., Jensen, K., Breen, W., Hartsough, K., Machemer, L., Radka, S., Jadhav, V., Vaish, N., Zinnen, S., Vargeese, C., Bowman, K., Shaffer, C.S, Jeffs, L.B., Judge, A., MacLachlan, I., and Polisky, B. 2005.** Potent and persistent in vivo anti-HBV activity of chemically modified siRNAs. *Nat. Biotechnol.* **23**:1002–1007.

- **Mounkes, L.C., Zhong, W., Cipres–Palacin, G., Heath, T.D., and Debs, R.J. 1998.** Proteoglycans mediate cationic liposome-DNA complex–based gene delivery in vitro and in vivo. *J. Biol. Chem.* **273**:26164–26170.

- **Mukhopadhyay, P., Monticelli, L., and Tieleman, D.P. 2004.** Molecular dynamics simulation of a palmitoyl-oleoyl phosphatidylserine bilayer with Na+ counterions and NaCl. *Biophys. J.* **86**:1601–1609.

- **Murzyn, K., Zhao, W., Karttunen, M., Kurdziel, M., and Róg, T. 2006.** Dynamics of water at membrane surfaces: effect of headgroup structure. *Biointerphases.* **1**:98–105.

- **Pandit, S. A. and Berkowitz, M. L. 2002.** Molecular Dynamics Simulation of Dipalmitoylphosphatidylserine Bilayer with Na+ counterions. *Biophysical Journal.* **82**:1818–1827.

- **Pandit, S., Bostick, D., and Berkowitz, M.L. 2003.** Molecular dynamics simulation of dipalmitoylphosphatidylcholine bilayer with NaCl. *Biophys. J.* **84**:3743–3750.

- **Panzner, S., Fankhänel, S., Essler, F., Panzner, C., and Gerold, E. 2002.** Amphoteric liposomes and the use thereof. **WO 02/066012.**

- **Panzner, S., Lutz, S., Siepi, E., and Claudia, M. 2008.** Improvements in or relating to amphoteric liposomes Amphoteric liposomes, a method of formulating an amphoteric liposome and a method of loading an amphoteric liposome. **WO 08/043575.**

- **Phillips, M.I.and Zhang, Y.C. 2000.** Basic principles of using antisense oligonucleotides in vivo. *Methods Enzymol.* **313**:46–56.

- **Plank, C., Mechtler, K., Szoka, F.C. Jr., and Wagner, E. 1996.** Activation of the complement system by synthetic DNA complexes: a potential barrier for intravenous gene delivery. *Hum. Gene Ther.* **7**:1437–46.

- **Pollack, G. H. 2001.** Cells, Gels and the Engines of Life. *Ebner and Sons Publishers.* **Chap. 6**, pp. 87-98.

- **Rappolt, M., Vidal, M.F., Kriechbaum, M., Stienhert, M., Amentisch, H., Bernstorff, S. and Laggner, P. 2003.** Structural, dynamic, and mechanical properties of POPC at low cholesterol concentration studied in pressure/temperature space. *Eur. Biophys. J.* **31**:575–585.

- **Reinsch, C., Siepi, E., Dieckmann, A., and Panzner, S. 2008.** Therapeutic Oligonucleotides; Chapter 10, "Strategies for the delivery of Oligonucleotides in vivo"; *RSC Biomolecular Sciences; Royal Society of Chemistry.*

- **Santel, A., Aleku, M., Keil, O., Endruschat, J., Esche, V., Durieux, B., Loeffler, K., Fechtner, M., Röhl, T., Fisch, G., Dames, S., Arnold, W., Giese, K., Klippel, A., and Kaufmann, J.A. 2006a.** RNA interference in the mouse vascular endothelium by systemic administration of siRNA–lipoplexes for cancer therapy. *Gene Therapy.* **18**:1360–1370.

- **Santel, A., Aleku, M., Keil, O., Endruschat, J., Esche, V., Fisch, G., Dames, S., Loeffler, K., Fechtner, M., Arnold, W., Giese, K., Klippel, A., and Kaufmann, J.A. 2006b.** Novel siRNA-lipoplex technology for RNA interference in the mouse vascular endothelium. *Gene Therapy.* **16**:1222–1234.

- **Sarapuk, J., Gabrielska, J., and Przestalski, S. 1997.** Modification of model membrane by new bifunctional surfactants. *Current Topics Biophys*. **21**:54–57.

- **Sarapuk, J., Kleszczynska, H., and Rozycka–Roszak, B. 1998.** The role of counterions in the interaction of bifunctional surface active compounds with model membranes. *Biochem. Mol. Biol. Int*. **44**:1105–1110.

- **Shi, F., Wasungu, L., Nomden, A., Stuart, M.C.A., Polushkin, E., Engberts, J.B.F.N., and Hoekstra, D. 2002.** Interference of polyethylene glycol-lipid analogues with cationic lipid-mediated delivery of oligonucleotides; role of lipid exchangeability and non-lamellar transitions. *Biochem. J.* **366**:333–341.

- **Shurety, W., Stewart, N.L., and Stow, J.L. 1998.** Fluid-phase markers in the basolateral endocytic pathway accumulate in response to the actin assembly-promoting drug Jasplakinolide. *Mol. Biol. Cell.* **9**:957–975.

- **Siegel, D.P. 1996.** The modified stalk mechanism of lamellar/inverted phase transitions and its implications for membrane fusion. *Biophys. J.* **76**:291–313.

- **Siegel, D.P. and Epand, R.M. 1997.** The mechanism of lamellar to inverted hexagonal phase transitions in phosphatidylethanolamine: Implications for membrane fusion mechanisms. *Biophys. J.* **73**:3089–3111.

- **Sioud M. 2005.** On the delivery of small interfering RNAs intomammalian cells. *Expert Opinion on Drug Delivery.* **2**:639–651.

- **Slepushkin, V.A., Simões, S., Dazin, P., Newman, M.S., Guo, L.S., Pedroso de Lima, M.C., and Düzgünes, N. 1997.** Sterically stabilized pH-sensitive liposomes. Intracellular delivery of aqueous contents and prolonged circulation in vivo. *J. Biol. Chem.* **272**:2382–2388.

- **Soutschek, J., Akinc, A., Bramlage, B., Charisse, K., Constien, R., Donoghue, M., Elbashir, S., Geick, A., Hadwiger, P., Harborth, J., John, M., Kesavan, V., Lavine, G., Pandey, R.K., Racie, T., Rajeev K.G., Rohl, I., Toudjarska, I., Wang, G., Wuschko, S., Bumcrot, D., Koteliansky, V., Limmer, S., Manoharan, M., and Vornlocher, H.P. 2004.** Therapeutic silencing of an endogenous gene by systemic administration of modified siRNAs. *Nature.* **432**:173–178.

- **Stephenson, M. L. and Zamecnik, P. C. 1978.** Inhibition of Rous sarcoma viral RNA translation by a specific oligodeoxyribonucleotide. *Proc. Natl. Acad. Sci*. *U.S.A*. **75**:285–288.

- **Straubinger, R.M., Düzgünes, N., and Papahadjopoulos, D. 1985.** pH-sensitive liposomes mediate cytoplasmic delivery of encapsulated macromolecules. *FEBS Lett.* **179**:148–154.

- **Straubinger, R.M., Hong, K., Friend, D.S., and Papahadjopoulos, D. 1983.** Endocytosis of liposomes and intracellular fate of encapsulated molecules: encounter with a low pH compartment after internalization in coated vesicles. *Cell* **32**:1069–1079.

- **Struck, D.K., Hoekstra, D., and Pagano, R.E. 1981.** Use of resonance energy transfer to monitor membrane fusion. *Biochemistry.* **20**:4093–4099.

- **Suits, F., Pitman, M.C., and Feller, S.E. 2005.** "Molecular dynamics investigation of the structural properties of phosphatidylethanolamine lipid bilayers." *J. Chem. Phys.* **122**:244714.

- **Takai, N., Hamanaka, R., Yoshimatsu, J., and Miyakawa, I. 2005.** Polo-like kinases (Plks) and cancer. *Oncogene.* **24**:287–291.

- **Tamaddon, A.M., Hosseini-Shirazi, F., and Moghimi, H.R. 2007.** Preparation of oligodeoxynucleotide encapsulated cationic liposomes and release study with models of cellular membranes. *DARU.* **15**:61–70.

- **Tarahovsky, Yu. S., Koynova, R., and MacDonald, R.C. 2004.** DNA release from lipoplexes by anionic lipids: correlation with lipid mesomorphism, interfacial curvature, and membrane fusion. *Biophys. J.* **87**:1054–1064.

- **Tilcock, C.P. and Cullis, P.R. 1981.** The polymorphic phase behaviour of mixed phosphatidylserine-phosphatidylethanolamine model systems as detected by 31P-NMR. *Biochim. Biophys. Acta.* **641**:189–201.

- **Tocanne, J.-F. and Teissie´, J. 1990.** Ionization of phospholipids and phospholipid-supported interfacial lateral diffusion of protons in model membrane systems. *Biochim. Biophys. Acta.* **1031**:111–142.

- **Whitehead, K. A., Langer, R., and Anderson, D. G. 2009.** Knocking down barriers: advances in siRNA delivery. *Nat. Rev. Drug. Discov.* **8**:129–138.

- **Wolf, G., Elez, R., Doermer, A., Holtrich, U., Ackermann, H., Stutte, H.J., Altmannsberger, H.M., Rubsamen-Waigmann, H., and Strebhardt, K. 1997.** Prognostic significance of Polo-like kinase (PLK) expression in non-small cell lung cancer. *Oncogene.* **14**:543–549.

- **Yakubov, L.A., Deeva, E.A., Zarytova, V.F., Ivanova, E.M., Ryte, A.S., Yurchenko, L.V., and Vlassov V.V. 1989.** Mechanism of oligonucleotide uptake by cells: involvement of specific receptors? *Proc. Natl. Acad. Sci. U. S. A.* **86**:6454–6458.

- **Yu, X.X., Murray, S.F., Pandey, S.K., Booten, S.L., Bao, D., Song, X.Z., Kelly, S., Chen, S., McKay, R., Monia B.P., and Bhanot, S. 2005.** Antisense oligonucleotide reduction of DGAT2 expression improves hepatic steatosis and hyperlipidemia in obese mice. *Hepatology.* **42**: 362–371.

- **Zelphati, O., and Szoka, F. C. 1996a.** Intracellular distribution and mechanism of delivery of oligonucleotides mediated by cationic lipids. *Pharm. Res.* **13**:1367–1372.

- **Zelphati, O., Uyechi, L.S., Barron, L.G., and Szoka, F.C. Jr. 1998.** Effect of serum components on the physico-chemical properties of cationic lipid/oligonucleotide complexes and on their interactions with cells. *Biochim. Biophys. Acta.* **1390**:119–133.

- **Zhang, H.Y., Du, Q., Wahlestedt, C., and Liang, Z. 2006.** RNA interference with chemically modified siRNA. *Curr. Top. Med. Chem.* **6**:893–900.

- **Zhang, Y.P., Sekirov, L., Saravolac, E.G., Wheeler, J.J., Tardi, P., Clow, K., Leng, E., Sun, R., Cullis, P.R., and Scherrer, P. 1999.** Stabilized plasmid-lipid particles for regional gene therapy: formulation and transfection properties. *Gene Ther.* **6**:1438–1447

- **Zhang, Z., Weinschenk, T., Guo, K., and Schluesener, H.J. 2006.** siRNA binding proteins of microglial cells: PKR is an unanticipated ligand. *J. Cell. Biochem.* **97**:1217–1229.

- **Zhao, Q., Matson, S., Herrera, C.J., Fisher, E., Yu, H., and Krieg, A.M. 1993.** Comparison of cellular binding and uptake of antisense phosphodiester, phosphorothioate, and mixed phosphorothioate and methylphosphonate oligonucleotides. *Antisense Res.Dev.* **3**:53–66.

- **Zhao, W., Rog, T., Gurtovenko, A.A., Vattulainen, I., and Karttunen, M. 2007.** Atomic-scale structure and electrostatics of anionic palmitoyloleoylphosphatidylglycerol lipid bilayers with Na^+ counterions. *Biophys. J.* **92**:1114–1124.

- **Zhou, X., and Huang, L. 1994.** DNA transfection mediated by cationic liposomes containing lipopolylysine: characterization and mechanism of action. *Biochim. Biophys. Acta.* **1189**:195–203.

- **Zimmermann, T.S., Lee, A.C., Akinc, A., Bramlage, B., Bumcrot, D., Fedoruk, M.N., Harborth, J., Heyes, J.A., Jeffs, L.B., John, M., Judge, A.D., Lam, K., McClintock, K., Nechev, L.V., Palmer, L.R., Racie, T., Rohl, I., Seiffert, S., Shanmugam, S., Sood, V., Soutschek, J., Toudjarska, I., Wheat, A.J., Yaworski, E., Zedalis, W., Koteliansky, V., Manoharan, M., Vornlocher, H.P., and MacLachlan, I. 2006.** RNAi-mediated gene silencing in non–human primates. *Nature*. **441**:111–114.

- **Zuhorn, I.S., and Hoekstra, D. 2002.** On the mechanism of cationic amphiphile-mediated transfection. To fuse or not to fuse: is that the question? *J. Membr. Biol.* **189**:167–179.

TABLES & FIGURES

TABLE 2.1: Application and corresponding counterions used in this study…….. 32

TABLE 2.2: Amphoteric liposomes for siRNA delivery into HeLa and RAW264.7 cells 35

TABLE 3.1: Amphoteric mixtures in combination with neutral lipids tested in the second step…… 59

TABLE 3.2: Lipid composition of model cellular membranes…….. 64

FIGURE 1.1: Schematic representation of cationic delivery agents for oligonucleotides and siRNA…….. 15

FIGURE 1.2: Chemical structures of typical amphiphiles used in liposome formation. 17

FIGURE 1.3: Schematic representation of positively and negatively charged lipids….. 20

FIGURE 1.4: Schematic illustration of lamellar L_α and inverted hexagonal H_{II} phase… 21

FIGURE 1.5: Schematic illustration of molecular lipid geometry and the related phase structures…… 22

FIGURE 1.6: Schematic illustration of an amphoteric membrane at different pH values …… 27

FIGURE 2.1: Fusion matrix of an Amphoter I system…….. 33

FIGURE 3.1: 3D schematic illustration of CHIM and CHEMS structures…….. 46

FIGURE 3.2: Counterion binding governs lipid fusion…….. 47

FIGURE 3.3: Counterions control lipid fusion…….. 49

FIGURE 3.4: Amphoteric liposomes display bistable phase behaviour…….. 51

FIGURE 3.5: pH-dependent fusion properties of Amphoter II system…….. 53

FIGURE 3.6: pH-dependent fusion properties of Amphoter III system…… 54

FIGURE 3.7: pH-dependent fusion properties of DOPA and POPG amphoteric liposomes…… 55

FIGURE 3.8: Fusion matrix of amphoteric liposomes obtained by HTS…… 56

FIGURE 3.9: For charged and neutral lipids, liposome fusion correlates with the headgroup volumes…….. 58

FIGURE 3.10: Impact of neutral and zwitterionic lipids on the fusion properties of amphoteric liposomes…….. 60

FIGURE 3.11: For neutral lipids, liposome fusion correlates with the head group volumes…… 62

FIGURE 3.12: pH-dependent fusion properties of amphoteric membranes upon incubation with model cellular membranes…….. 65

FIGURE 3.13: Intracellular localisation of MoChol/CHEMS liposomes…….. 67

FIGURE 3.14: Schematic illustration of a 96 well transfection plate…… 69

FIGURE 3.15: *In vitro* screen of amphoteric liposomes for siRNA delivery…….. 71

FIGURE 3.16: The shape parameter κ determinate cation to anion ratio for transfection efficiency…….. 73

FIGURE 3.17: The fusion determinant κ_{MIN} governs the siRNA transfection into HeLa or macrophages cells with amphoteric liposomes…… 75

FIGURE 3.18: κ_{MIN}, but not κ_{pH8} governs the transfection of cells with amphoteric liposomes…… 76

ACKNOWLEDGEMENTS

To my supervisor, Dr. Steffen Panzner, I am so grateful to be member of the novosom family and work closely with you in the past years. After finishing my studies and without having any research experience, I made a big switch to be a scientist in your group. It turns out to be such a memorial experience to work in your lab. Thank you for your trust, which ensured me a great freedom to do experiments. Your enthusiasm led me through the hard times of the project. Last but not least, through our joint working, I have learned to appreciate and love science… "ΕΥΧΑΡΙΣΤΩ"

I would like to thank Dr. Silke Lutz for the critical discussions concerning the results of this thesis and for the helpful suggestions. I am very grateful to Claudia Müller and Ute Vinzens for their technical assistance. I appreciate their technical expertise and readiness to help, which have been highly crucial for this work.

Sebastian Kehres, thank you for correcting the manuscript of my thesis; for your helpful and interesting suggestions and for lifelong friendship.

I am grateful to Prof. Dr. Sven-Erik Behrens for reviewing the thesis, providing relevant criticism and comments and enabling the accomplishment of the dissertation.

At last, I would like to thank Elias Papatheodorou. Elias, thanks a lot for all your help and support in my career development.

CURRICULUM VITAE

Name: Evgenios Siepi
Born: 19th August 1978 in Larnaca, Cyprus
Nationality: Cypriot
e-mail: **esiepi@hotmail.com**

EDUCATION

May 2006 – Dec 2009 **Ph.D. student,** Institute of Biochemistry/Biotechnollogy – Martin-Luther-University Halle-Wittenberg, Germany. Thesis title: "Mechanism of Amphoteric Liposomes & Application for siRNA Delivery".

Oct 2004 – May 2005 **Diploma Thesis,** Institute of Clinical Immunology and Transfusion Medicine, Medical Faculty – University of Leipzig, Germany. Thesis title: "Construction and functional characterisation of GFP-fusions of proteins for the analysis of protein-interactions with the transcription factor Stat3 using fluorescence microscopy and FRET".

Apr 2003 – Jun 2003 **Research work,** Research group "Protein engineering" at Biotechnological and Biomedical Center – University of Leipzig, Germany. Title: "Introduction of disulfide bridge in exonuclease III from *E.coli*".

Oct 1999 –Oct 2004 **Studies of Science in Biochemistry,** Faculty of Biosciences, Pharmacy and Psychology – University of Leipzig, Germany.

Oct 1998 – Jul 1999 **German language course,** Herder Institut – University of Leipzig, Germany.

PROFESSIONAL EXPERIENCE

Jul 2009 **Manager Drug Delivery,** Novosom AG – Biopharmaceutical Company, Germany.

Mar 2007 – Jul 2009 **Project Leader,** Novosom AG – Biopharmaceutical Company, Germany.

Oct 2005 – Mar 2007 **Research Scientist,** Novosom AG – Biopharmaceutical Company, Germany.

Oct 2003 – Jan 2004 **Research Assistant,** Research group "Protein engineering" at Biotechnological and Biomedical Center – University of Leipzig, Germany.

Apr 2001 – Jul 2001 **Research Assistant**, Institute of Human Genetics – University of Leipzig, Germany.

Oct 1996 – Jul 1998 **Military service,** Cyprus.

PUBLICATIONS & PATENTS

- **Siepi, E., Lutz S., Reinsch C., and Panzner, S.** "An Ion Switch Regulates Membrane Fusion and Allows the Rational Design of Cellular Transfectants". *Submitted for publication in Science in January 2010.*

- **Reinsch, C., Siepi, E., Dieckmann, A., and Panzner, S. 2008.** Therapeutic Oligonucleotides; Chapter 10, "Strategies for the delivery of Oligonucleotides in vivo"; *RSC Biomolecular Sciences; Royal Society of Chemistry.*

- PubDate: 2008-04-17 **Improvements in or relating to amphoteric liposomes.**
  Document No: 2008/043575
  Application No: PCT/EP2007/008917
  Publication No: WO/2008/043575
  Application Date: 2007-10-12

- PubDate: 2008-04-17 **Amphoteric liposomes, a method of formulating an amphoteric liposome and a method of loading an amphoteric liposome.**
  Document No: 20080089932
  Application No: 974350
  Publication No: 20080089932
  Application Date: 2007-10-12

- PubDate: 2008-06-26 **Lipids and lipid assemblies comprising transfection enhancer elements.**
  Document No: 2008/074487
  Application No: PCT/EP2007/011187
  Publication No: WO/2008/074487
  Application Date: 2007-12-19

- PubDate: 2009-04-16 **Improvements in or relating to amphoteric liposomes comprising neutral lipids.**
  Document No: 2009/047006
  Application No: PCT/EP2008/008621
  Publication No: WO/2009/047006
  Application Date: 2008-10-12

STATEMENT/ERKLÄRUNG

Hiermit erkläre ich, dass die vorliegende Arbeit selbständig verfasst habe und keine anderen als die angegebenen Quellen und Hilfsmittel verwendet habe. Die anderen Arbeiten entnommenen Angaben, wurden dem Wortlaut oder Sinn entsprechend wiedergegeben und sind durch Quellenangaben gekennzeichnet.

_____

Evgenios Siepi Halle (Saale), February 2010